

**EVALUATION OF FEDERAL REFERENCE METHOD PM10 INLET FOR
SAMPLING LARGE PARTICLES**

A Thesis

by

RALEIGH ALLEN SMITH

Submitted to the Office of Graduate and Professional Studies of
Texas A&M University
in partial fulfillment of the requirements for the degree of

MASTER OF SCIENCE

Chair of Committee,
Committee Members,
Head of Department,

Ronald E. Lacey
John Haglund
Gerald Riskowski
Stephen W. Searcy

May 2017

Major Subject: Biological and Agricultural Engineering

Copyright 2017 Raleigh Allen Smith

ABSTRACT

Particulate matter (PM) is one of the six criteria pollutants regulated under the National Ambient Air Quality Standards (NAAQS). Regional compliance with PM NAAQS is monitored using networks of Federal Reference Method (FRM) designated PM₁₀ sampling inlets. Several previous studies have suggested that FRM PM₁₀ inlets sampling PM from rural sources will not perform as designed and that a significant number of particles with larger diameters will penetrate the inlet. This research sought to characterize a common FRM PM₁₀ inlet, the SA246b, using a combination of the original developmental steps, FRM designation testing procedures, and new techniques.

The wind tunnel originally used as part of the designing and testing of the SA246b was reassembled and evaluated against Subpart D standards. The SA246b was evaluated as described in Subpart D at a wind speed of 8 km h⁻¹ with two adjustments: an aerosol particle sizer and testing times were specifically scheduled to meet minimum signal requirements. Measured and corrected data showed that particles with diameters of 20 and 25 micrometers had non-trivial penetration of 5.7% and 3.5%, respectively. A lognormal curve was found to be most descriptive of the collected data (p-value of 0.686). The Subpart D mass concentration analysis yielded a concentration of 152.694 $\mu\text{g m}^{-3}$ which was within 10% of the ideal concentration value, 143.889 $\mu\text{g m}^{-3}$. When the empirical SA246b lognormal performance curve was applied to the PSDs for several different rural PM sources, the mass concentration values for those sources were between 10% and 34% greater than that of the Subpart D ideal mass concentration. It was

determined that the impact of large particle penetration was non-trivial and dependent upon the PSD of the PM being sampled.

A low volume total suspended particulate (LVTSP) inlet developed at Texas A&M University was evaluated in the Subpart D wind tunnel in an effort to fully characterize the true performance of the inlet. The inlet was evaluated at wind speeds of 2, 8, and 24 km h⁻¹ according to the procedures of Subpart D and the experimental additions employed during the SA246b testing. It was determined that piecewise models were more descriptive across all three wind speeds (p-values were greater than 0.84). Data collected in the wind tunnel was shown to be wind speed dependent and no further analysis of inlet performance was conducted. It was concluded that further analysis of the wind tunnel at the wind speeds of two and 24 km h⁻¹ need to be conducted before further studies could be reliable.

Computational fluid dynamics was used to analyze the performance of the impactor section (the lower section) of the SA246b FRM PM10 inlet for the particle sizes listed in Subpart D. The CFD for the impactor assembly produced a cutpoint of 14.79 micrometers and a performance slope of 1.19 resulting in a 34.88% higher mass concentration for CFD results than the ideal Subpart D inlet mass concentration. This result is outside the 10% difference allowed. It was concluded that the characterization of the inlet must include the aspirator as well as the impactor section as the aspirator assembly also has sampling performance characteristics.

DEDICATION

This thesis is dedicated to my loving wife, Kayla, and the late Dr. Brock Faulkner.

They never gave up on me. Ever.

ACKNOWLEDGMENTS

I would like to thank Dr. Ronald Lacey, my committee chair, who stepped up to help me finish this thesis with his experience and guidance after the loss of Dr. Faulkner. I would also like to thank Dr. John Haglund, whose past experience with this equipment and the methods we've employed were invaluable to the project's success, and Dr. Gerald Riskowski, who has graciously agreed to help finalize this work.

Additional thanks go to folks and organizations who provided integral contributions without which this body of work would never have been completed:

- BGI Instruments which provided drawings and equipment that facilitated this research and were always willing to help out;
- CD-adapco (now Siemens) for the student license of STAR-CCM+ used to conduct the CFD analysis presented in this thesis;
- Dr. Robert Vanderpool of the EPA who was a great asset in developing the wind tunnel and the testing procedures used in this work;
- Dr. Kalbasi for all his help with pictures and equipment information; and,
- Walter Oosthuizen for his friendship and willingness to always lend a hand.

A special thanks to Keith who has been my partner in crime through this entire journey. We've done it, buddy!

I'd like to thank my mother and father for their constant support and my wife who never let me quit, no matter what.

NOMENCLATURE

AED	Aerodynamic Equivalent Diameter
ANOVA	Analysis of Variance
APS	Aerosol Particles Sizer
CAA	Clean Air Act
CAAQES	Center for Agricultural Air Quality Engineering and Science
CFD	Computational Fluid Dynamics
CFR	Code of Federal Regulations
COV	Coefficient of Variation
EPA	United States Environmental Protection Agency
FEC	Fractional Efficiency Curve
FEM	Federal Equivalent Method
FRM	Federal Reference Method
GSD	Geometric Standard Deviation
HEPA	High-Efficiency Particulate Air
LV	Low Volume
LVTSP	Low Volume Total Suspended Particulate
MMD	Mass Median Diameter
NAAQS	National Ambient Air Quality Standards
PM	Particulate Matter
PSD	Particle Size Distribution

PTFE	Polytetrafluoroethylene
TAMU	Texas A&M University
TSP	Total Suspended Particulate
US	United States
VOAG	Vibrating Orifice Aerosol Generator

TABLE OF CONTENTS

	Page
ABSTRACT	ii
DEDICATION	iv
ACKNOWLEDGMENTS	v
NOMENCLATURE	vi
TABLE OF CONTENTS	viii
LIST OF FIGURES	x
LIST OF TABLES	xii
CHAPTER I INTRODUCTION	1
Objectives	8
CHAPTER II SUBPART D WIND TUNNEL EVALUATION OF FRM PM10 SAMPLER	10
Introduction	10
Methodology	20
Results and Discussion	47
Conclusion	56
CHAPTER III SUBPART D WIND TUNNEL EVALUATION OF TAMU LVTSP SAMPLER	58
Introduction	58
Methodology	62
Results and Discussion	79
Conclusion	88
CHAPTER IV COMPUTATIONAL FLUID DYNAMICS ANALYSIS OF PM10 INLET	89

Introduction	89
Methodology	93
Results and Discussion.....	103
Conclusion and Future Work	110
REFERENCES	114
APPENDIX A.....	116
APPENDIX B.....	125
APPENDIX C.....	130
APPENDIX D.....	136
APPENDIX E	139

LIST OF FIGURES

	Page
Figure 1. FEC based on desired penetration of particles in FRM PM10 inlets from Subpart D (CFR, 1987b).....	4
Figure 2. Annotated hatched view of the SA246b PM10 inlet.	6
Figure 3. Concentrations of PM10 emitting from a cotton gin measured by and estimated for (operating with a cut point and slope of 10.5 micrometers and 1.6, respectively) the PM10 inlet, compared with the “true” concentration of PM10 present in each test PSD (Buser et al., 2008).....	15
Figure 4. Hatched view of the PM10 inlet (BGI Instruments, 1997).....	18
Figure 5. Schematic of the Scoates Wind Tunnel used for testing.	21
Figure 6. Velocity measurement sampling grid used in the Scoates wind tunnel for tunnel speeds of 8 km h ⁻¹ ; displayed dimensions are in meters.	23
Figure 7. The (a) PM10 and (b) isokinetic inlet in the same sampling planes.....	25
Figure 8. Labeled photo of the 8 km h ⁻¹ isokinetic nozzle.....	35
Figure 9. Fluorometric measurement error resulting from the signal-to-noise ratio of fluorometric solutions.....	37
Figure 10. Isokinetic temporal uniformity.	39
Figure 11. Example of expected sampling efficiency for polydisperse test aerosol generated by a VOAG.	44
Figure 12. Liquid particle penetration data (green triangles) Subpart D “ideal sampler” FEC (blue line), Lognormal FEC (purple line) and Sigmoidal FEC at 8 km h ⁻¹	49
Figure 13. Multiplet corrected best-fit lognormal curve.	50
Figure 14. Surface plot of percent difference between the Subpart D “ideal sampler” sampling effectiveness and lognormal sampling effectiveness curve constructed with observed liquid particle data passing Subpart D testing at 8 km h ⁻¹	53
Figure 15. Design view of the cone-top LVTSP inlet (Wanjura et al, 2005).....	60
Figure 16. The LVTSP inlet inside the wind tunnel.	62
Figure 17. Sampling effectiveness results from the wind tunnel testing of the LVTSP.....	81

Figure 18. 2, 8, and 24 km h ⁻¹ wind speed data graphed with the corresponding piecewise performance models.....	83
Figure 19. Data collected during the performance testing of the LVTSP by the EPA for each nominal wind speed (Vanderpool, 2015).	85
Figure 20. Hatched view of the SA246b FRM PM10 inlet by BGI Instruments.	93
Figure 21. "Lower Inlet Assembly" of the SA246b inlet (BGI Instruments). No dimensions are included to prevent the divulging of proprietary information.	94
Figure 22. Volume mesh results.....	97
Figure 23. Resulting (a) laminar vector flow field simulation and (b) turbulent vector field simulation.	99
Figure 24. Laminar CFD lognormal curve fitting of modeling results with all three slope calculations.....	106
Figure 25. Graphical comparison of CFD results, the ideal sampling effectiveness for FRM PM10 inlets, and the Subpart D wind tunnel testing results.	108
Figure 26. Preliminary flow field work for the SA246b taken from the (a) z-direction and (b) x-direction.	112

LIST OF TABLES

	Page
Table 1. Subpart D (Table D-2) particle size and testing requirements (CFR, 1987b).....	3
Table 2. Parameters of observed PSDs of aerosols emitted from common rural sources (Faulkner et al., 2007).	14
Table 3. Sampling effectiveness values presented in Tolocka et al. (2001)	19
Table 4. Summary of wind tunnel performance requirements for Subpart D FRM PM10 inlet testing (CFR, 1987b).	22
Table 5. Sampling effectiveness results for SA246 PM10 sampler at 8 km h ⁻¹	47
Table 6. Model parameters calculated based on uncorrected, empirical wind tunnel data collected.	48
Table 7. Expected mass concentration for PM10 samplers (40 CFR Part 53 Subpart D – Table D-3).....	51
Table 8. Percent difference between the Subpart D “ideal sampler” sampling effectiveness curve and the lognormal model for various rural PM sources (PSDs from Faulkner et al., 2007).....	54
Table 9. Sampling effectiveness results for the LVTSP.	80
Table 10. Lognormal distribution model parameters for the LVTSP at each wind speed.	82
Table 11. Performance piecewise models for the LVTSP at each wind speed.	82
Table 12. ANOVA comparisons of EPA data and the piecewise performance functions developed in this study.	86
Table 13. CFD simulation sampling effectiveness results.	104
Table 14. Interpolation results of critical diameters.....	105
Table 15. Sum of Square error results between simulation and lognormal model.	106
Table 16. Expected mass concentration for PM10 samplers (40 CFR Part 53 Subpart D - Table D-3).....	109

CHAPTER I

INTRODUCTION

The Federal Clean Air Act (CAA) was originally enacted in 1963 in an effort to begin the monitoring and regulation of pollutants that may endanger public health and welfare. The National Environmental Policy Act of 1970 established the Environmental Protection Agency (EPA), which is the agency responsible for developing and implementing air quality regulations under the authority of the CAA. The CAA amendments of 1970 established the National Ambient Air Quality Standards (NAAQS) for six criteria pollutants, including particulate matter (PM). PM₁₀, defined in the Code of Federal Regulations (CFR) (1987a) Title 40, Part 53 as the fraction of PM with aerodynamic equivalent diameters (AED) that can penetrate to and deposit within the thoracic region of the human respiratory system, is one of the two fractions of PM currently regulated by EPA (2011).

PM₁₀ is currently regulated under both a primary and secondary standard. The purpose of the primary standard is to protect public health, chiefly the more sensitive human populations: the elderly and children. The primary standard is a 24-hour average concentration of 150 micrograms per cubic meter ($\mu\text{g m}^{-3}$) that is not to be exceeded more than once per year on average over 3 years (EPA, 2006). The secondary standard is concerned with the protection of environment, infrastructure and other non-health related welfare from damage by large concentrations of PM₁₀. This standard is based on a

24-hour average concentration not to be exceeded and is currently equivalent to the primary standard, $150 \mu\text{g m}^{-3}$.

The CAA defines air quality and pollution control as the “primary responsibility of states and local governments” and requires states to implement monitoring and enforcement regulations to ensure compliance with the NAAQS (CAA, 2004). Ambient concentrations of PM₁₀ are measured using networks of Federal Reference Method (FRM) and Federal Equivalent Method (FEM) PM₁₀ samplers and inlets. FRM PM₁₀ inlets such as the SA246b (BGI Instruments; Waltham, MA) are widely deployed to measure PM₁₀ concentrations in monitoring networks, including areas dominated primarily by crustal emissions such as those associated with agricultural operations, mining, and wind-blown dust. The size of the PM contained in the air of any region can be characterized using a particle size distribution (PSD). PSDs can be generated using the fractional mass, volume or number of specifically sized particles contained in the aerosol. The majority of PSDs describing ambient aerosols can be represented by lognormal distributions characterized by the mass median diameter (MMD) and the geometric standard deviation (GSD) of the aerosol (Hinds, 1999).

The CFR Title 40, Part 53 (1987a) states that any inlet that is to be used in monitoring networks for PM₁₀ NAAQS compliance must be designated as either a FRM or FEM sampler. Inlets are classified as FRM inlets if they meet the requirements of the CFR (1987a) Title 40, Part 53, Subpart D. Title 40, Part 53, Subpart D of the CFR (1987b; hereafter “Subpart D”) states that FRM PM₁₀ inlets are designed to perform with a cut point (d₅₀) of 10 ± 0.5 microns. The d₅₀ of a sampler is the particle size at which 50% of

the particles of that size penetrate the inlet to the filter and the remaining 50% are removed from the air stream prior to the filter. Candidate inlets must also pass a series of rigorous tests, including what is referred to as Subpart D testing to achieve FRM designation. Subpart D outlines the procedures and requirements for testing candidate PM10 inlets with mono-dispersed liquid and solid particles. Per Subpart D, the penetration efficiency for 10 specific particle sizes across 3 wind speeds is determined with a minimum of 3 replicates per particle diameter to establish repeatability.

Table 1. Subpart D (Table D-2) particle size and testing requirements (CFR, 1987b).

Particle Size (μm)	Wind Speed (km h^{-1}) ^[a]		
	2	8	24
3 \pm 0.5	L	L	L
5 \pm 0.5	L	L	L
7 \pm 0.5	L	L	L
9 \pm 0.5	L	L	L
10 \pm 0.5	L	L	L
11 \pm 0.5	L	L	L
13 \pm 1.0	L	L	L
15 \pm 1.0	L	L	L
20 \pm 1.0	L	L	L
25 \pm 1.0	L	L/S	L/S

[a] L and S represent liquid and solid particle testing, respectively

Sampler penetration efficiencies for particles within the size ranges in table 1 are used to generate the performance curve of the inlet, and is often referred to as the “Fractional Efficiency Curve” (FEC) (figure 1).

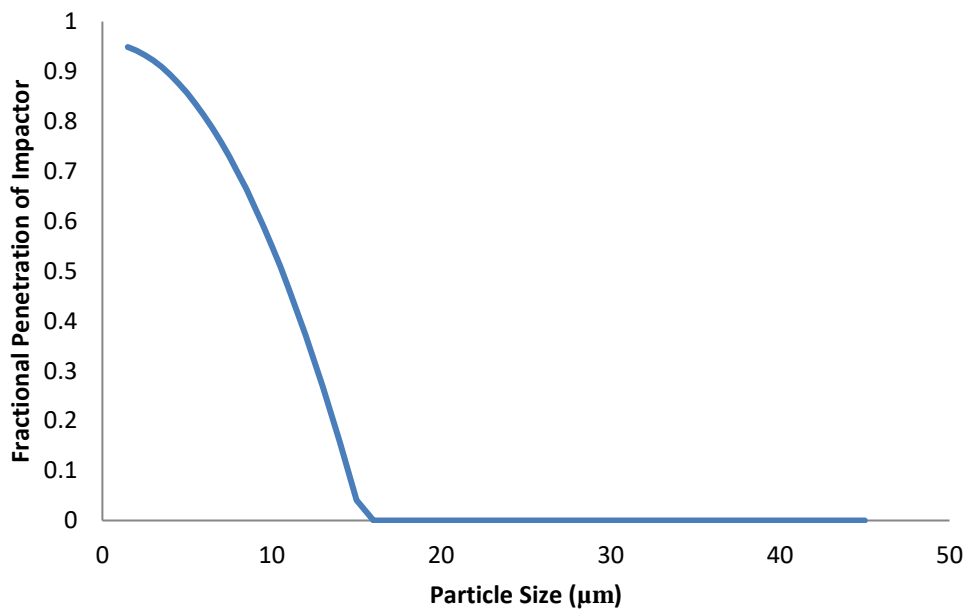


Figure 1. FEC based on desired penetration of particles in FRM PM10 inlets from Subpart D (CFR, 1987b).

The FEC shown in figure 1 was constructed using the desired penetration (CFR, 1987b) of specific particle sizes through an FRM PM10 sampling inlet by the EPA and published in Subpart D. This curve is not characterized by a lognormal distribution; however, Hinds (1999) has suggested that the performance curve desired by the EPA can be approximated using a cumulative lognormal distribution in which the distribution mean and standard deviation are the natural log of the inlet cut point and the natural log of the GSD, respectively.

Faulkner et al. (2007) reported that the MMD and GSD of PSDs found in rural regions is typically around 20 micrometers and 2.0, respectively. However, the performance of many PM inlets, including the SA246b, was originally designed with a

primary focus around the region of the cut point. Thus, inlet performance when challenged with the PM emitted in rural settings is less certain than inlet performance when challenged by the smaller particles characteristic of urban environments. According to EPA (1996), the PSD of the coarse mode of PM found in urban areas has a MMD and GSD of approximately 5.7 micrometers and 2.25, respectively. Because of the large difference between the MMDs of urban and rural PM, it is possible that the inlets designed primarily for urban sampling may not perform as expected when used in rural areas.

Many size-selective, low volume (LV) FRM PM samplers remove unwanted fractions of sampled PM through a process called inertial impaction. In this process, PM-laden air is drawn into an inlet at a constant flow rate and through the impaction section of the inlet. Here, the flow streams are sharply redirected upwards. Ideally, the larger, unwanted fraction of particles is unable to follow the redirected flow streams due to their inertial energy and separates out of the streams. The separated particles are then collected on an impaction plate or in a virtual impactor. The remaining PM passes through the impaction section and is deposited on a filter or transferred to a secondary separation device. A cross-sectional diagram of the SA246b PM10 inlet is shown below in figure 2.

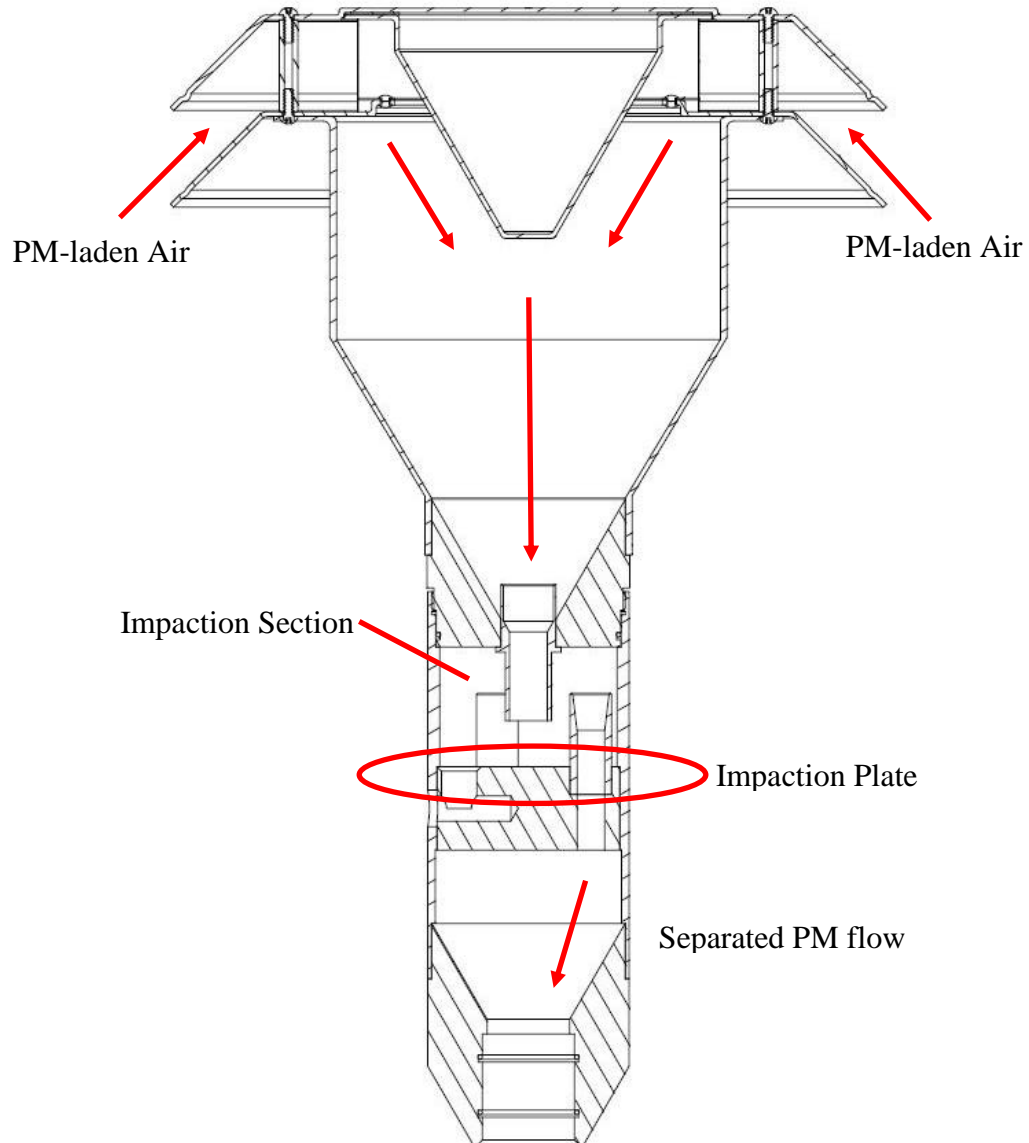


Figure 2. Annotated hatched view of the SA246b PM10 inlet.

Several studies have involved the measurement ambient particulate matter using collocated PM10 inlets, a SA246b inlet and a LV total suspended particulate (LVTSP) inlet developed by Texas A&M. The LVTSP inlet was used to collect a representative sample of particulate emissions from various rural and agricultural operations. These

samples were used to develop a particle size distribution which allowed researchers to estimate the mass of PM10 in the samples. One of the most prominent studies published by Buser et al.(2008), showed that the mass of PM10 collected by the LVTSP and the PM0 inlet differed by an amount between 145% and 287%. These studies concluded that the likely source of the mass discrepancy between the samples collected by the two inlets was the penetration of larger particles through the impactor section of the PM10 inlet.

The hypothesis that large particles may penetrate the impactor of some FRM PM10 inlets warranted further study after personal interactions and collaboration with Carlos Ortiz. Mr. Ortiz worked with Andy McFarland in the 1980s to develop a PM10 inlet and a process for demonstrating that the inlet sampled PM10 (McFarland and Ortiz, 1984). Much of their testing methodology was integrated into the Subpart D testing procedures. The inlet they originally designed was denoted as the SA246. Since then, the SA246 has evolved into the SA246b which sports a louvered inlet for rain protection and other changes that make the inlet easier to manufacture and assemble but does not adversely impact its performance. The inlet is one of the most widely deployed PM10 inlets in the EPA PM monitoring networks. The PM10 inlet performance curve their work generated is the same curve shown in figure 1 from Subpart D. According to Carlos, their original concern when developing a PM10 inlet was producing an inlet performance curve with a cutpoint of ten micrometers and a performance slope as sharp as possible. They were not so concerned with the performance of the inlet at larger particles sizes (Carlos Ortiz, TAMU-MEEN, personal communication, 2010).

Dr. John Haglund corroborated the focus of the PM10 sampler research and development conducted by Ortiz and Mr. McFarland (Dr. John Haglund, TAMU-MEEN, personal communication, 2010). Dr. Haglund further added that the analysis of inlet performance for the larger particles was sensitive to small changes in particle concentrations due to the way particles were constructed and that the analysis could be improved by setting different testing requirements (Dr. John Haglund, TAMU-MEEN, personal communication, 2010). Part of this research included the development and definition of these requirements for the purpose of increasing the accuracy of performance measurements for larger particles.

Objectives

The primary goal of this research was to evaluate the penetration of large particles through the internal inertial impactor of the SA246b PM10 inlet using Subpart D procedures in conjunction with new testing methods that should decrease uncertainty when compared with previous research.

Specifically, the objectives of this research were to:

1. Empirically evaluate the SA246 PM10 inlet performance in accordance with Subpart D procedures at 8 kilometers per hour with a primary focus on the penetration of larger particles, similar in size to those present in rural environments, through the inlet.

2. Using Subpart D testing methodology, evaluate the LVTSP inlet performance and develop a performance model for the inlet that can be used to correct the PSD measured by the LVTSP to the true PSD.

3. Perform computational fluid dynamics (CFD) modeling on the impactor section of the SA246b and compare the results to those collected during Subpart D wind tunnel testing in order to evaluate the validity of using CFD modeling as a supplement to the design and development of inlets in the future.

The specific methodologies and their results as they pertain to completing the listed objectives are contained in subsequent chapters.

CHAPTER II

SUBPART D WIND TUNNEL EVALUATION OF FRM PM10 SAMPLER¹

Introduction

The Federal Clean Air Act (CAA) was originally enacted in 1963 in an effort to begin monitoring and regulating air pollutants that may endanger public health and welfare. The National Environmental Policy Act of 1970 established the Environmental Protection Agency (EPA), which is now responsible for developing and implementing air quality regulations under the authority of the CAA. The CAA amendments of 1970 required EPA to establish National Ambient Air Quality Standards (NAAQS) for six criteria pollutants, including particulate matter (PM). PM₁₀, defined as the fraction of “PM with an aerodynamic diameter (AED) less than or equal to a nominal 10 micrometers,” is one of the two fractions of PM currently regulated by EPA because it can penetrate to and deposit within the thoracic region of the human respiratory system (EPA, 2011).

For regulatory purposes, ambient concentrations of PM₁₀ are measured using Federal Reference Method (FRM) and Federal Equivalent Method (FEM) PM₁₀ samplers. Inlets for FRM PM₁₀ samplers, such as the PQ/PM₁₀ dichotomous louvered PM₁₀ inlet

¹ Reprinted with permission from “Large Particle Penetration During PM₁₀ Sampling” by William B. Faulkner, Raleigh Smith & John Haglund, 2014. *Aerosol Science and Technology*, 48:6, 676-687, Copyright 2014 by Aerosol Science and Technology.

(PQ/PM10; BGI Instruments; Waltham, MA), are widely deployed to measure PM10 and PM2.5 concentrations.

The size distribution of the PM in any given region can be characterized by a particle size distribution (PSD), which may describe the distribution of particle mass, volume, or number of specifically sized particles contained in the aerosol. Ambient aerosols are often characterized by PSDs with one or more modes. Each mode can be characterized by a lognormal distribution described by a mass median diameter (MMD) and geometric standard deviation (GSD) (Hinds, 1999). The MMD describes the particle diameter at 50% of the total mass. The GSD is related to the ratio between the MMD and the particle diameters at specific mass fractions (equation 1).

$$\text{GSD} = \frac{d_{84.1}}{\text{MMD}} = \frac{\text{MMD}}{d_{15.9}} = \sqrt{\frac{d_{84.1}}{d_{15.9}}} \quad (1)$$

where:

$d_{84.1}$ = the particle diameter at 84.1% of the total mass; and

$d_{15.9}$ = the particle diameter at 15.9% of the total mass.

The Code of Federal Regulations (CFR) Title 40, Part 53 (1987a) states that any inlet that is to be used in monitoring networks for PM10 NAAQS compliance must be designated as either a FRM or FEM sampler inlet. Inlets are classified as FRM inlets if they meet the requirements of 40 CFR Part 53. Subpart D of 40 CFR Part 53 (hereafter “Subpart D”) states that FRM PM10 inlets are designed to perform with a cut point (d50) of 10 ± 0.5 micrometers (μm). The d50 of a sampler is the particle size at which 50% of the particles of that size penetrate the inlet to the filter and the remaining 50% are removed from the sampled air upstream of the filter. Candidate inlets must also pass a series of

rigorous tests to achieve FRM designation. Subpart D outlines the procedures and requirements for testing candidate PM10 inlets with mono-dispersed liquid and solid particles in the controlled confines of a wind tunnel. Per Subpart D, the sampling effectiveness for ten specific particle sizes across three wind speeds is determined with a minimum of three replicates per particle diameter to establish repeatability (table 1).

Sampling effectiveness values for particles of various sizes are used to generate a performance curve for the sampler. This curve is considered the performance curve of the inlet and is often referred to as the Fractional Efficiency Curve (FEC). The FEC shown in figure 1 was constructed using the “ideal” sampler penetrations of specific particle sizes shown in Table D-3 (CFR, 1987b) of Subpart D.

The curve shown in figure 1 is not characterized by a lognormal distribution, however Hinds (1999) has suggested that the performance curve desired by the EPA can be approximated using a cumulative lognormal distribution in which the distribution mean and standard deviation are the natural log of the inlet cut point and the natural log of the performance slope, respectively. The parameters used to approximate the “ideal” sampling effectiveness curve shown in figure 1 are a cut point and slope of 10.5 micrometers and 1.6, respectively (Buser et al, 2008).

The performance of the PQ/PM10 inlet (henceforth, PM10 inlet) has been characterized by several studies following Subpart D standards (McFarland and Ortiz, 1984; VanOsdell and Chen 1990; and Tolocka et al., 2001). There are, however, two main issues concerning previous studies:

1. The focus of the work was to produce the sharpest performance curve around the desired cutoff of 10 micrometers (Carlos Ortiz, TAMU-MEEN, personal communication, 2010); and,
2. Analysis methodologies previously employed were often designed to detect changes in sampling efficiency near the cut point and may not have had the sensitivity to accurately determine the small sampling efficiencies expected when testing large particles

The phrase “large particles” in this study refers to particles with an AED of 16 micrometers and greater. The diameter of 16 micrometers was selected for the minimum diameter of large particles because Table D-3 in Subpart D contends that particles of 16 micrometers in diameter and larger do not penetrate an “ideal” PM10 inlet.

According to EPA (1996), the average PSD of the coarse mode of PM found in urban areas has a MMD and GSD of approximately 5.7 micrometers and 2.25, respectively. Faulkner et al. (2007) reported the PSDs of PM emitted from several common rural sources (table 2), all of which are characterized by significantly larger MMDs than urban aerosols.

Table 2. Parameters of observed PSDs of aerosols emitted from common rural sources (Faulkner et al., 2007).

Rural PM Source	MMD (μm)	GSD	% Particles w/ diameter $>16 \mu\text{m}$
Feed yard	20	2.2	42
Broiler	24	1.6	40
Dairy	15	2.1	33
Cotton Gin	23	1.8	42

Buser et al. (2008) performed an analysis on data collected during field testing of the PM10 inlet with collocated low volume total suspended particulate (LVTSP) samplers at a cotton gin. During the study the following were calculated:

- Estimation of the performance characteristics for the PM10 inlet.
- The maximum possible concentrations of PM10 that could be collected assuming the “ideal” sampling effectiveness curve for the PM10 inlet and the PSD of the inlet.

The results of the concentrations measured by the PM10 inlet placed in the field, the theoretical concentrations of PM10, and the “true” concentrations of PM10 are shown in figure 3. Theoretical PM10 concentrations were estimated by integrating the multiplication of the particle size distribution for the particulates emitting from the cotton gin and the lognormal PM10 sampler performance curve characterized by a cutpoint of 10.5 micrometers and a slope of 1.6. The “true” PM10 concentration was calculated by analyzing the particle size distribution of the PM collected by the LVTSP inlet, believing

the LVTSP to collect representative aerosol samples, and summing the concentration of all particles with a diameter of ten micrometers or less.

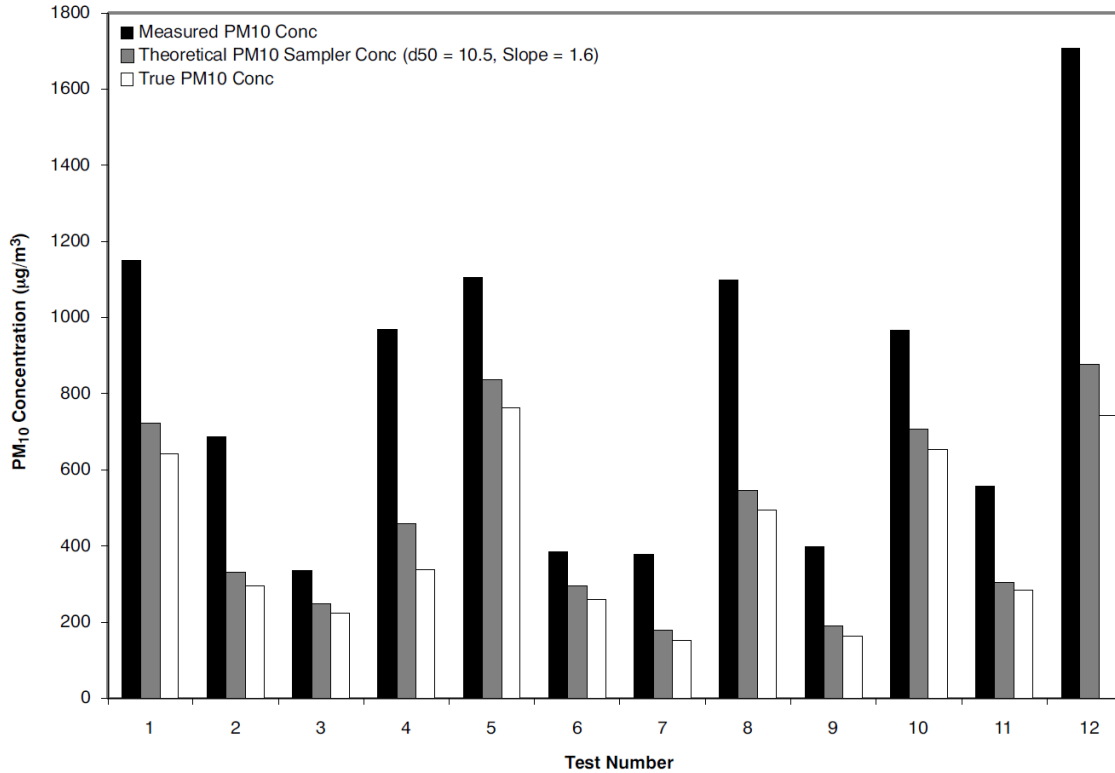


Figure 3. Concentrations of PM10 emitting from a cotton gin measured by and estimated for (operating with a cut point and slope of 10.5 micrometers and 1.6, respectively) the PM10 inlet, compared with the “true” concentration of PM10 present in each test PSD (Buser et al., 2008).

When comparing the PM10 concentrations measured by the inlets in the field with the theoretical PM10 concentration in figure 3, the concentrations collected by the deployed PM10 inlets were significantly larger than those predicted by the theoretical analysis of the PM10 inlet operating with ideal performance characteristics. Based on the federal definition of PM10, the “true” PM10 concentration was not applicable.

Buser et al. (2008) hypothesized that the PM10 inlet does not operate as specified by the EPA when challenged with PSDs typical of operations in rural areas; that the performance of the inlet is most likely impacted by the greater concentration of large diameter particles characteristic of rural PM compared to urban environments. Because of the large difference between the MMDs of urban and rural PM, it is possible that the inlets designed primarily for urban sampling may exhibit biases when challenged with large particles emitted in rural settings. The reliability of the inlets to produce accurate measurements of PM10 is, therefore, questionable when challenged by the large particles characteristic of rural environments.

Many size-selective PM samplers remove unwanted fractions of sampled PM through inertial impaction. In this process, PM-laden air is drawn into an inlet at a constant flow rate (figure 4, point 1) and through the impactor of the inlet (figure 4, point 2). The flow streams are sharply redirected to inertially separate the larger particles from the flow streams. The Stokes Number is the principle governor of impactor collection efficiency and is calculated as the ratio of particle stopping distance at the average impactor nozzle exit velocity to the diameter of the impactor jet (Hinds, 1999). The Stokes number for an impactor is calculated using equation 2.

$$Stk = \frac{\tau U}{D_j/2} = \frac{\rho_p d_p^2 U C_c}{9\eta D_j} \quad (2)$$

where:

τ = particle relaxation time (s),

U = average impactor nozzle exit velocity (m s^{-1}),

D_j = inlet jet diameter (m),

ρ_p = particle density (kg m^{-3}),

d_p = particle diameter (m),

C_c = Cunningham's correction factor (1.015), and

η = gas viscosity (N s).

Ideally, the particles with larger Stokes numbers are unable to follow the redirected flow streams due to their inertial energy and separate out of the streams. The separated particles are collected on an impaction plate. The remaining PM passes through the impaction section and is deposited on a filter or transferred to a secondary separation device (figure 4, point 3).

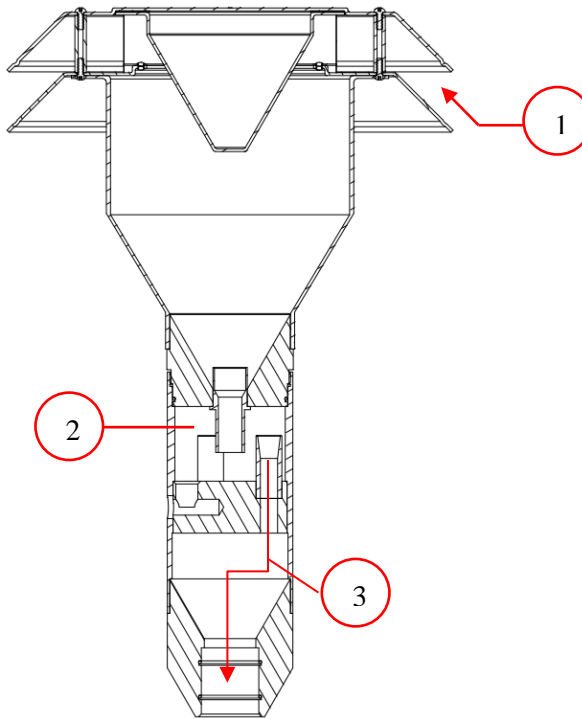


Figure 4. Hatched view of the PM10 inlet (BGI Instruments, 1997).

It is hypothesized that the combination of the particle physics involved with inertial separation and impaction of particles combined with the drastically greater concentrations of larger particles in rural environments result in the sampling error examined by Buser et al. (2008). Examples of particle physics include particle bounce and the reduced velocity of particles in the boundaries of laminar flow.

Several evaluations of the performance of PM10 inlets have provided evidence of non-zero penetration of large particles through the PM10 inlet to the filter. Tolocka et al. (2001) conducted Subpart D performance testing of both the louvered PM10 inlet and its predecessor, the flat top PM10 inlet, to ensure equivalent performance for the modified inlet. The results from their study contained non-zero penetration of both liquid and solid

particles for particles of diameters greater than or equal to sixteen micrometers, at wind speeds of eight and twenty-four km h⁻¹ (table 3).

Table 3. Sampling effectiveness values presented in Tolocka et al. (2001)

	Sampling Effectiveness					
	20 μm Particles			25 μm Particles		
	2 km h ⁻¹	8 km h ⁻¹	24 km h ⁻¹	2 km h ⁻¹	8 km h ⁻¹	24 km h ⁻¹
MacFarland and Ortiz (1984) ^[a]	0.1%	1.0%	0.9%	--	--	--
VanOsdell and Chen (1990) ^[a]	--	--	--	2.3%	0.3%	3.1%
VanOsdell (1991)	--	--	--	1.2%	--	4.6%
Tolocka et al. (2001)	--	--	--	0.1%	0.2%	0.0%

[a] Multiplet corrected values; all other averages reported are not multiplet corrected

The inlet tested by Tolocka et al. (2001) met the wind tunnel performance requirements of Subpart D; however, the study results demonstrated that nonzero penetration of particles exists with this PM10 inlet and still meet the requirements for FRM designation. For rural aerosols, where a significant portion of the total aerosol mass is comprised of particles larger than 16 micrometers, even relatively small penetration values may lead to non-trivial changes in measured PM10 concentrations.

Based on the studies by Tolocka et al. (2001) and Buser et al. (2008), the combination of nonzero penetration of particles with diameters larger than 16 micrometers (Tolocka et al., 2001) and the discrepancies between the theoretical and actual sampling concentrations for this PM10 inlet (Buser et al., 2008), the capability of FRM PM10 inlets to reliably generate inertial separation of large, unwanted particles from any ambient aerosol and prevent those particles from depositing on sample filters is uncertain.

McFarland and Ortiz (1984) performed the initial evaluation of the SA246b PM10 inlet. The process utilized in their study was integral in the development of the testing requirements published in Subpart D.

The objective of this research was to study the performance of the PQ/PM10 inlet with particular emphasis on the penetration of large particles characteristic of agricultural aerosols. This study performed a full performance analysis of the inlet for the wind speed of 8 km h⁻¹ to better characterize and study the penetration of large particles through the inlet.

Methodology

Subpart D Wind Tunnel

Wind tunnels to be used for the evaluation of PM10 inlets are required to meet specific criteria outlined in 40 CFR Part 53, Subpart D. A 0.61 m x 0.61 m (2 ft x 2 ft) wind tunnel located in Scoates Hall at Texas A&M University (henceforth referred to as “Scoates wind tunnel”) was originally fabricated in the early 1980s for the development and evaluation of PM10 inlets (McFarland and Ortiz, 1982, 1984). The 0.61 x 0.61-m (2 x 2-foot) wind tunnel was comprised of 3 sections, each 1.22 meters (4 feet) in length, a HEPA filter doubling as a laminar flow device, a flow straightener, a Stermann disk, and a flared inlet (figure 5).

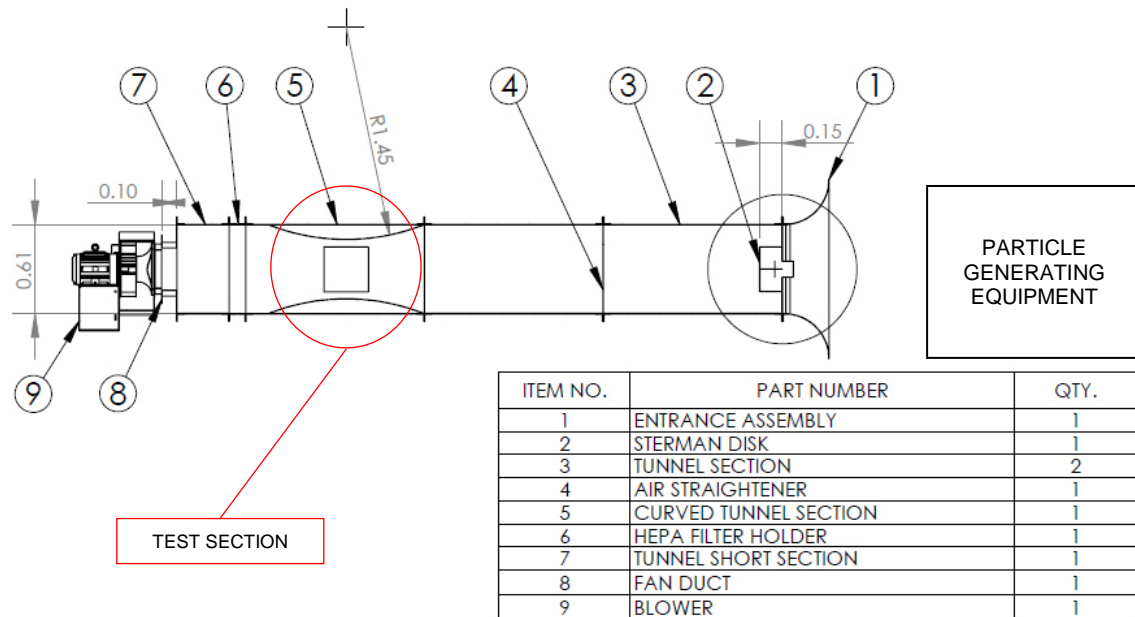


Figure 5. Schematic of the Scoates Wind Tunnel used for testing.

Air was drawn into the wind tunnel by a centrifugal blower [9] (18ACF; New York Blower; Willowbrook, Ill.) that was controlled with a variable frequency motor controller (VS1PF27-1; Baldor Drives; Fort Smith, AR). The air was pulled into the wind tunnel through the entrance assembly [1] and across the sterman disk [2]. The sterman disk was used to disperse the flow and the test aerosols so as to produce a more uniform cross sectional profile of particle concentration and flow. The air then flows down the tunnel [3] and through the air straightener [4]. The purpose of the air straightener was to correct any twisting or rotation of the flow prior to passing through the test section [5]. The test section has several access ports for the insertion of inlets and sampling probes in various configurations as well as windows for observation. A HEPA filter [6] was used to both help straighten air flow and prevent aerosols from entering the fan duct [8] and blower [9].

A wind tunnel must conform to the requirements summarized in table 4 in order to be used for inlet testing according to Subpart standards.

Table 4. Summary of wind tunnel performance requirements for Subpart D FRM PM10 inlet testing (CFR, 1987b).

Parameter	Subpart D Section	Category	Requirement
Air Velocity	53.42(e)	Uniformity	$\pm 10\%$ of nominal wind speeds of 2, 8 and 24 km h ⁻¹
		Measurement	Measured at a minimum of 12 points with technique capable of precision of $\leq 5\%$ Determine the longitudinal turbulence intensity at each sampling point
Particle Concentration	53.42(d)	Uniformity	Concentration in zones must differ $\leq 10\%$
		Measurement	5 equally spaced isokinetic samplers in the sampling plane
Blockage	53.42(a)	Measurement	Maximum of 15% blockage of sampling zone cross sectional area

A hot wire anemometer (VelociCalc 8386, TSI, Inc., Shoreview, MN) with an accuracy of $\pm 3.0\%$ of reading was used to measure air velocity in the wind tunnel across 11 points spaced in 50.8 mm (2 inch) intervals at three heights in the sampling plane for a total of 33 points of measurement. Curved 101.6 millimeter (4 inch) high panels were installed on the roof and the base of the test section of the wind tunnel to make it easier to achieve 8 km h⁻¹. Velocity measurements were conducted at 76.2, 203.2, and 330.2 mm (3, 8, and 13 inches) above the raised base of the wind tunnel (figure 6). The anemometer was programmed to sample at a rate of 1 Hz for a total of 15 seconds. After 15 seconds

of sampling, the measurements were averaged and recorded. This was repeated at least 12 times per measurement point for a total of 396 wind speed measurements across the test section of the wind tunnel.

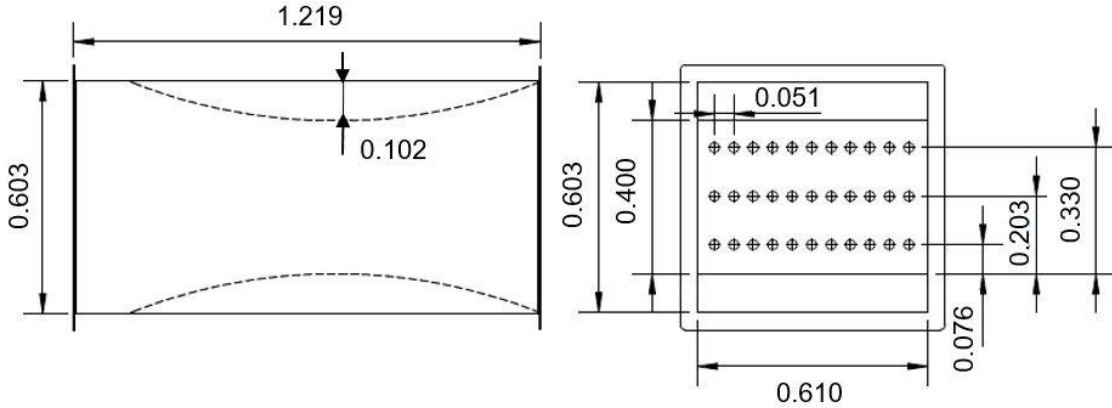


Figure 6. Velocity measurement sampling grid used in the Scoates wind tunnel for tunnel speeds of 8 km h⁻¹; displayed dimensions are in meters.

The longitudinal turbulence intensity describes the degree of turbulence in the direction of the air flow. The turbulence intensity value, I , was calculated as the percentage of turbulent flow using equation 3,

$$I = \frac{u'}{U} \quad (3)$$

where:

u' = standard deviation of the flow measurements at each point, and

U = average wind speed measured at each point.

For a nominal wind speed of 8 km h⁻¹, an average wind speed of 8.05 km h⁻¹ was measured with a COV and maximum standard deviation of 1.32% and 7.83, respectively.

The calculated maximum turbulence intensity was 1.79%. Therefore, all criteria for wind speed required by 40 CFR 53.42(e) were satisfied in the Scoates wind tunnel.

Two reference sampler configurations were used in the Scoates wind tunnel. The first configuration consisted of the PM10 inlet and two isokinetic samplers collocated on either side of the inlet (aka. the dual isokinetic reference procedure). The isokinetic inlets sampled concurrently with the PM10 inlet to establish spatial uniformity. Flow was supplied to both the isokinetic samplers and the PM10 inlet by a 0.56 kW (0.75 hp) pump (5KC49NN0194AX; GE Motor & Industrial Systems; Benton Harbor, MI) and flow to each sampler was controlled using rotometers (RMB-53-SSV; Dwyer Instruments, Inc.; Michigan City, IN). The pressure drop across each sampler was measured (2050; Dwyer Instruments, Inc.; Michigan City, IN) and recorded. The isokinetic nozzles in this configuration were designed so that the volumetric flow rate applied to the nozzles divided by the cross-sectional area of the inlet to the nozzle was equivalent to the wind speed of the wind tunnel. A 12.70 mm inlet diameter isokinetic nozzle with a volumetric flow rate of 17.5 L min⁻¹ was used for the 8-km h⁻¹ tests.

The collocated isokinetic and sampling inlet setup was removed from use in the Scoates wind tunnel partway through testing at the suggestion of a senior EPA aerosol scientist. New isokinetic nozzles were manufactured and used in a second configuration denoted as “hot swapping.” This configuration was used to reduce uncertainty in the inlet tests resulting from lack of spatial uniformity of particle concentration across the sampling plane. The appropriate isokinetic inlet was placed in the wind tunnel and then swapped with the candidate sampler inlet during testing so that the inlets of the isokinetic sampler

and the sampler under evaluation were located in the same point in the sampling plane (figure 7). The hot swapping procedure is outlined in Subpart D, specifically, 40 CFR 53.43(a)(2)(x). Temporal uniformity tests indicated that coefficients of variation were less than 10%. The temporal uniformity was checked for each particle size evaluated at 8 km h^{-1} . Data collected with the collocated process that met various requirements, was retained as valid and not retested using the hot swap procedure.

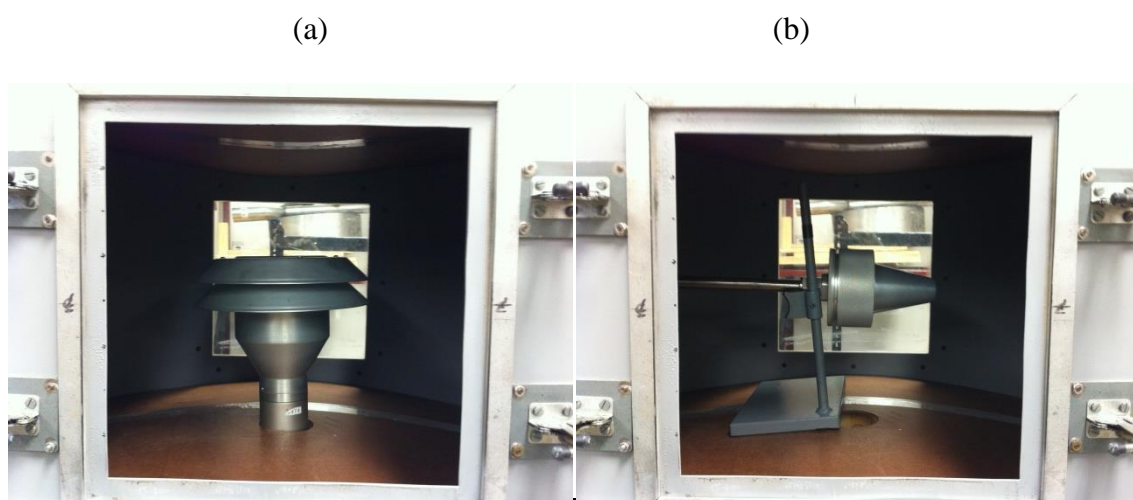


Figure 7. The (a) PM10 and (b) isokinetic inlet in the same sampling planes.

The isokinetic nozzles used with the hot swapping procedure were designed so that the volumetric flow rate applied to the inlet divided by the cross-sectional area of the inlet to the nozzle was equivalent to the wind speed of the wind tunnel. The isokinetic nozzle used in the Scoates wind tunnel was designed with a 33.02 mm (1.3 inches) diameter inlet to operate at a flow of 114 L min^{-1} to achieve an equivalent sampling velocity of 8 km h^{-1} .

Isokinetic air flow was provided by a 0.56 kW (0.75 hp) pump (5KC49NN0194AX, GE Motor & Industrial Systems, Benton Harbor, MI) and the flow

controlled with a ball valve. The actual flow rate supplied to the sampler was monitored by a HI-Q flow meter (D-AFC-09, HI-Q, San Diego, CA). The target set point for the pump was calculated using equation 4,

$$Q_s = 44.1375 * \frac{P_a}{T} \quad (4)$$

where:

P_a = ambient pressure (mm Hg),

T = ambient temperature (K), and

44.1375 = constant (sL K min⁻¹ mm Hg⁻¹) = 114 aL min⁻¹ * 293 K / 760 mm Hg.

The pump was allowed to warm up at the beginning of each day of testing. The pump was then set to the appropriate flow rate at the beginning of each isokinetic test using the flow meter. At the end of an isokinetic test, the flow rate was again verified. Observed flow rates did not vary from the original set point established prior to each isokinetic test by more than 10%. Typical observed variation was approximately 7%, or 8 L min⁻¹.

Per 40 CFR 53.42(a), inlets placed in a Subpart D wind tunnel cannot block more than 15% of the cross-sectional area. The largest inlet placed in the Scoates wind tunnel was the SA246b PM10 inlet (SSI2.5; BGI Instruments; Waltham, MA). The blunt surface area of the inlet in the wind tunnel blocks approximately 13% of the sampling plane with the 101.6 mm (4 inch) panels installed.

Inlet Flow Systems

The SA246 PM10 sampler was designed for a flow rate of 1 cubic meter per hour (16.7 L min^{-1}) of air to be drawn through the inlet. To provide the air flow, a PQ200 (BGI Instruments; Waltham, MA), FRM flow control unit was used. The PQ200 measures the ambient air temperature and pressure in order to adjust sampler air flow to deliver a constant 16.7 L min^{-1} of flow rate. The flow rate calibration and system integrity of the PQ200 was checked and verified every day per manufacturer specifications prior to running any tests with a candidate inlet. The flow rate was verified and calibrated using a tetraCal system (tetraCal; BGI Instruments; Waltham, MA). System integrity was determined by running the leak check procedure on the PQ200 per manufacturer instructions.

Liquid and Solid Aerosols

Specially constructed solutions were used in conjunction with a vibrating orifice aerosol generator (VOAG; Model 3450; TSI, Inc.; Shoreview, MN) to produce either liquid or solid, mono-dispersed particles of various sizes. Solutions were constructed to produce a desired particle size based on equations 5-7 adapted from the VOAG user manual and the original VOAG development work by Berglund and Liu (1973). Most solutions were constructed for use with a flow rate and VOAG vibration frequency of $0.225 \text{ mL min}^{-1}$ and 57,000 Hz, respectively. Particles with diameters of 3 micrometers and smaller were designed for a flow rate and VOAG vibration frequency of $0.093 \text{ mL min}^{-1}$ and 150,000 Hz, respectively. Orifice vibrating frequency was optimized

for different orifice diameters and adjusted during particle generation to minimize the formation of “satellite” droplets.

$$D_{p_p} = \left(\frac{6 * Q * C}{\pi * f} \right)^{1/3} \quad (5)$$

where:

D_{p_p} = physical particle diameter (μm),

Q = solution flow rate (mL min^{-1}) = $0.225 \text{ mL min}^{-1}$,

C = volumetric concentration of aerosol material in the solution, and

f = VOAG frequency (Hz) = approximately 57,000 Hz.

$$C = \frac{m_i}{\rho_i * V_c} \quad (6)$$

where:

m_i = mass of fluorometric material used (g),

ρ_i = density of fluorometric material (g mL^{-1}), and

V_c = volume of the solution container (mL).

$$D_{p_a} = D_{p_p} * \sqrt{\rho_{p,i}} \quad (7)$$

where:

D_{p_a} = the aerodynamic particle diameter (μm), and

$\rho_{p,i}$ = particle density (g cm^{-3}).

Subpart D testing requires the evaluation of the inlet performance with specific particle sizes (table 1). Liquid particle solutions were made to achieve the desired particle size by combining specific amounts of oleic acid and uranine (CAS 518-47-8). Uranine was used to provide fluorescent signal. The ratio of uranine to oleic acid in the particle

was 1:10 or 0.10 g uranine per mL of oleic acid. Ethanol made up the remaining volume of the solution. Equations 8-10 are specific to generating liquid particles and were combined with equations 5-7 to determine the expected aerodynamic particle size.

$$m_u = \rho_u * (V_o * C - V_o) \quad (8)$$

where:

m_u = mass of uranine in the solution (g),

ρ_u = density of uranine (g mL^{-1}) = 1.53 g mL^{-1} , and

V_o = volume of oleic acid in solution (mL) = $m_o * \rho_o$.

$$m_o = \frac{\rho_o * V_c * C}{1 + R/\rho_u} \quad (9)$$

where:

m_o = mass of oleic acid (g),

ρ_o = density of oleic acid (g mL^{-1}) = 0.8935 g mL^{-1} , and

R = mass of uranine (g) per volume of oleic acid (mL) = 0.10 g mL^{-1} .

$$\rho_{p,l} = \frac{R * V_o + m_o}{V_u + V_o} \quad (10)$$

where:

$\rho_{p,l}$ = density of liquid particle (g mL^{-1}), and

V_u = volume of uranine in the solution (mL) = $m_u * \rho_u$.

For solid particles, fluorescein (CAS 2321-07-05) was combined with ammonium hydroxide to form ammonium fluorescein. Three times the stoichiometrically-required amount of ammonium hydroxide was used to ensure that all of the fluorescein was reacted. Once aerosolized, the remaining ammonium hydroxide was volatilized. The ammonium-fluorescein/ammonium hydroxide mixture was diluted with an appropriate volume of

deionized (DI) water to produce the final solution. This solution forms solid, spherical beads after being aerosolized. The amount of fluorescein and ammonium hydroxide required for the solution was determined using equations 11-13 and then combined with equations 5-7 to calculate the aerosol particle size.

$$m_f = \rho_f * C * V_c \quad (11)$$

where:

m_f = mass of fluorescein (g), and

ρ_f = density of fluorescein (g mL⁻¹).

$$\rho_f = \rho_{af} * \left(\frac{MW_f}{MW_f + MW_{NH_4} - MW_H} \right) \quad (12)$$

where:

ρ_{af} = density of ammonium fluorescein (g mL⁻¹) = 1.35 g mL⁻¹,

MW_f = molecular weight of fluorescein (g gmol⁻¹) = 332.32 g gmol⁻¹,

MW_{NH_4} = molecular weight of ammonia (g gmol⁻¹) = 18.04 g gmol⁻¹, and

MW_H = molecular weight of hydrogen (g gmol⁻¹) = 1.0 g gmol⁻¹.

$$V_{NH_4OH} = \left(\frac{m_f}{MW_f} \right) * C_{NH_4OH} * F \quad (13)$$

where:

V_{NH_4OH} = volume of NH₄OH to add to the solution (mL),

C_{NH_4OH} = concentration of NH₄OH in anhydrous ammonia solution (mL gmol⁻¹)

= 68.97 mL gmol⁻¹, and

F = ammonia molar concentration factor (unit less) = 3.0.

Particle sizes and distribution were verified post generation. An Aerodynamic Particle Sizer (APS; Model 3321; TSI; Shoreview, MN) was used to check the uniformity of particle sizes produced. If the particle stream was not mono-dispersed, the VOAG frequency was adjusted and the stream retested with the APS until the APS indicated a nominally mono-disperse PSD. However, due to the stretching of particles as they are accelerated through the APS, the APS was not used to determine the size of the generated particles, only if the aerosol was mono-dispersed.

Once the generated particles were deemed to be nominally mono-dispersed, particles were impacted onto slides in order to manually measure their diameters. The slides were coated with either Dow Corning high vacuum grease for solid particles or an oleophobic solution, Nyebar (Type Q), for liquid particles. The slides were then placed under a microscope with 400X magnification. A line slider was used to measure the impacted particle diameters by the number of tick marks counted from one side of the particle to the other. The line slider was calibrated using a stage slide etched with lines spaced at 10 micrometers. The number of ticks per 10 micrometers was determined to be 42. Doublets and triplets, known as multiplets, were accounted for post particle sizing. The procedures used in the study for slide coating, particle impaction, and particle measurement were described in detail by Faulkner and Haglund (2012).

Multiplets were accounted for by applying the multiplet correction described by Haglund et al. (2002). This process also corrects liquid particle “stretching” that affects liquid particle measured by the APS. As the liquid particles are accelerated through the APS, the spherical particles stretch into an oblong shape and are then measured by the

laser in the APS. For each nominal particle size shown in table 1, measurements of particle sizes collected with the APS were used to quantify the relative mass concentrations of satellites and multiplets. (Due to the APS's maximum particle detection size of 20 micrometers, a single effectiveness value was used for the 25-micrometer data point based on microscopy measurements). A particle size correction factor, f_d , was generated for each nominal particle size shown in table 1 to correct APS-measured particle diameters and distributions using equation 14. The particle size correction factor was applied during model development to correct the models for multiplets present in the data the models are fit to. This process is explained in a later section.

$$f_d = \frac{D_{pa}}{D_{APS,VMD}} \quad (14)$$

where :

f_d = particle size correction factor, and

$D_{APS,VMD}$ = volume mean diameter reported by the APS.

Previous studies and Subpart D accounted for multiplets by physically counting particles with diameters that fall outside the acceptable diameter range from the impacted particles on the glass slide. The percentage of particles with acceptable diameters was then determined and used to correct sampler performance results. This method is required by Subpart D. However, the APS correction method was both quicker and more accurate as much less human judgment was involved in the counting process, the effects of smaller satellite droplets can also be considered, and the sample size was much larger yielding more representative values.

It was uncommon for large numbers of multiplets to be present when observing particles under the microscope because the APS was used to verify the monodisperse nature of PSDs prior to slide impaction and testing. If large numbers of multiplets were observed, the aerosol was regenerated and impacted again prior to running a test.

The observed diameter of liquid droplets measured on the microscope, D_a , was not representative of the actual diameter of the aerosol particles. When liquid particles are impacted on slides, they flatten to form a plano-convex shape. This final shape was a product of droplet surface tension and interactions of the droplet with the oleophobic coating on the slide. Faulkner and Haglund (2012) determined the appropriate flattening coefficient factors for 10% uranine-oleic acid droplets impacted on slides treated with Nyebar Type Q to be 1.358. This flattening coefficient was used in equation 15 to determine the physical aerosol particle diameter. The particle diameter was then converted to the aerodynamic particle size using equation 7.

$$D_{p_p} = \frac{D_a}{F_Q} \quad (15)$$

where:

D_a = measured impacted droplet diameter (μm), and

F_Q = flattening coefficient for Nyebar Type Q.

Experimental Design

The performance of the PM10 Inlet was evaluated using the Subpart D Scoates wind tunnel at a wind speed of 8 km h^{-1} . Isokinetic samplers were used in the same sampling plane in the in the test section of the wind tunnel as the PM10 inlet. As stated

previously, two different processes were used in the Scoates wind tunnel for the collection of the representative wind tunnel concentration sample; the collocated and hot swapping procedures.

In the collocation procedure, two identical isokinetic samplers were installed on either side of the PM₁₀ inlet in the wind tunnel for concurrent sampling. Forty-seven-millimeter diameter PTFE filters were cut from full PTFE sheets (PSPJ001; Pall Corporation; Port Washington, NY) and used to collect the sampled particles for all three samplers. The filters used in the isokinetic samplers were placed directly in the sampler and secured in place by tightly screwing the isokinetic nozzle to the sampler base. The filters used for the PM₁₀ inlet were placed into filter cartridges and filter holders manufactured by Texas A&M University.

For the hot swapping procedure, the PM₁₀ inlet and the isokinetic samplers were placed in the wind tunnel one after the other in an alternating fashion beginning with the isokinetic nozzle and were not collocated. Filters were used to capture the particles sampled by isokinetic and PM₁₀ inlets. Forty-seven-millimeter diameter, PTFE, ring supported filters (P5PQ047; Pall Corporation; Port Washington, NY) and 90 mm glass fiber filters (61664; Pall Corporation; Port Washington, NY) were used to collect the particles sampled by the PM₁₀ inlet and isokinetic samplers, respectively. The 47 mm filters were placed in a filter cartridge (F21; BGI Instruments; Waltham, MA) and installed in the filter holder (F20; BGI Instruments; Waltham, MA) that attaches to the base of the PM₁₀ inlet. The 90mm filters were placed directly into the isokinetic sampler and are held in place by the nozzle and knurled sleeve (figure 8).

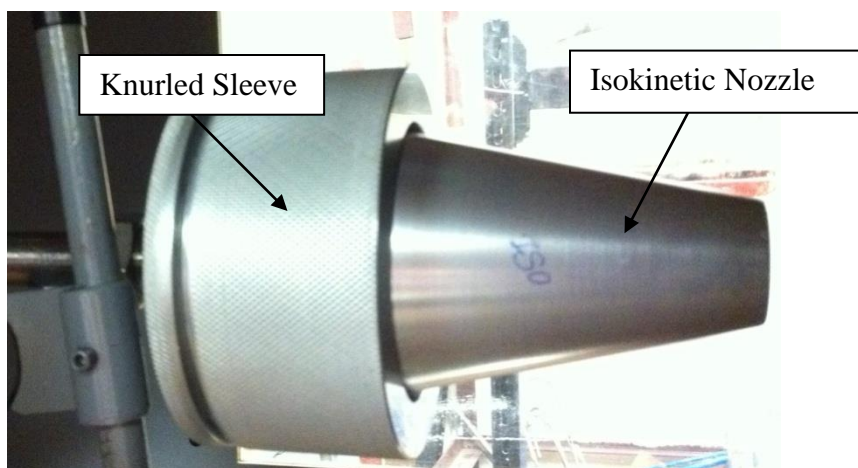


Figure 8. Labeled photo of the 8 km h⁻¹ isokinetic nozzle.

Inlet performance evaluation was performed using a minimum of three pairs of isokinetic and PM10 inlet tests. An isokinetic sample was collected first, followed by evaluation of the PM10 inlet. Test durations were developed based on experience and the need to meet the required signal to noise ratio of the measured fluorescence with a fluorometer (FM109515; Barnstead International; Dubuque, IA). See Appendix D for the procedures used to evaluate the PM10 inlet.

Fluorometric Analysis

After each round of inlet testing, the filters were removed and placed into a measured mass of 0.01 N sodium hydroxide (for liquid particles) or 0.01 N ammonium hydroxide (for solid particles) to elute the fluorometric material from the filters. Filters soaked overnight and were then analyzed with the fluorometer. See Appendix D for procedures used to operate the fluorometer and analyze the filters.

For the fluorometric analysis, a small volume (approximately 2 mL) of the solution from each of the jars with soaking filters was transferred to individual disposable test tubes using a different disposable pipette for each solution in order to avoid contamination. A separate test tube was filled with approximately 2 mL of unused extraction solution for background measurements. The fluorometer was then used to measure the raw fluorometric intensity units (FIUs) of each tube according to the procedures described in Appendix D. The FIU measurements of the background solution were subtracted from the measurements for each filter source and the resulting values for each filter were averaged together. The resulting value was considered the fluorometric intensity of material captured by that particular filter.

Establishing the Signal-to-Background Ratio

The chemicals used to elute the fluorescent material from the filters have their own fluorometric signal which was considered to be background signal. The signal-to-background requirements of the PM10 inlet performance tests were established through sets of serial dilutions of fluorometric test solutions of uranine and sodium hydroxide. The fluorometric signal of the 0.01 N sodium hydroxide solution was measured and considered the background signal in this case study. The fluorometric intensity of the test solutions were initially measured and then diluted with known amounts of the sodium hydroxide solution. The fluorometric intensity of the diluted test solutions was then measured. With known dilution ratios, the fluorometric intensity of the test solution was predicted and compared to the intensity measured by the fluorometer. Figure 9 was generated using the

ratio of the signal (i.e., the measured intensity of the test solution minus the background signal) to the background signal of the 0.01N sodium hydroxide solution and the percent error between the predicted and measured fluorometric intensity of the test solutions.

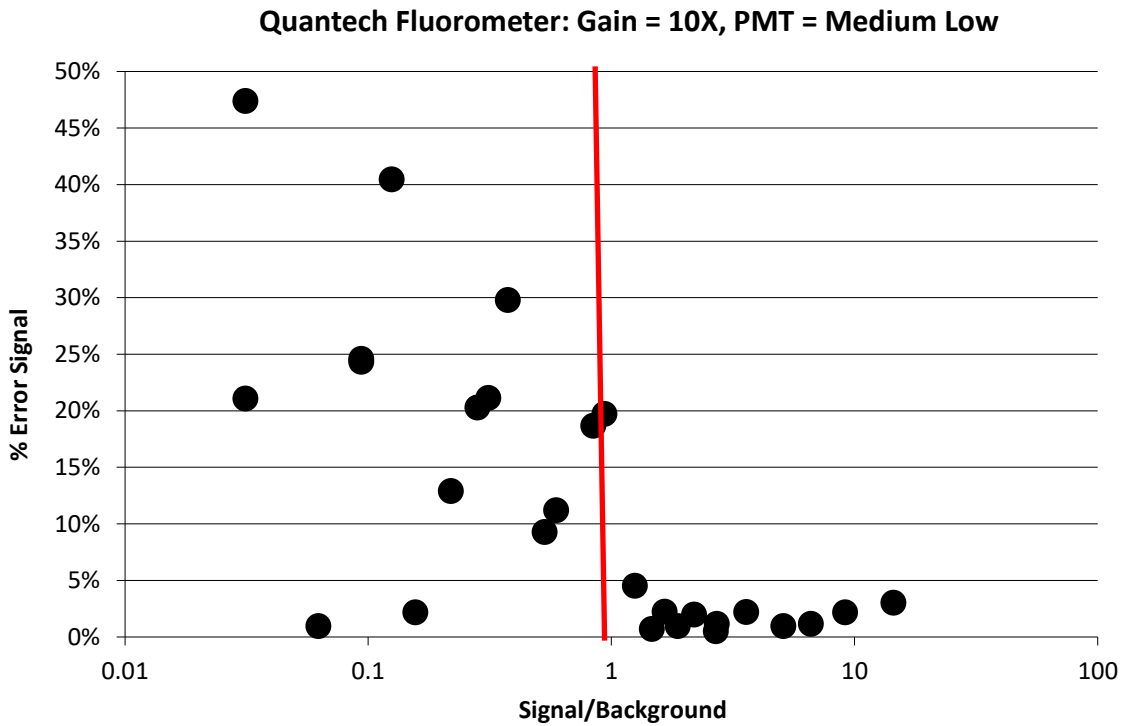


Figure 9. Fluorometric measurement error resulting from the signal-to-noise ratio of fluorometric solutions.

The error of the fluorometric measurements are consistent and less than five percent when the fluorometric intensity produced by the captured particles was at least equal to the intensity of the pure elution solution (i.e., signal/background = 1.0). To reduce uncertainty of the fluorometric measurements in the Scoates wind tunnel tests, the signal-to-noise ratio between the total measured signal from the filters to the measured noise of the elution solutions was required to be at least two to one (i.e., signal/background = 1.0).

In previous Subpart D performance testing, such as in the original testing of the unit by McFarland and Ortiz (1984), the fluorometer was zeroed using a sample of the elution solution, or a “blank.” This was supposed to account for the background signal of the solvent, stray light, or contamination by only reading out values greater than the zeroed set point. While this procedure simplifies the analysis, it can mask significant errors when solution concentration was not sufficiently above background signal. In contrast, by requiring a minimum signal-to-background ratio to qualify data as acceptable, any background masking effects are removed.

Concentration and Penetration Analysis

The concentration of particles deposited on the PM10 inlet filter was determined using equation 16.

$$C_i = \frac{FIU * m_L}{Q} \quad (16)$$

where:

C_i = calculated concentration of particles on a sampler inlet filter (FIU g min sL⁻¹),

FIU = Average net fluorometric intensity (FIU),

m_L = mass of liquid in which filter was soaked (g), and

Q = flow rate through the sampler inlet (sL min⁻¹).

Because the isokinetic sampler design and flow rate combination were chosen in order to sample with an air velocity equivalent to the wind speed in the wind tunnel (i.e., isokinetically), the concentration of particles collected by the isokinetic sampler was considered to be representative of the concentration of particles in the wind tunnel. As

such, the isokinetic sampler concentration was considered the reference concentration used to evaluate the sampling effectiveness of the PM10 inlet. Fluorometric intensity was linearly related ($R^2 > 0.99$) to test duration (figure 10) such that, for the isokinetic nozzle, a time ratio between the isokinetic sampler and PM10 inlet testing durations can be used to modify equation 16.

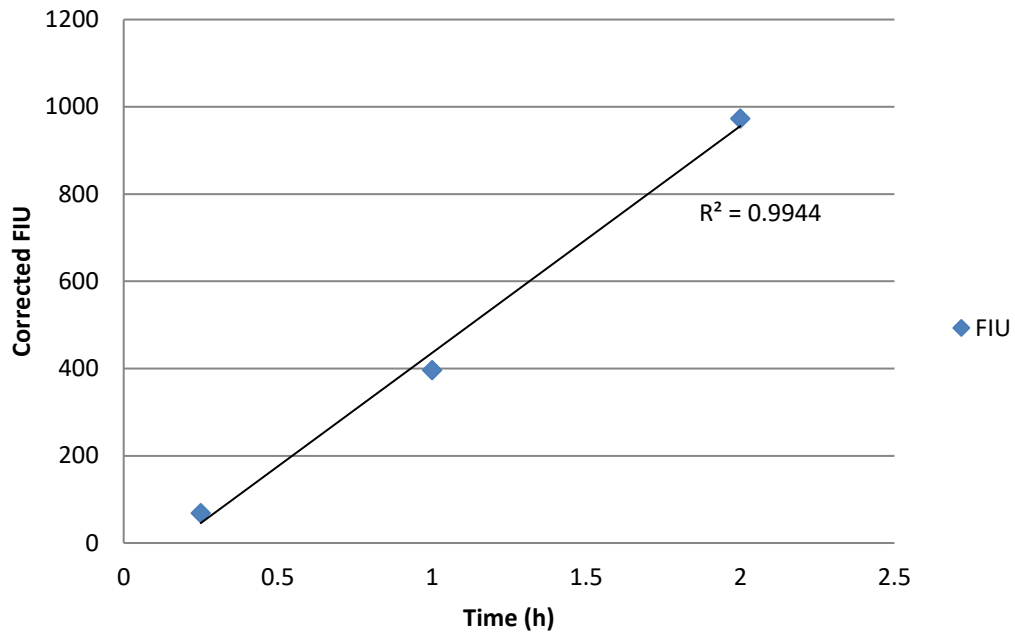


Figure 10. Isokinetic temporal uniformity.

Modifying equation 16 with the time ratio results in equation 17.

$$C_i = \frac{FIU * m_L}{Q} * \frac{t_{inlet}}{t_{ref}} \quad (17)$$

where:

t_{inlet} = the testing duration for the PM10 inlet (h), and

t_{ref} = the testing duration for the isokinetic sampler (h).

The inclusion of this time factor allowed for shorter overall testing periods as the isokinetic testing times can be greatly reduced relative to the candidate inlet while still maintaining acceptable signal to noise ratios.

The performance of the PM10 inlet is described by the penetration curve of the inlet, which relates sampling efficiency to particle size. The sampling effectiveness curve for the PM10 inlet was constructed by plotting the fractional penetration of different particle sizes through the PM10 inlet. In Subpart D PM10 inlet testing, the particle sizes that make up the penetration curve are those that are listed in table 1. The fractional penetration for each particle size was determined by dividing the concentration of particles collected by the PM10 inlet by the reference concentration from the isokinetic sampler as shown in equation 18.

$$\text{Effectiveness} = \frac{C_{\text{inlet}}}{C_{\text{ref}}} \quad (18)$$

The penetration of the particles was calculated for each PM10 inlet-isokinetic inlet pair. The fractional penetration of all tests for a given particle size must have a coefficient of variation (COV) less than 10% (CFR, 1987b). COV was calculated using equation 19.

$$\text{COV} = \frac{s}{\bar{x}} \quad (19)$$

where:

s = the sample standard deviation of the calculated fractional penetrations, and

\bar{x} = the average of the calculated fractional penetrations.

Models and Model Evaluation

Two curves were fit to the data to estimate and model the sampler effectiveness. Subpart D inlets are designed to mimic the human respiratory system and collect the respirable fraction of PM (CFR, 1987b). The lognormal distribution function was used to generate the fractional efficiency curve for the performance of an inlet. Equation 20 was the lognormal distribution function used to predict the sampling effectiveness of any given particle size based on the cut point and slope performance parameters of a sampler.

$$\eta_{p,ln} = 1 - \frac{1}{d_p * \ln(\text{slope}) * \sqrt{2\pi}} \exp \left[\frac{-(\ln(d_p) - \ln d_{50})^2}{2 * (\ln(\text{slope}))^2} \right] \quad (20)$$

where:

$\eta_{p,ln}$ = fractional sampling effectiveness for particle size d_p calculated with the lognormal function

d_p = particle size (μm),

d_{50} = cut point or the particle size at which a sampler has a 50% sampling effectiveness, and

slope = the performance slope of the PM10 inlet.

The “slope” of the lognormal distribution can be calculated as shown in equation 21 (Cooper and Alley, 2002).

$$\text{slope} = \frac{d_{84.1}}{d_{50}} = \frac{d_{50}}{d_{15.9}} = \sqrt{\frac{d_{84.1}}{d_{15.9}}} \quad (21)$$

where:

$d_{84.1}$ = particle size at which a sampler has a 84.1% collection efficiency, and

$d_{15.9}$ = particle size at which a sampler has a 15.9% collection efficiency.

Tolocka et al. (2001) used a sigmoidal function to model sampler effectiveness.

The sigmoidal function is shown in equation 22.

$$\eta_{p,s} = \frac{1}{1 + \left(\frac{d_p}{d_{50}}\right)^p} \quad (22)$$

where:

$\eta_{p,s}$ = fractional sampling effectiveness for particle size d_p calculated with the sigmoidal function,

p = empirical constant.

Microsoft Excel® was used to fit the both the lognormal and sigmoidal curves to the data by minimizing the sum of square errors between observed effectiveness values and the fitted curves (equation 23). This generates the parameters for the two models.

$$\left(\sum(E_i - \eta_{ex,i})^2\right) = \text{minimum} \quad (23)$$

where:

E_i = measured sampling effectiveness for particle size i , and

$\eta_{ex,i}$ = expected (i.e. modeled) sampling effectiveness for particle size i .

The performance models were then corrected for polydisperse particle distribution generated by the VOAG and measured by the APS using equation 24.

$$\eta_i = \int [\eta(d_{p,c}) * f_{m,i}(d_p)] dd_p \quad (24)$$

where:

η_i = expected sampling efficiency for test aerosol i ,

$\eta(d_{p,c})$ = modeled sampling efficiency for particles of size d_p , and

$f_{m,i}(d_p)$ = relative, corrected mass frequency of particles of size d_p in test aerosol i
as measured by the APS

In equation 24, the particle sizes used in the modeled sampling efficiency were corrected using the particle size correction factor f_d . Equation 23 was applied to the models using the corrected particle sizes to fit the new curves to the data.

Graphically, the expected sampling efficiency is represented by the area within the product of the sampling efficiency curve and the relative mass frequency distribution (figure 11).

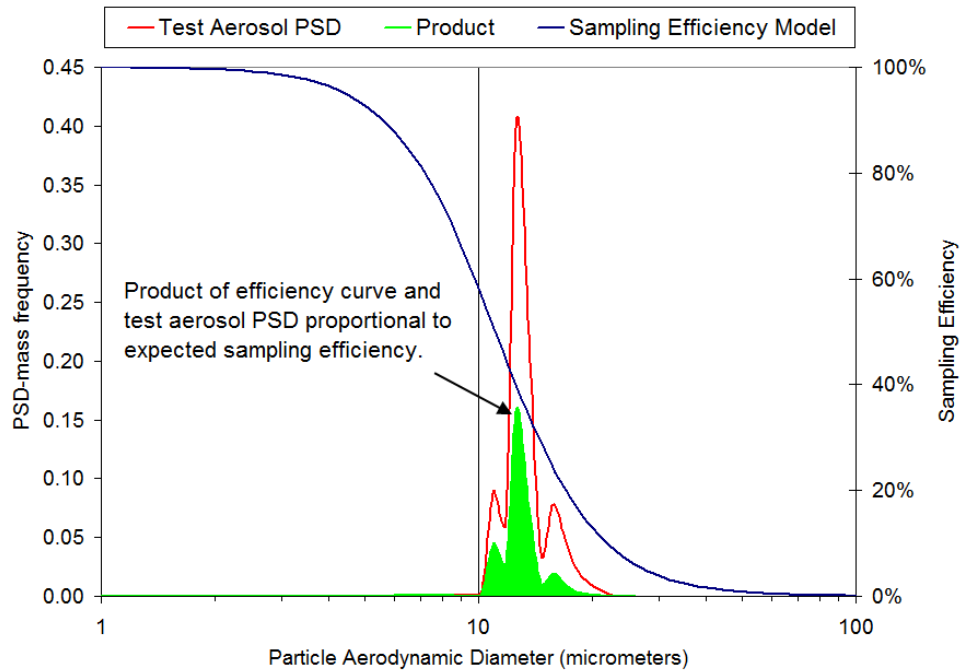


Figure 11. Example of expected sampling efficiency for polydisperse test aerosol generated by a VOAG.

Model Comparison

Subpart D specifies a procedure to evaluate the performance curve generated for the inlet during testing in a wind tunnel. In this procedure, the data collected from wind tunnel testing was placed on logarithmic graphing paper. Sampling effectiveness for the particle diameters of 1 and 50 micrometers was assumed to be one hundred and zero percent, respectively. A smooth curve was then drawn through the plotted points to generate the performance curve for the inlet. Using the smooth curve, the sampling effectiveness of the tested inlet for particles of varying sizes was estimated. The estimated effectiveness was multiplied with the corresponding interval mass concentrations provided by the EPA in Table D-3 of Subpart D to obtain the expected mass concentration.

The expected mass concentrations are then summed across all the sizes to determine the expected sampler mass concentration, $C_{\text{sam}(\text{exp})}$ ($\mu\text{g m}^{-3}$). This value was then compared to the “ideal” expected mass concentration ($C_{\text{ideal}(\text{exp})}$) for PM10 inlets (equation 25):

$$\Delta C = \frac{C_{\text{sam}(\text{exp})} - C_{\text{ideal}(\text{exp})}}{C_{\text{ideal}(\text{exp})}} * 100\% \quad (25)$$

According to Table D-1 of Subpart D, the expected and “ideal” mass concentrations, ΔC , must be within ten percent of each other. However, the mass distribution curve of the particle intervals provided in Table D-3 is not a typical distribution but a multi-modal distribution. This may be a representative distribution for specific regions in the US, such as urban areas, but is not representative of areas with large fractions of PM comprised of primary, crustal particles, such as rural regions, as the largest interval of the mass in the curve lies in the interval for particles with diameters of 1.0 micrometers or less.

Mass Collection Difference Analysis

An important comparison between the “ideal sampler” performance as defined in Subpart D and the expected performance of the same PM₁₀ inlets as estimated by the lognormal and sigmoidal functions was the mass collection difference. The mass collection difference was defined as the difference between the fractions of mass collected by the “ideal” sampler operated strictly based on the Subpart D performance curve and that which would be collected by the same inlet operating based on the lognormal and sigmoidal curves that better fit observed data. Equation 26 was used to calculate the mass collection difference.

$$\% \text{ Diff} = \left| 1 - \frac{\text{MF}_{\text{SubD}}}{\text{MF}_j} \right| * 100\% \quad (26)$$

where:

% Diff = the mass collection difference (%),

MF_{SubD} = mass fraction collected by the inlet based on the “ideal” sampling efficiency as defined in Subpart D, and

MF_j = mass fraction collected by the inlet based on the lognormal or sigmoidal FECs.

Equation 27 was used to calculate the mass fraction over the particle sizes 1.0 to 100 micrometers.

$$\text{MF}_i = \int_{1.0}^{100} \text{FEC}(dp)_i * \text{PSD}(dp)_i \text{ ddp} \quad (27)$$

where:

MF_i = estimated fraction of aerosol mass that penetrates the sampler based on the sampler FEC and i^{th} PSD

$\text{FEC}(dp)_i$ = fractional efficiency curve as a function of dp and based on Subpart D, lognormal or sigmoidal models

$\text{PSD}(dp)_i$ = fraction of total aerosol comprised of “p” size particles determined using a lognormal particle size distribution described by a combination of MMD (5-30 μm) and GSD (1.5-3) values

This difference was calculated over a range of PSDs built using a combination of MMD, ranging from 5 to 30 micrometers in 1 micrometer increments, and GSD, ranging

from 1.5 to 3 in 0.1 increments, values to replicate the ambient PSDs to which FRM PM10 inlets may be exposed in both urban and rural environments.

Results and Discussion

Table 5 shows corrected and uncorrected sampling effectiveness values for wind tunnel testing of the louvered FRM PM10 inlet at 8 km h⁻¹.

Table 5. Sampling effectiveness results for SA246 PM10 sampler at 8 km h⁻¹.

Required Particle Size (µm)	Particle Size (µm)		Sampling Effectiveness		COV (%)	Std Dev
	Calculated ^[a]	Measured ^[b]	Not corrected ^[c,d]	Corrected ^[e]		
3±0.5	3.01	3.03	1.152±0.171	0.996	6.0	0.069
5±0.5	5.22	5.20	0.916±0.110 ^[f]	0.916	4.8	0.044
7±0.5	7.22	7.50	0.759±0.093 ^[f]	0.788	4.9	0.038
9±0.5	8.82	8.90	0.591±0.041	0.619	2.8	0.017
10±0.5	10.38	9.80	0.596±0.083 ^[f]	0.477	8.8	0.052
11±0.5	10.63	10.72	0.403±0.065 ^[f]	0.462	6.5	0.026
13±1.0	13.14	12.79	0.272±0.047	0.273	6.8	0.019
15±1.0	14.10	14.50	0.191±0.047 ^[f]	0.200	9.9	0.019
20±1.0	19.71	20.00	0.034±0.028 ^[g]	0.057	33.2	0.011
25±1.0	24.22 (liquid)	28.40	0.035±0.008	0.035	8.9	0.003
	24.95 (solid)	25.51	0.032±0.011 ^[g]		14.3	0.005

[a] Calculated based on VOAG operating parameters and solution composition.

[b] Measured microscopically using flattening factor of 1.358 for liquid particles (Faulkner and Haglund, 2012).

[c] Mean ±95% confidence interval.

[d] Measured sampling effectiveness, not corrected for multiplets and satellites.

[e] Corrected for multiplets and satellites.

[f] Results produced with data collected from the collocated isokinetic nozzle testing process.

[g] COV exceeds 10%.

Several particles have COV values that are greater than the maximum COV allowed for Subpart D testing. However, for larger particle sizes that have low average penetration values, the COV was highly sensitive to small variations in penetration values

across tests. In these cases, the standard deviation, which was small for all of the tests in question, was a more reliable indicator of data consistency than the COV. Furthermore, in all cases, the mean was significantly greater than zero ($\alpha = 0.05$).

Using the data collected with the Scoates wind tunnel, lognormal and sigmoidal functions were fit to the data by minimizing the sum of the squared error between the predict penetration value of the model and the actual data. The model parameters calculated are shown in table 6.

Table 6. Model parameters calculated based on uncorrected, empirical wind tunnel data collected.

Model	d₅₀ (μm)	Slope	P	R²	p-value
Lognormal	10.07	1.54	N/A	0.9833	0.686
Sigmoidal	10.10	N/A	3.93	0.9845	0.671

Figure 12 showcases the model curves based on the parameters of table 7 and the raw data results for the liquid particle testing.

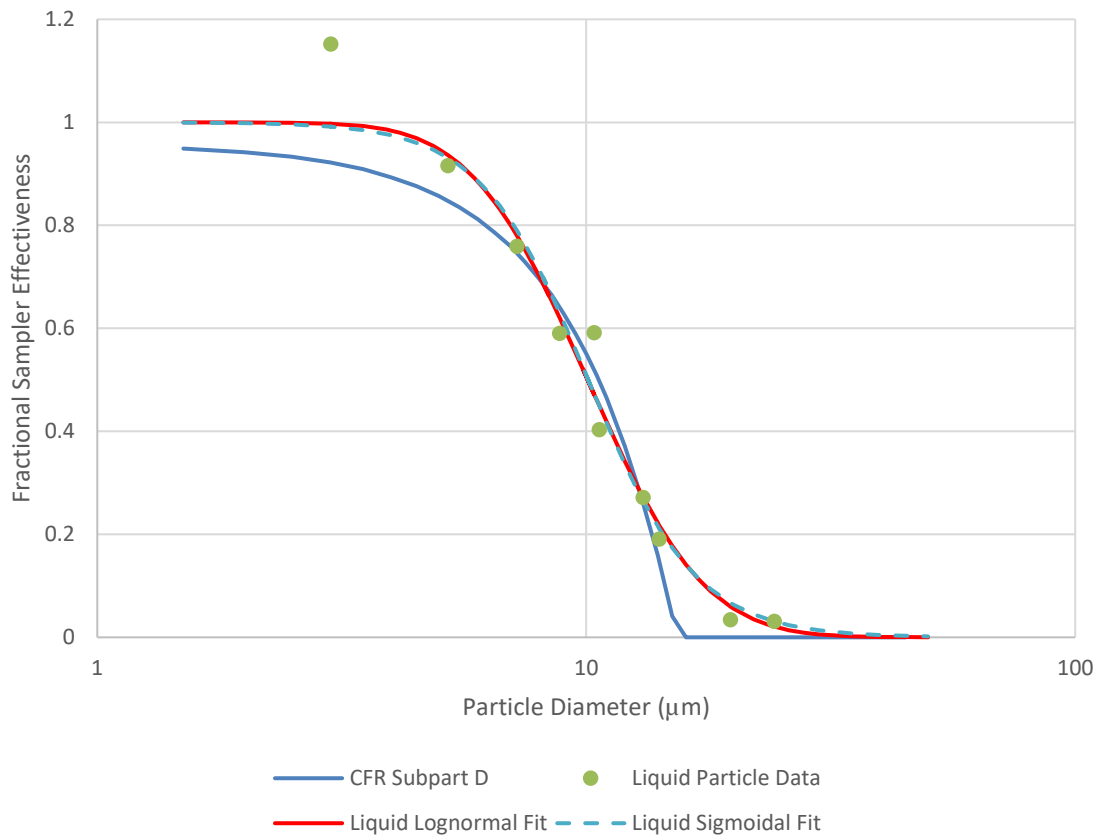


Figure 12. Liquid particle penetration data (green triangles) Subpart D “ideal sampler” FEC (blue line), Lognormal FEC (purple line) and Sigmoidal FEC at 8 km h⁻¹.

The sigmoidal and lognormal models were not significantly different from one another (p -value > 0.05). The lognormal performance model was selected to represent the performance of the inlet and was used for all further analysis because of its historical and prevalent use in representing past aerosol inlet and impactor performance.

The correction procedure resulted in a best-fit lognormal curve ($R^2 = 0.985$; $p = 0.657$) characterized by a cut point of 10.18 with a slope of 1.52 (figure 13).

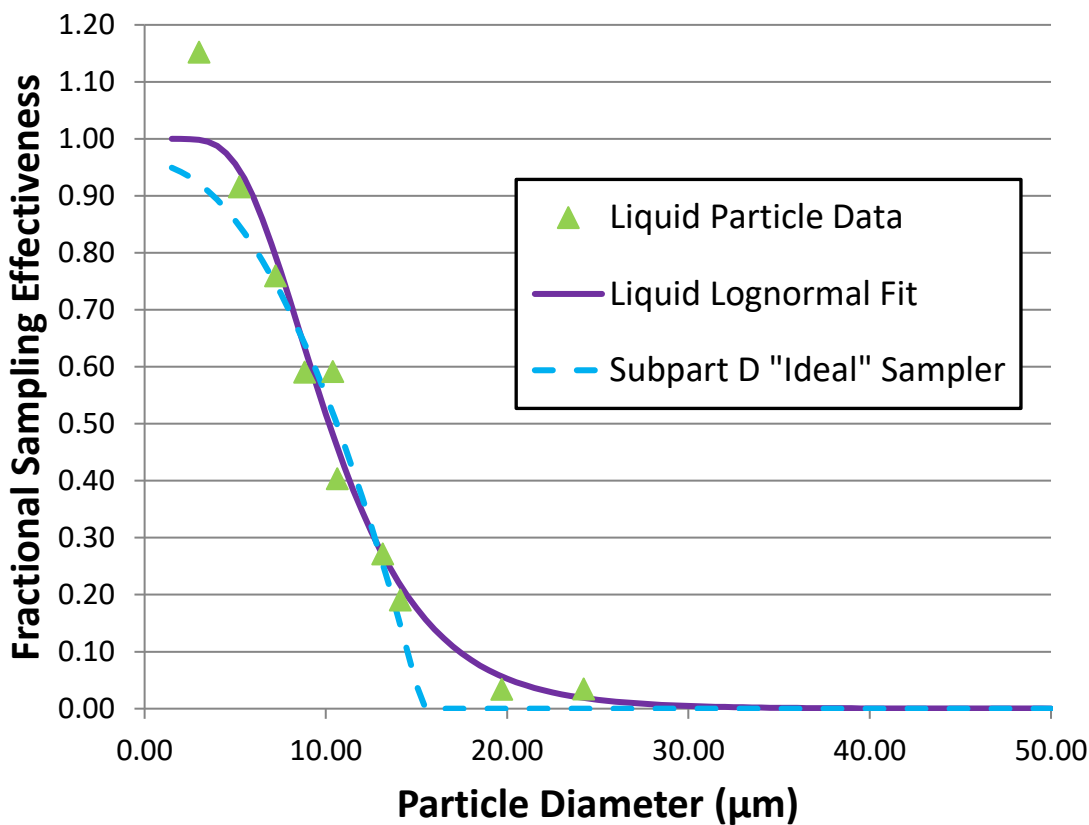


Figure 13. Multiplet corrected best-fit lognormal curve.

The sampling effectiveness was calculated using the lognormal model and the model comparison procedures described by Subpart D. Table D-3 from Subpart D was adapted and completed as shown in table 7.

Table 7. Expected mass concentration for PM10 samplers (40 CFR Part 53 Subpart D – Table D-3).

d_p (μm)	Test Sampler ^[a]			Ideal Sampler			
	Sampling Eff.	Interval Mass Concen. ($\mu\text{g m}^{-3}$)	Expected Mass Concen. ($\mu\text{g m}^{-3}$)	Sampling Eff.s	Interval Mass Concen. ($\mu\text{g m}^{-3}$)	Expected Mass Concen. ($\mu\text{g m}^{-3}$)	
<1.0	1.000	62.813	62.813	1.000	62.813	62.813	
1.5	1.000	9.554	9.554	0.949	9.554	9.067	
2.0	1.000	2.164	2.164	0.942	2.164	2.038	
2.5	1.000	1.785	1.784	0.933	1.785	1.665	
3.0	0.998	2.084	2.080	0.922	2.084	1.921	
3.5	0.995	2.618	2.604	0.909	2.618	2.380	
4.0	0.987	3.211	3.171	0.893	3.211	2.867	
4.5	0.975	3.784	3.689	0.876	3.784	3.315	
5.0	0.956	4.300	4.111	0.857	4.300	3.685	
5.5	0.930	4.742	4.411	0.835	4.742	3.960	
6.0	0.898	5.105	4.582	0.812	5.105	4.145	
6.5	0.859	5.389	4.629	0.786	5.389	4.236	
7.0	0.815	5.601	4.567	0.759	5.601	4.251	
7.5	0.768	5.746	4.414	0.729	5.746	4.189	
8.0	0.718	5.834	4.191	0.697	5.834	4.066	
8.5	0.667	5.871	3.917	0.664	5.871	3.898	
9.0	0.616	5.864	3.613	0.628	5.864	3.683	
9.5	0.566	5.822	3.293	0.590	5.822	3.435	
10.0	0.517	5.750	2.972	0.551	5.750	3.168	
10.5	0.470	5.653	2.658	0.509	5.653	2.877	
11.0	0.426	8.257	3.518	0.465	8.257	3.840	
12.0	0.346	10.521	3.644	0.371	10.521	3.903	
13.0	0.278	9.902	2.758	0.269	9.902	2.664	
14.0	0.222	9.250	2.054	0.159	9.250	1.471	
15.0	0.176	8.593	1.512	0.041	8.593	0.352	
16.0	0.139	7.948	1.103	0.000	7.948	0.000	
17.0	0.109	7.329	0.800	0.000	7.329	0.000	
18.0	0.086	9.904	0.848	0.000	9.904	0.000	
20.0	0.052	11.366	0.597	0.000	11.366	0.000	
22.0	0.032	9.540	0.307	0.000	9.540	0.000	
24.0	0.020	7.997	0.158	0.000	7.997	0.000	
26.0	0.012	6.704	0.082	0.000	6.704	0.000	
28.0	0.008	5.627	0.043	0.000	5.627	0.000	
30.0	0.005	7.785	0.037	0.000	7.785	0.000	
35.0	0.002	7.800	0.012	0.000	7.800	0.000	
40.0	0.001	5.192	0.003	0.000	5.192	0.000	
45.0	0.000	4.959	0.001	0.000	4.959	0.000	
		C_{sam} =	152.694			C_{ideal} =	143.889

[a] The sampling effectiveness model used accounts for multiplet correction.

The ΔC was determined to be 6.12% for the lognormal model comparison. The calculated percent difference between the “ideal” and model concentrations was within the 10% requirement of Subpart D even with nonzero penetration of larger particles. However, the interval mass concentration provided in Table D-3 was not indicative of the mass fractions of particles of rural PSDs. Because the provided mass distribution was so heavily weighted towards the fine fraction, the calculated ΔC primarily describes the gap between the two curves associated with particle sizes less than ten micrometers. As such, the “mass collection difference analysis” using a multitude of PSDs representative of aerosol characteristics encountered throughout the US was a more robust tool to examine the sampling performance of a candidate PM10 inlet.

The mass collection percent difference between the “ideal” inlet performance curve and the lognormal model was calculated for every combination of MMD and GSD of the PSD as previously described. The results of the calculation based on liquid particles when using the lognormal model is shown in figure 14.

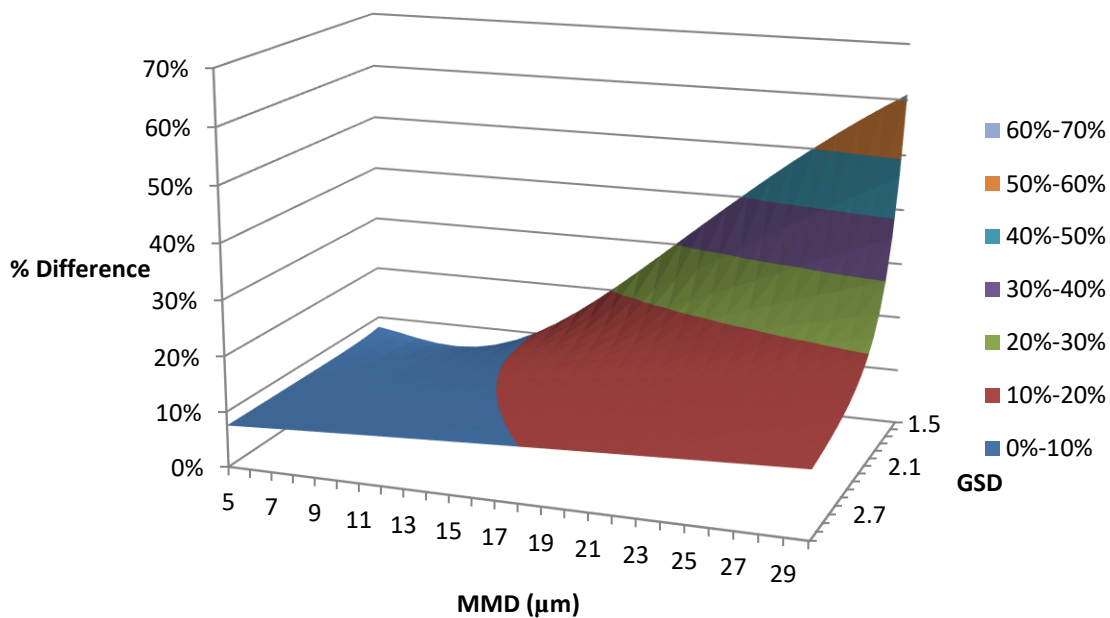


Figure 14. Surface plot of percent difference between the Subpart D “ideal sampler” sampling effectiveness and lognormal sampling effectiveness curve constructed with observed liquid particle data passing Subpart D testing at 8 km h⁻¹.

As the MMD and GSD of ambient aerosols increase and decrease, respectively, the mass collection difference increases exponentially. This is primarily caused by the increased mass contributions of particles greater than 16 micrometers. The mass of a 25-micrometer particle is nearly four times that of a 16-micrometer particle and fifteen times that of a ten-micrometer particle. Therefore, even small values of penetration by large particles can lead to significant differences in measured concentrations.

To further illustrate, PSDs were produced for several common, rural sources of PM using a single mode, lognormal distribution based on previously determined MMD

and GSD parameters. The resulting PSD was then multiplied by both the lognormal and “ideal” sampling effectiveness curves and the percent difference in mass analysis conducted. Table 8 showcases the percent difference in theoretical mass collection between the “ideal” and the lognormal model effectiveness curves.

Table 8. Percent difference between the Subpart D “ideal sampler” sampling effectiveness curve and the lognormal model for various rural PM sources (PSDs from Faulkner et al., 2007).

Rural PM Source	MMD (µm)	GSD	% Difference Lognormal Model
Dairy	15	2.1	10.69
Feed yard	20	2.2	12.77
Cotton Gin	23	1.8	21.20
Broiler	24	1.6	33.74

PM10 inlets sampling the PM emitted by common agricultural sources have the potential to measure concentrations that are more than 10% greater than that which would be measured by the same inlet operating “ideally,” as defined by 40 CFR 53 Subpart D. This non-trivial percent difference in mass not only shows that the SA246b inlet is unfit for universal deployment but that inlets which can perform to Subpart D standards in rural environments should be used in areas where ambient aerosols are estimated to contain larger fractions of crustal particles.

Subpart F, the subpart related to FEM requirements for PM2.5 inlets, requires the fitted FEC of the candidate PM2.5 inlet to be integrated against three separate PSDs: typical, fine and coarse. This type of comparison would greatly benefit the development of future PM10 inlets as it requires the developers to gauge the sampling effectiveness of

their inlet in the presence of more representative environments. Further, applying the Subpart F method to currently designated FRM and FEM inlets would ensure that those inlets do, indeed, meet the requirements of their designations.

As previously stated, Stokes number is the principle governor of impactor collection efficiency. Based on equation 2, the Stokes number for a given particle will increase as particle AED increases under constant flow conditions. The impactor of the “ideal” PM10 sampler is supposed to inertially separate any particles greater than sixteen micrometers from the flow streams based on Stokes number. The Stokes number for a sixteen micrometer AED particle is 0.257. Due to the design of the inlet, a particle with a Stokes number greater than 0.257 should not physically be able to penetrate the impactor section of a PM10 inlet. However, Kim et al. (2004) showed that, even though a particle should not be able to penetrate an impactor based on the Stokes number analysis, non-trivial penetration of particles much larger than the cut point may occur.

Kim et al. (2004) examined the effect of Stokes number on a virtual impactor being used to separate large particles from fine powders for the construction of superconducting filaments, which are broken by contamination by large particles. In their study, the effect of Stokes number on virtual impactor collection efficiency was examined. The Stk50 number (i.e., the Stokes number corresponding to d50) for the virtual impactor in the study was approximately 0.85. Particles with Stokes numbers ten times greater than the Stk50 value were able to penetrate the major flow of the virtual impactor with an efficiency of approximately 1%. This was concluded to be the result of decreased local velocities and, consequentially, local Stokes numbers, for particles located near the boundary layer

adjacent to the nozzle walls. It seems likely that such effects may have occurred in the impactor of the tested PM10 nozzle in the present study as well.

The particle physics of virtual impactors are similar to those of FRM samplers. The Stokes number for 10-micrometer particles in the PM10 inlet is 0.098. The Stokes value ten times larger corresponds to a particle over 30 micrometers in diameter. Applying the conclusions of Kim et al. (2004) to the PM10 inlet, larger particles located in the boundary region of the inlet flow passing through the PM10 jet may have local Stokes values sufficiently low enough to remain in the streamlines of the sampled air, pass through the impactor, and deposit on the filter. This would result in the penetration of said particles through the impactor, as was observed for particles up to 25 micrometers in size.

Considering all of the data and evidence presented, non-trivial penetration of particles greater than 16 micrometers in aerodynamic diameter should no longer be considered an isolated or rare occurrence. The significance of the penetration of these larger particles is dependent on the concentration of the larger particles in the ambient PSD. PM10 inlets placed in areas dominated by PSDs characterized by larger MMDs, such as rural or agricultural regions, will produce more biased sampling results than those inlets placed in urban environments because of the number of larger particles present in those dusts.

Conclusion

In order for concentrations of PM to be measured accurately, inlets used to sample desired fractions of ambient PM must be carefully characterized. The performance of a

FRM PM10 sampler was evaluated following Subpart D specifications in conjunction with newly developed, modified analyses to produce more accurate observations than previous studies concerning the penetration of particles larger than 16 micrometers. Results indicate non-trivial penetration of large particles. This finding was supported by both the field observations of Buser et al. (2008) and the theoretical and empirical analysis of Kim et al. (2004). The inlet performance curves generated using data collected during wind tunnel testing pass all EPA FRM certification testing requirements for a single wind speed and were not significantly different from the “ideal” curve for PM10 inlets.

The effect the larger particle penetration will have on calculated PM10 concentrations is dependent upon the PSD of the sampled PM. This result should have little consequence to urban areas as PM in these areas contains small quantities of larger PM. However, PM10 concentrations from monitors placed in rural areas where PSDs are dominated by MMDs and quantities of particles with diameters larger than sixteen micrometers are much more susceptible to the penetration of the larger particles. This raises the question of whether or not PM is being appropriately regulated in rural or agricultural areas.

CHAPTER III

SUBPART D WIND TUNNEL EVALUATION OF TAMU LVTSP SAMPLER

Introduction

The Federal Clean Air Act (CAA) was originally enacted in 1963 in an effort to begin monitoring and regulating air pollutants that may endanger public health and welfare. The National Environmental Policy Act of 1970 established the Environmental Protection Agency (EPA), which is now responsible for developing and implementing air quality regulations under the authority of the CAA. The CAA amendments of 1970 required EPA to establish National Ambient Air Quality Standards (NAAQS) for six criteria pollutants, including particulate matter (PM). Historically, PM has been regulated based on a concentration of total suspended particulates, or TSP, as measured by a standard high-volume (“hi-vol”) sampler (AP-42, 1995). In 1987, standards for PM₁₀, defined as the fraction of “PM with an aerodynamic diameter (AED) less than or equal to a nominal 10 micrometers” (EPA, 2011), were promulgated and the TSP standards slowly phased out moving forward. However, TSP measurements are still used as both an indicator for the smaller PM fractions as well as for collecting representative aerosol samples.

The size of the PM in any given region can be characterized by a particle size distribution (PSD), which describes the distribution of particle mass, volume, or number of specifically sized particles contained in the aerosol. Ambient aerosols are often

characterized by PSDs with one or more modes. Each mode can be characterized by a lognormal distribution described by a mass median diameter (MMD) and geometric standard deviation (GSD) (Hinds, 1999). The MMD describes the particle diameter at 50% of the total mass. The GSD is related to the ratio between the MMD and the particle diameters at specific mass fractions (equation 28).

$$\text{GSD} = \frac{d_{84.1}}{\text{MMD}} = \frac{\text{MMD}}{d_{15.9}} = \sqrt{\frac{d_{84.1}}{d_{15.9}}} \quad (28)$$

where:

$d_{84.1}$ = the particle diameter at 84.1% of the total mass; and

$d_{15.9}$ = the particle diameter at 15.9% of the total mass.

The Biological and Agricultural Engineering Department at Texas A&M University in conjunction with the Center for Agricultural Air Quality Engineering and Science (CAAQES) developed a low-volume total suspended particulate (LVTSP) inlet, henceforth referred to as the “LVTSP inlet,” and sampling system (Wanjura et al., 2005). This inlet, shown in the figure 15, was designed to operate at the same volumetric flow rate as the SA246 PM10 inlet, henceforth referred to as “the PM10 inlet”, of 16.7 L min^{-1} for ease of deployment and use with existing PM10 sampling equipment (Wanjura et al., 2005). The cone shape of the LVTSP shown in figure 15 was eventually redesigned to a dome shape for safety reasons, but no critical dimensions were changed.

for ten specific particle sizes across three wind speeds was determined with a minimum of three replicates per particle diameter to establish repeatability (table 1).

The resulting sampling effectiveness values for the particle sizes and types listed in table 1 are used to develop the performance curve. The performance curve for a sampler is often referred to as the Fractional Efficiency Curve (FEC).

The LVTSP has been used in several studies seeking to demonstrate that there are issues concerning the use of certain PM₁₀ inlets in areas with large fractions of PM comprised of primary, crustal particles such as rural regions. In Wang et al. (2005), Buser et al. (2007), and Buser et al. (2008), FRM PM₁₀ inlets and the LVTSP inlets were collocated at various agricultural operations in order to compare and evaluate the particulates collected by both inlets sampling the same aerosol. For the studies, PSDs of the ambient aerosol were produced from the particulates collected by the LVTSP inlet and compared to what was collected by the PM₁₀ inlet to evaluate the existence and magnitude of sampling error.

The objective of this research was to accurately develop a performance curve for the LVTSP inlet for future use in inlet research. This study performed a full performance analysis of in the inlet for the nominal wind speeds of 2, 8, and 24 km h⁻¹ to better characterize and study the penetration of particles through the inlet. The results of this research were used to estimate the error between a PSD generated from a sample of an ambient aerosol collected by the LVTSP and the actual PSD of the ambient aerosol.

Methodology

For the testing of the TAMU LVTSP inlet, a Subpart D wind tunnel was not necessarily required. However, in order to generate LVTSP inlet data for comparison with FRM PM10 inlets, it was determined that the LVTSP inlet should be tested and characterized using Subpart D procedures.

Subpart D Wind Tunnel

The Scoates wind tunnel utilized in Chapter 2, that was shown to meet the requirements of Subpart D, was used to develop performance curves for the LVTSP inlet at the nominal wind speeds of 2, 8, and 24 km h⁻¹. The curved panels installed in the wind tunnel for the analysis in Chapter 2 were retained (figure 16).



Figure 16. The LVTSP inlet inside the wind tunnel.

Isokinetic nozzles were manufactured and used in a configuration denoted as “hot swapping.” This configuration was used to reduce uncertainty in the inlet tests resulting from a lack of spatial uniformity of particle concentration across the sampling plane. The

appropriate isokinetic inlet was placed in the wind tunnel and then swapped with the candidate sampler inlet during testing so that the inlets of the isokinetic sampler and the sampler under evaluation were located in the same point in the sampling plane. The hot swapping procedure is outlined in Subpart D, specifically, 40 CFR 53.43(a)(2)(x). Temporal uniformity tests indicated that coefficients of variation were less than 10%. The temporal uniformity was routinely checked with each particle size-wind speed combination evaluated.

The isokinetic nozzles used with the hot swapping procedure were designed so that the volumetric flow rate applied to the inlet divided by the cross sectional area of the inlet to the nozzle was equivalent to the wind speed of the wind tunnel. The isokinetic nozzles used in the Scoates wind tunnel had inlet diameters of 66.04 mm (2.6 inches), 33.02 mm (1.3 inches), and 19.05 mm (0.75 inches) so as to produce the equivalent sampling velocities of 2, 8, and 24 km h⁻¹, respectively, under the same volumetric flow of 114 L min⁻¹.

The isokinetic air flow was provided by a 0.56 kW (0.75 hp) pump (5KC49NN0194AX, GE Motor & Industrial Systems, Benton Harbor, MI) and the flow controlled with a ball valve. The actual flow rate supplied to the sampler was monitored by a HI-Q flow meter (D-AFC-09; HI-Q; San Diego, CA). The target set point for the pump was calculated using equation 29,

$$Q_s = 44.1375 * \frac{P_a}{T} \quad (29)$$

where:

P_a = ambient pressure (mm Hg),

T = ambient temperature (K), and

$$44.1375 = \text{constant (sL min}^{-1} \text{ K mm Hg}^{-1}) = 114 \text{ L min}^{-1} * 293 \text{ K} / 760 \text{ mm Hg}.$$

The pump was allowed to warm up at the beginning of each day of testing. The pump was then set to the appropriate flow rate at the beginning of each isokinetic test using the flow meter. At the end of an isokinetic test, the flow rate was again verified. Observed flow rates did not vary from the original set point established prior to each isokinetic test by more than 10%. Typical observed variation was approximately 7%, or 8 L min⁻¹.

Per 40 CFR 53.42(a), inlets placed in a Subpart D wind tunnel cannot block more than 15% of the cross-sectional area. The blunt surface area of the inlet and the inlet holder in the wind tunnel block less than 15% of the sampling plane with the 101.6 mm (4 inch) panels installed.

Inlet Flow Systems

The LVTSP inlet was designed for a flow rate of 1 cubic meter per hour (16.7 liters per minute) of air to be drawn through the inlet. This design allowed the TSP inlet to be used with the same flow equipment utilized by certified PM10 inlets. To provide the air flow, a PQ200 (BGI Instruments; Waltham, MA), FRM flow control unit was used. The PQ200 measures the ambient air temperature and pressure in order to adjust sampler air flow to deliver a constant 16.7 aL m⁻¹ of flow rate. The flow rate calibration and system integrity of the PQ200 was checked and verified every day per manufacturer specifications prior to running any tests with a candidate inlet. The flow rate was verified and calibrated

using a tetraCal system (tetraCal; BGI Instruments; Waltham, MA). System integrity was determined by running the leak check procedure on the PQ200 per manufacturer instructions.

Liquid Aerosols

Specially constructed solutions were used in conjunction with a vibrating orifice aerosol generator (VOAG; Model 3450, TSI, Inc., Shoreview, MN) to produce liquid, mono-dispersed particles of various sizes. Solutions were constructed to produce a desired particle size based on equations 30-32 adapted from the VOAG user manual and the original VOAG development work by Berglund and Liu (1973). Most solutions were constructed for use with a flow rate and VOAG vibration frequency of 0.225 mL min⁻¹ and 57,000 Hz, respectively. Particles with diameters of 3 micrometers and smaller were designed for a flow rate and VOAG vibration frequency of 0.093 mL min⁻¹ and 150,000 Hz, respectively. Orifice vibrating frequency was optimized for different orifice diameters and adjusted during particle generation to minimize the formation of “satellite” droplets.

$$D_{pp} = \left(\frac{6 * Q * C}{\pi * f} \right)^{1/3} \quad (30)$$

where:

D_{pp} = physical particle diameter (μm),

Q = solution flow rate (mL s^{-1}) = 0.225 mL min⁻¹,

C = volumetric concentration of aerosol material in the solution, and

f = VOAG frequency (Hz) = approximately 57,000 Hz.

$$C = \frac{m_i}{\rho_i * V_c} \quad (31)$$

where:

m_i = mass of fluorometric material used (g),

ρ_i = density of fluorometric material (g mL^{-1}), and

V_c = volume of the solution container (mL).

$$Dp_a = Dp_p * \sqrt{\rho_{p,i}} \quad (32)$$

where:

Dp_a = the aerodynamic particle diameter (μm), and

$\rho_{p,i}$ = particle density (g cm^{-3}).

Subpart D testing requires the evaluation of the inlet performance with specific particle sizes (table 11). Liquid particle solutions were made to achieve the desired particle size by combining specific amounts of oleic acid and uranine (CAS 518-47-8). Uranine was used to provide fluorescent signal. The ratio of uranine to oleic acid in the particle was 1:10 or 0.10g uranine per mL of oleic acid. Ethanol made up the remaining volume of the solution. Equations 33-35 are specific to generating liquid particles and were combined with equations 30-32 to determine the expected aerodynamic particle size.

$$m_u = \rho_u * (V_o * C - V_o) \quad (33)$$

where:

m_u = mass of uranine in the solution (g),

ρ_u = density of uranine (g mL^{-1}) = 1.53 g mL^{-1} , and

V_o = volume of oleic acid in solution (mL) = $m_o * \rho_o$.

$$m_o = \frac{\rho_o * V_c * C}{1 + R/\rho_u} \quad (34)$$

where:

m_o = mass of oleic acid (g),

ρ_o = density of oleic acid (g mL^{-1}) = 0.8935 g mL^{-1} , and

R = mass of uranine (g) per volume of oleic acid (mL) = 0.10 g mL^{-1} .

$$\rho_{p,l} = \frac{R * V_o + m_o}{V_u + V_o} \quad (35)$$

where:

$\rho_{p,l}$ = density of liquid particle (g mL^{-1}), and,

V_u = volume of uranine in the solution (mL) = $m_u * \rho_u$.

Particle sizes and distribution were verified post generation. An Aerodynamic Particle Sizer (APS, Model 3321, TSI, Shoreview, MN) was used to check the uniformity of particle sizes produced. If the particle stream was not mono-dispersed, the VOAG frequency was adjusted and the stream retested with the APS until the APS indicated a nominally mono-disperse PSD. Once the generated particles were deemed to be nominally mono-dispersed, the liquid particles were impacted onto slides coated with an oleophobic solution, Nyebar (Type Q). The slides were then placed under a microscope with 400X magnification. A line slider was used to measure the impacted particle diameters by the number of tick marks counted from one side of the particle to the other. The line slider was calibrated using a stage slide etched with lines spaced at 10 micrometers. The number of ticks per 10 micrometers was determined to be 42. Doublets and triplets, known as multiplets, were accounted for post particle sizing.

Multiplets were accounted for by applying the multiplet correction described by Haglund et al. (2002). This process also corrects liquid particle “stretching” that affects liquid particle measured by the APS. As the liquid particles are accelerated through the APS, the spherical particles stretch into an oblong shape and are then measured by the laser in the APS. For each nominal particle size shown in table 11, measurements of particle sizes collected with the APS were used to quantify the relative mass concentrations of satellites and multiplets. (Due to the APS’s maximum particle detection size of 20 micrometers, a single effectiveness value was used for the 25-micrometer data point based on microscopy measurements). A particle size correction factor, f_d , was generated for each nominal particle size shown in table 11 to correct APS-measured particle diameters and distributions using equation 36. The particle size correction factor was applied during model development to correct the models for multiplets present in the data the models are fit to. This process is explained in a later section.

$$f_d = \frac{D_{pa}}{D_{APS,VMD}} \quad (36)$$

where :

f_d = particle size correction factor, and

$D_{APS,VMD}$ = volume mean diameter reported by the APS.

Previous studies and Subpart D accounted for multiplets by physically counting particles with diameters that fall outside the acceptable diameter range from the impacted particles on the glass slide. The percentage of particles with acceptable diameters was then determined and used to correct sampler performance results. This method is required by Subpart D. However, the APS correction method was both quicker and more accurate

as much less human judgment was involved in the counting process, the effects of smaller satellite droplets can also be considered, and the sample size was much larger yielding more representative values.

It was uncommon for large numbers of multiplets to be present when observing particles under the microscope because the APS was used to verify the mono-disperse nature of PSDs prior to slide impaction and testing. If large numbers of multiplets were observed, the aerosol was regenerated and impacted again prior to running a test.

The observed diameter of liquid droplets measured on the microscope, D_a , was not representative of the actual diameter of the aerosol particles. When liquid particles are impacted on slides, they flatten to form a plano-convex shape. This final shape was a product of droplet surface tension and interactions of the droplet with the oleophobic coating on the slide. Faulkner and Haglund (2012) determined the appropriate flattening coefficient factors for 10% uranine-oleic acid droplets impacted on slides treated with Nyebar Type Q to be 1.358. This flattening coefficient was used in equation 36 to determine the physical aerosol particle diameter. The particle diameter was then converted to the aerodynamic particle size using equation 37.

$$D_{p_p} = \frac{D_a}{F_Q} \quad (37)$$

where:

D_a = measured impacted droplet diameter (μm); and

F_Q = flattening coefficient for Nyebar Type Q.

Experimental Design

The performance of the TSP Inlet was evaluated using the Subpart D Scoates wind tunnel at nominal wind speeds of 2, 8, and 24 km h⁻¹. Isokinetic samplers were used in the same sampling plane in the in the test section of the wind tunnel as the TSP inlet. As stated previously, two different processes were used in the Scoates wind tunnel for the collection of the representative wind tunnel concentration sample; the collocated and hot swapping procedures.

In the collocation procedure, two identical isokinetic samplers were installed on either side of the PM10 inlet in the wind tunnel for concurrent sampling. Forty-seven-millimeter diameter PTFE filters were cut from full PTFE sheets (PSPJ001, Pall, Port Washington, NY) and used to collect the sampled particles for all three samplers. The filters used in the isokinetic samplers were placed directly within in the sampler and secured in place by tightly screwing the isokinetic nozzle to the sampler base. The filters used for the TSP inlet were placed into aluminum filter holders manufactured by Texas A&M University to fit securely inside the TSP inlet.

For the hot swapping procedure, the TSP inlet and the isokinetic samplers were placed in the wind tunnel one after the other in an alternating fashion beginning with the isokinetic nozzle and were not collocated. Filters were used to capture the particles sampled by isokinetic and TSP inlets. Forty-seven-millimeter diameter, PTFE, ring supported filters (P5PQ047, Pall Corporation, Port Washington, NY) and 90 mm glass fiber filters (61664, Pall Corporation, Port Washington, NY) were used to collect the particles sampled by the PM₁₀ inlet and isokinetic samplers, respectively. The 47-mm

filters were placed in filter holders and installed in the TSP inlet prior to placing the inlet within the wind tunnel. The 90 mm filters were placed directly into the isokinetic sampler and are held in place by the nozzle and knurled sleeve (figure 8).

Inlet performance evaluation was performed using a minimum of three pairs of isokinetic and TSP inlet tests. An isokinetic sample was collected first, followed by evaluation of the PM10 inlet. Test durations were developed based on experience and the need to meet the required signal to noise ratio of the measured fluorescence with a fluorometer (FM109515, Barnstead International, Dubuque, IA). See Appendix C for the procedures used to evaluate the TSP inlet.

Fluorometric Analysis

After each round of inlet testing, the filters were removed and placed into a measured mass of 0.01 N sodium hydroxide (for liquid particles) or 0.01 N ammonium hydroxide (for solid particles) to elute the fluorometric material from the filters. Filters were soaked overnight and then analyzed with the fluorometer. See Appendix D for procedures used to operate the fluorometer and analyze the filters.

For the fluorometric analysis, a small volume (approximately 2mL) of the solution from each of the jars with soaking filters was transferred to individual disposable test tubes using a different disposable pipette for each solution in order to avoid contamination. A separate test tube was filled with approximately 2 mL of unused extraction solution for background measurements. The fluorometer was then used to measure the raw fluorometric intensity units (FIUs) of each tube according the procedures described in

Appendix D. The FIU measurements of the background solution were subtracted from the measurements for each filter source and the resulting values for each filter were averaged together. The resulting value was considered the fluorometric intensity of material captured by that particular filter.

Establishing the Signal-to-Background Ratio

After each round of inlet testing, the filters were removed and placed into a measured mass of 0.01 N sodium hydroxide (for liquid particles) or 0.01 N ammonium hydroxide (for solid particles) to elute the fluorometric material from the filters. Filters were soaked overnight and then analyzed with the fluorometer. See Appendix D for procedures used to operate the fluorometer and analyze the filters.

For the fluorometric analysis, a small volume (approximately 2mL) of the solution from each of the jars with soaking filters was transferred to individual disposable test tubes using a different disposable pipette for each solution in order to avoid contamination. A separate test tube was filled with approximately 2 mL of unused extraction solution for background measurements. The fluorometer was then used to measure the raw fluorometric intensity units (FIUs) of each tube according the procedures described in Appendix D. The FIU measurements of the background solution were subtracted from the measurements for each filter source and the resulting values for each filter were averaged together. The resulting value was considered the fluorometric intensity of material captured by that particular filter.

Concentration and Penetration Analysis

The concentration of particles deposited on the PM10 inlet filter was determined using equation 38.

$$C_i = \frac{FIU * m_L}{Q} \quad (38)$$

where:

C_i = calculated concentration of particles on a sampler inlet filter (FIU g min sL⁻¹),

FIU = Average net fluorometric intensity (FIU),

m_L = mass of liquid in which filter was soaked (g), and

Q = flow rate through the sampler inlet (sL min⁻¹).

Because the isokinetic sampler design and flow rate combination were chosen in order to sample with an air velocity equivalent to the wind speed in the wind tunnel, the concentration of particles collected by the isokinetic sampler was considered to be representative of the concentration of particles in the wind tunnel. As such, the isokinetic sampler concentration was considered the reference concentration used to evaluate the sampling effectiveness of the PM10 inlet. Fluorometric intensity was linearly related ($R^2 > 0.99$) to test duration (figure 10) such that, for the isokinetic nozzle, a time ratio between the isokinetic sampler and PM10 inlet testing durations can be used to modify equation 38.

Modifying equation 38 with the time ratio results in equation 39,

$$C_i = \frac{FIU * m_L}{Q} * \frac{t_{inlet}}{t_{ref}} \quad (39)$$

where:

t_{inlet} = the testing duration for the PM10 inlet (hr), and

t_{ref} = the testing duration for the isokinetic sampler (hr).

The inclusion of a time factor allowed for shorter overall testing periods as the isokinetic testing times could be reduced relative to the candidate inlet while still maintaining acceptable signal-to-background ratios.

The performance of the PM10 inlet was described by the penetration curve of the inlet, which relates sampling efficiency to particle size. The sampling effectiveness curve for the PM10 inlet was constructed by plotting the fractional penetration of different particle sizes through the PM10 inlet. In Subpart D PM10 inlet testing, the particle sizes that make up the penetration curve are listed in table 1. The fractional penetration for each particle size was determined by dividing the concentration of particles collected through the PM10 inlet by the reference concentration from the isokinetic sampler as shown in equation 40.

$$\text{Effectiveness} = \frac{C_{\text{inlet}}}{C_{\text{ref}}} \quad (40)$$

The penetration of the particles was calculated for each PM10 inlet-isokinetic inlet pair. The fractional penetration of all tests for a given particle size were required to have a coefficient of variation (COV) less than 10% to be considered valid (CFR, 1987b). COV was calculated using equation 41.

$$\text{COV} = \frac{s}{\bar{x}} \quad (41)$$

where:

s = the sample standard deviation of the calculated fractional penetrations, and

\bar{x} = the average of the calculated fractional penetrations.

Model Development and Selection

Two curves were fit to the data to estimate and model the sampler effectiveness: the lognormal distribution and a piecewise function. The lognormal distribution function was used to generate the fractional efficiency curve for the performance of an inlet. Equation 42 was the lognormal distribution function used to predict the sampling effectiveness of any given particle size based on the cut point and slope performance parameters of a sampler.

$$\eta_{p,ln} = 1 - \frac{1}{d_p * \ln(\text{slope}) * \sqrt{2\pi}} \exp \left[\frac{-(\ln(d_p) - \ln(d_{50}))^2}{2 * (\ln(\text{slope}))^2} \right] \quad (42)$$

where:

$\eta_{p,ln}$ = fractional sampling effectiveness for particle size d_p calculated with the lognormal function

d_p = particle size (um),

d_{50} = cut point or the particle size at which a sampler has a 50% sampling effectiveness, and

slope = the performance slope of the PM10 inlet.

The “slope” of the lognormal distribution can be calculated as shown in equation 43 (Cooper and Alley, 2002). Calculating the slope was done the same way as calculating the GSD (equation 28).

$$\text{slope} = \frac{d_{84.1}}{d_{50}} = \frac{d_{50}}{d_{15.9}} = \sqrt{\frac{d_{84.1}}{d_{15.9}}} \quad (43)$$

where:

$d_{84.1}$ = particle size at which a sampler has a 84.1% collection efficiency, and

$d_{15.9}$ = particle size at which a sampler has a 15.9% collection efficiency.

Microsoft Excel® was used to fit the lognormal curve to the data by minimizing the sum of square errors between observed effectiveness values and the fitted curves (equation 44). Once the best fit curve was found, the cut point and slope were calculated.

$$\left(\sum(E_i - \eta_{ex,i})^2\right) = \text{minimum} \quad (44)$$

where:

E_i = measured sampling effectiveness for particle size i , and

$\eta_{ex,i}$ = expected (i.e. modeled) sampling effectiveness for particle size i .

A second model, using piecewise functions, was used to fit several sub-functions to different sections of the data collected and produce a fractional efficiency curve for the inlet. The functions were derived and fit to the data in such a way as to maximize the coefficient of determination (R^2) between the data and the piecewise sub-functions. Specific piecewise functions were generated for each wind speed.

The fractional efficiency curves generated by the two models for each wind speed were then compared to the data collected at that wind speed using a single factor Analysis of Variance (ANOVA). This comparison was conducted at a confidence level of 95%. The model that fit collected data best, denoted as having the lowest p-value from the ANOVA, was used for the remainder of the analyses.

Particle Size Distribution Correction

Historically, it was believed that the samples collected by the LVTSP inlet were representative of the ambient PSD being sampled. The samples were used to produce a

“measured” PSD and closely followed a lognormal distribution with characterized by a MMD and GSD. Using the FEC described by the model selected in the previous analysis and the measured PSD, the real ambient PSD was predicted. Equations 45 and 46 were used to predict the amount of a particle with diameter d_p present in the ambient PSD.

$$PSD_{amb}(d_p, WS) = \frac{\eta_{PSDm, \ln(MMD, GSD, d_p)}}{FEC(d_p, WS)} \quad (45)$$

where:

$PSD_{amb}(d_p, WS)$ = the ambient particle size distribution at a particle with diameter d_p (um) and wind speed of WS ($km\ h^{-1}$);

$\eta_{PSDm, \ln(MMD, GSD, d_p)}$ = the measured particle distribution as a function of a specified MMD and GSD and at a particle with a diameter d_p (equation 46); and

$FEC(d_p, WS)$ = the fractional efficiency curve of the inlet at a wind speed of WS ($km\ h^{-1}$) evaluated for a particle of diameter d_p (um).

$$\eta_{PSDm, \ln(MMD_m, GSD_m, d_p)} = \frac{1}{d_p * \ln(GSD_m) * \sqrt{2\pi}} \exp \left[\frac{-(\ln(d_p) - \ln(MMD_m))^2}{2 * (\ln(GSD_m))^2} \right] \quad (46)$$

where:

MMD_m = the MMD of the measured PSD (um); and

GSD_m = the GSD of the measured PSD.

Using equation 45, the ambient PSD of the sampled material was predicted across a range of particle sizes from 0.1 to 100 micrometers. A lognormal curve (equation 46) was fit to the ambient PSD while minimizing the sum of square error (equation 44) between the predicted ambient PSD and the lognormal curve, following the same process that was used to fit the lognormal distribution to the collected data. The fitted curve was

then normalized by dividing the predicted PSD fraction for a particular particle size by the sum of all fractions for the predicted PSD across the range. The normalized, predicted PSD developed through this process was considered the idealized ambient PSD, or simply, the ideal PSD. It was believed this ideal PSD would closely resemble the ambient PSD.

The ideal PSD was characterized by an expected MMD and GSD, determined during lognormal curve fitting, which were then compared to the MMD and GSD values of the measured PSD to determine how similar the two values were. The percent error between the measured and predicted MMDs and GSDs were calculated with equations 47 and 48.

$$\%Err\ MMD_m = \frac{MMD_m - MMD_T}{MMD_m} * 100\% \quad (47)$$

where:

$\%Err\ MMD_m$ = the percent error of the measured MMD; and

MMD_T = the MMD of the idealized PSD (μm).

$$\%Err\ GSD_m = \frac{GSD_m - GSD_T}{GSD_m} * 100\% \quad (48)$$

where:

$\%Err\ GSD_m$ = the percent error of the measured GSD; and

GSD_T = the GSD of the idealized PSD.

The process described above was repeated for a number of measured PSDs described by all combinations of MMDs, ranging from five to 30 micrometers in one-micrometer increments, and GSDs, ranging from 1.5 to 4 in 0.1 increments. This yielded an expected MMD and GSD for each combination of measured MMD and GSD. The percent error between the expected and measured MMDs and GSDs described how under

(negative) or over (positive) representative the measured MMD and GSD are of the expected PSD.

After evaluating the true MMD and GSD, the expected PSD was directly compared to the measured PSD to determine the difference between the two curves. This delta was denoted as the “bias” and was calculated for each particle size from 0.1 to 100 micrometers.

$$\text{bias}(d_p, WS) = \frac{\text{PSD}_{\text{amb}}(d_p, WS)}{\eta_{\text{PSDm,ln}}(\text{MMD}_m, \text{GSD}_m, d_p)} = \frac{1}{\text{FEC}(d_p, WS)} \quad (49)$$

The sum of all the bias for a measured MMD and GSD and wind speed combination for across the particle range was known as the correction error and described the amount of error between the measured PSD and the true PSD.

Results and Discussion

Table 9 shows the sampling effectiveness values for wind tunnel testing of the LVTSP inlet at the nominal wind speeds of 2, 8, and 24 km h⁻¹. This data is shown graphically in figure 17.

Table 9. Sampling effectiveness results for the LVTSP.

Nominal Wind Speed (km h ⁻¹)	Particle Size		Sampling Effectiveness ^[b,c]	COV (%)	Standard Deviation
	Nominal (µm)	Measured ^[a] (µm)			
2	5±0.5	5.31	1.41±0.114	4.18	0.059
	10±0.5	9.90	1.36±0.150	5.74	0.078
	11±0.5	10.80	1.38±0.198	7.46	0.103
	13±1.0	12.40	1.29±0.164	6.59	0.085
		13.41	1.26±0.208	8.57	0.108
	17±1.0	17.59	1.26±0.242	10.00	0.126
	20±1.0	20.09	1.02±0.142	7.25	0.074
	25±1.0	25.01	0.943±0.073	4.03	0.038
8	3±0.5	3.10	1.206±0.030	1.29	0.016
	5±0.5	5.03	1.147±0.096	4.36	0.050
	7±0.5	7.10	1.063±0.117	5.73	0.061
	9±0.5	8.80	0.938±0.134	7.45	0.070
	10±0.5	10.05	0.903±0.080	4.62	0.042
	13±1.0	13.60	0.799±0.100	6.54	0.052
	15±1.0	15.20	0.561±0.081	7.49	0.042
	20±1.0	20.20	0.572±0.026	2.39	0.014
24	25±1.0	24.86	0.506±0.071	7.33	0.037
	5±0.5	5.29	0.465±0.084	9.41	0.044
	11±0.5	10.99	0.359±0.083 ^[d]	12.06	0.043
	15±1.0	14.02	0.305±0.052	8.85	0.027
		15.22	0.249±0.045	9.36	0.023
	18±1.0	18.76	0.161±0.029	9.38	0.015
	20±1.0	21.11	0.111±0.019	8.87	0.010
	25±1.0	24.48	0.057±0.010	8.95	0.005

[a] Measured microscopically using flattening factor of 1.358 for liquid particles (Faulkner and Haglund, 2012).

[b] Mean ±95% confidence interval.

[c] Measured sampling effectiveness, not corrected for multipliants and satellites.

[d] COV exceeds 10%.

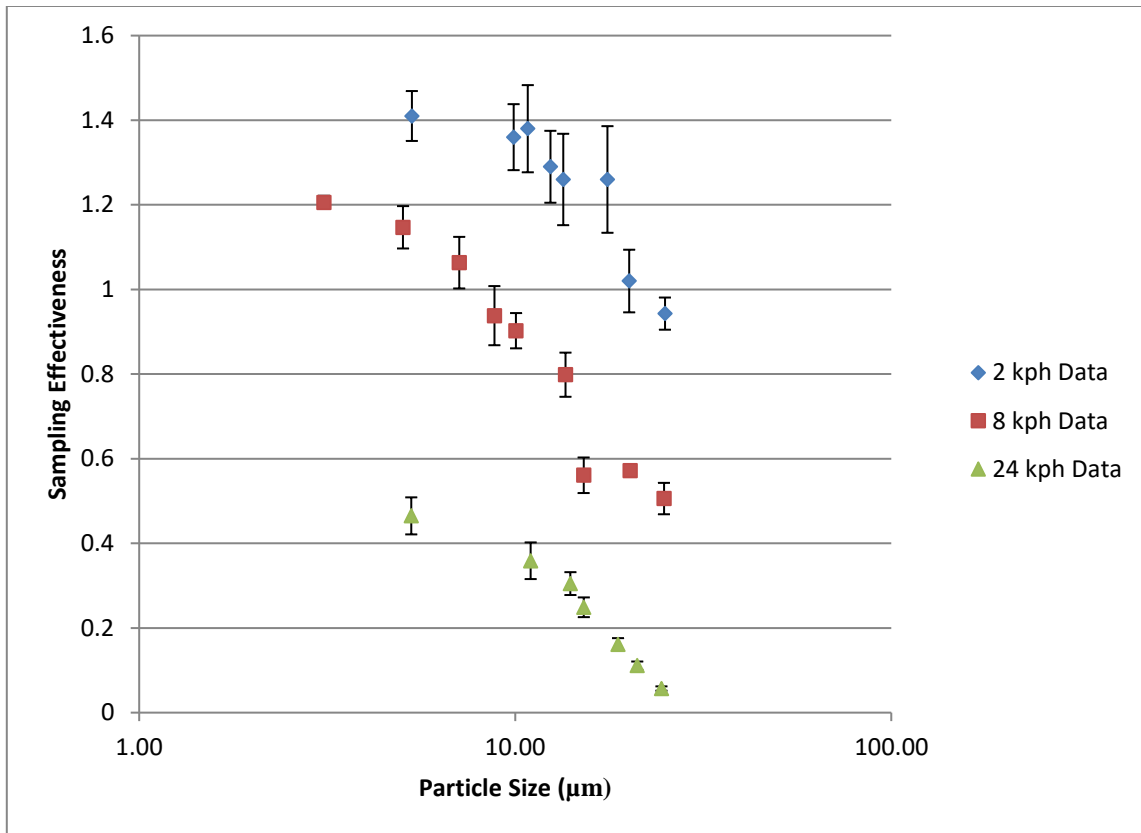


Figure 17. Sampling effectiveness results from the wind tunnel testing of the LVTSP.

According to the data shown in table 9 and the graph in figure 17, the performance of the LVTSP was heavily dependent upon wind speed.

Using the data collected with the Scoates Wind Tunnel, the lognormal and piecewise models were developed and fit to the data as described previously. The lognormal model parameters are shown in table 10 and the piecewise functions shown in table 11.

Table 10. Lognormal distribution model parameters for the LVTSP at each wind speed.

Nominal Wind Speed (km h ⁻¹)	d50 (um)	Slope	p-value
2	29.08	1.10	0.001
8	20.14	1.72	0.593
24	5.49	3.42	0.890

Table 11. Performance piecewise models for the LVTSP at each wind speed.

Nominal Wind Speed (km h ⁻¹)	Upper Bound (um)	Particle Size (um)	Lower Bound (um)	Functions	p-value
2	0	< d _p	≤ 8.1	1.4	0.841
	8.1	< d _p	≤ 44.2	1.61 - 0.026d _p	
	44.2	< d _p		0.46	
8	0	< d _p	≤ 5.3	1.05	0.890
	5.3	< d _p	≤ 30.4	$(-52E-7)d_p^4 - (4.1E-4)d_p^3 - 0.0102d_p^2 + 0.06348d_p + 0.93934$	
	30.4	< d _p		0.52	
24	0	d _p	≤ 25	0.59 - 0.022d _p	0.890
	25	< d _p		0.04	

As described previously, an ANOVA was conducted between the measured particle penetration data and the penetration predicted by the models for the particle sizes tested. As shown in table 10, the lognormal distribution models were not significantly different (p-value > 0.05) from the collected data ($\alpha = 0.05$), except for 2 km h⁻¹ wind speed (p-value < 0.05). However, in table 11 there was no significant difference between the data and the piecewise model for each wind speed. The piecewise models were selected to represent the performance of the inlet for continued analysis as they were

shown to be more statistically similar to collected data for each wind speed than the lognormal models. Figure 18 shows the piecewise models graphed alongside the collected data.

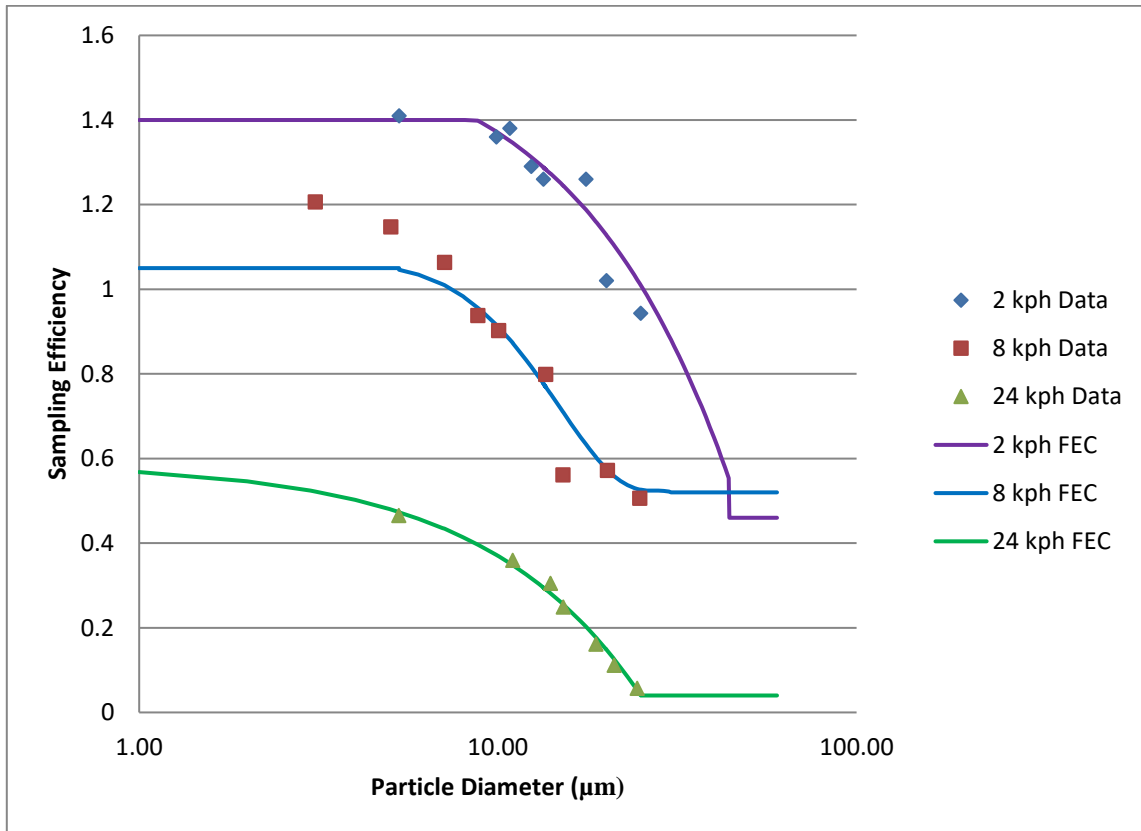


Figure 18. 2, 8, and 24 km h⁻¹ wind speed data graphed with the corresponding piecewise performance models.

While the piecewise models were selected as the more descriptive models of the sampler performance data, the particle size correction analysis was not conducted due to concerns about the collected data. Specifically, there was little agreement in inlet performance across the three wind speeds. It was hypothesized that the cause of the

discrepancies between the wind speeds could be one of or a combination of the following factors:

1. The LVTSP is susceptible to the variability in ambient wind speeds.
2. The design of the LVTSP is such that particles cannot consistently penetrate the sampler and impact on the filter.
3. There exists an unidentified issue with the wind tunnel or testing apparatus.

As part of an effort to generate a reference point for the sampling effectiveness of the LVTSP inlet, a second LVTSP inlet was provided to Dr. Robert Vanderpool of the EPA for testing in the Subpart D wind tunnel they maintain at Research Triangle Park in North Carolina. The wind tunnel used by the EPA is designed differently than the one used in this study (Vanderpool, 2016). Figure 19 showcases the result of the EPA testing of the LVTSP in their Subpart D wind tunnel.

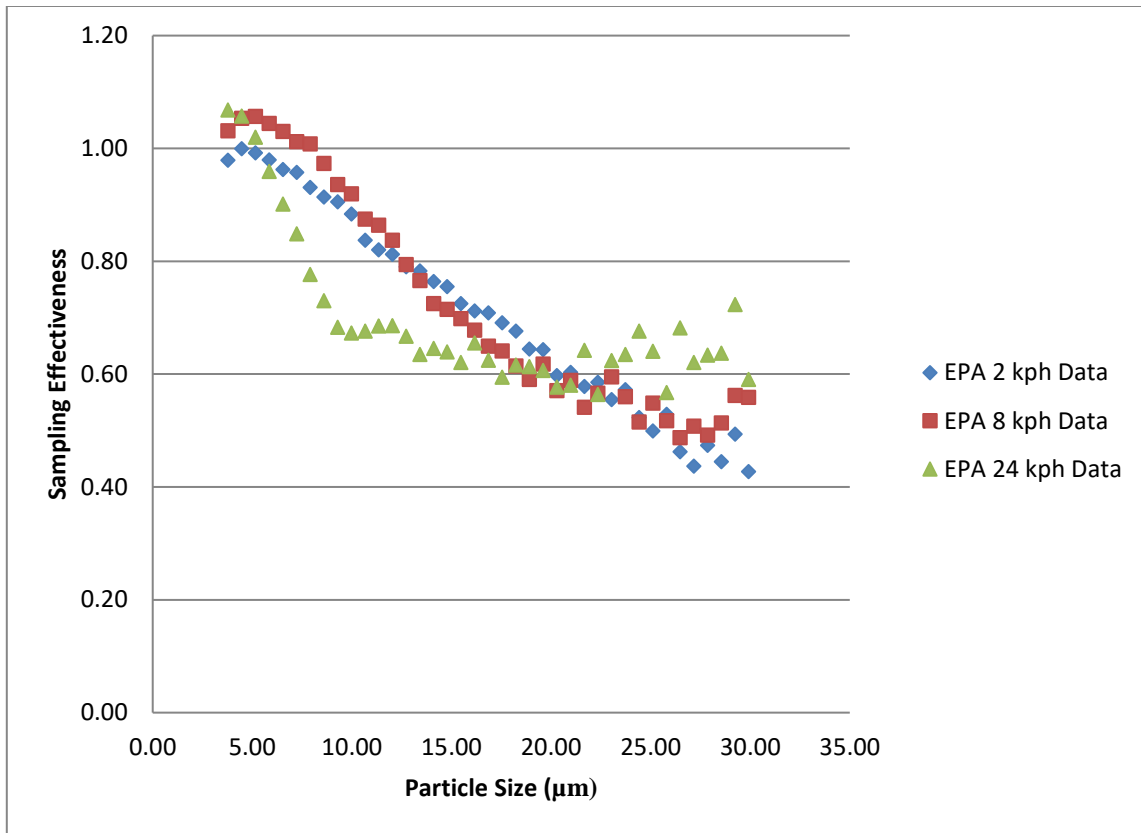


Figure 19. Data collected during the performance testing of the LVTSP by the EPA for each nominal wind speed (Vanderpool, 2015).

The data collected by the EPA shows a much tighter grouping than what was collect in the Scoates wind tunnel. To determine if the data collected by the EPA for the three wind speeds was significantly different across the nominal speeds, an ANOVA was conducted to compare each wind speed data set to the other. Additionally, each set of data collected by the EPA was compared to the piecewise performance curve developed in this study for the corresponding wind speed. The statistical results are shown in table 12.

Table 12. ANOVA comparisons of EPA data and the piecewise performance functions developed in this study.

Data Comparison ^[a,b]	p-value ^[c]	Significantly Different?
EPA 2 km h ⁻¹ v EPA 8 km h ⁻¹	0.72	No
EPA 2 km h ⁻¹ v EPA 24 km h ⁻¹	0.69	No
EPA 8 km h ⁻¹ v EPA 24 km h ⁻¹	0.43	No
EPA 2 km h ⁻¹ v TAMU 2 km h ⁻¹	0.00	Yes
EPA 8 km h ⁻¹ v TAMU 8 km h ⁻¹	0.94	No
EPA 24 km h ⁻¹ v TAMU 24 km h ⁻¹	0.00	Yes
EPA 2 km h ⁻¹ v TAMU 8 km h ⁻¹	0.77	No
EPA 24 km h ⁻¹ v TAMU 8 km h ⁻¹	0.48	No

[a] EPA refers to the data collected at each wind speed by the EPA when testing the LVTSP at their facilities.

[b] TAMU refers to the piecewise functions developed for each wind speed based on the data collected for the LVTSP with the Scoates wind tunnel.

[c] alpha = 0.05

The performance of the LVTSP inlet, as measured by the EPA, at each nominal wind speed was found to not be dependent on wind speed because there was no statistical difference between the three curves (table 12). The data sets collected by the EPA were then compared to the piecewise performance functions developed for the LVTSP inlet for each corresponding wind speed. While the curves for the EPA and TAMU data at 2 and 24 km h⁻¹ were statistically different from one another, there was no reason to reject the null hypothesis that the piecewise performance function at 8 km h⁻¹ was the same as the EPA 8 km h⁻¹ data (table 12). There were several possibilities for the differences in data sets and the discrepancies in the TAMU data:

1. The two inlets tested by Texas A&M and the EPA are different. Neither testing facility examined the same inlet and it is possible that there exists manufacturing defects in one or both inlets that will drastically affect performance.
2. While the wind tunnel initially met Subpart D requirements, the tunnel was not revalidated over the course of inlet testing. Regular, prolonged use or modifications to testing apparatuses may have had an effect on results.
3. Operator error and environmental changes (e.g. temperature, relative humidity, etc.).

There is currently no additional evidence to suggest which, if any, of the potential causes listed above may be responsible for the observed variations in the data.

Performance curves were developed for the LVTSP based on data collected in the Scoates wind tunnel. Current testing results of the LVTSP suggest that the inlet is sensitive to ambient wind speeds. A similar study of the LVTSP inlet conducted by the EPA produced performance results at 8 km h^{-1} that statistically agreed with the 8-km h^{-1} data collected in this study. However, the testing results from this study and the EPA at the wind speeds of 2 and 24 km h^{-1} were statistically different. Further investigation found that the 8-km h^{-1} performance curve developed for the LVTSP inlet was not statistically different from that data collected by the EPA at the wind speeds of 2 and 24 km h^{-1} . Based on this result, the 8-km h^{-1} curve may be suitable for use in estimating the performance of the LVTSP inlet with wind speeds up to 24 km h^{-1} in lieu of developing wind speed dependent functions.

Conclusion

The LVTSP was originally designed to provide a low flow, easily deployable option for collecting representative samples of ambient PM from which accurate ambient PSDs could be derived. The performance of the LVTSP inlet was evaluated following the methodology developed for evaluating FRM PM₁₀ inlets. Results indicated that the LVTSP did not collect a representative sample of ambient particulate matter and was susceptible to wind speed variability. Methodology was developed to mathematically predict ambient PSD after analyzing the collected sample, however analysis was not conducted due the wind speed dependency of LVTSP inlet performance. Further evaluation of the performance curves determined that of the three performance curves developed for the LVTSP inlet, only the 8-km h⁻¹ model was statistically similar to the data collected by the EPA for all wind speeds. It was concluded that the 8-km h⁻¹ performance model would best estimate the performance of the LVTSP inlet when exposed to wind speeds of up to 24 km h⁻¹. This performance curve could also be used to correct the results of previous studies that used this inlet or to correct field samples collected with the inlet for further analysis. However, additional studies should be conducted to further evaluate the performance of the LVTSP and its observed wind speed dependency prior to attempting to quantify the sampling bias of the inlet and using this process to reassess previous studies utilizing the LVTSP sampling results.

CHAPTER IV

COMPUTATIONAL FLUID DYNAMICS ANALYSIS OF PM10 INLET

Introduction

The Federal Clean Air Act (CAA) was originally enacted in 1963 in an effort to begin monitoring and regulating air pollutants that may endanger public health and welfare. The National Environmental Policy Act of 1970 established the Environmental Protection Agency (EPA), which is now responsible for developing and implementing air quality regulations under the authority of the CAA. The CAA amendments of 1970 required EPA to establish National Ambient Air Quality Standards (NAAQS) for six criteria pollutants, including particulate matter (PM). PM₁₀, defined as the fraction of “PM with an aerodynamic diameter (AED) less than or equal to a nominal 10 micrometers,” is one of the two fractions of PM currently regulated by EPA because it can penetrate to and deposit within the thoracic region of the human respiratory system (EPA, 2011).

For regulatory purposes, ambient concentrations of PM₁₀ are measured using Federal Reference Method (FRM) and Federal Equivalent Method (FEM) PM₁₀ samplers. Inlets for FRM PM₁₀ samplers, such as the PQ/PM₁₀ dichotomous louvered PM₁₀ inlet (PQ/PM₁₀; BGI Instruments; Waltham, MA), are widely deployed to measure PM₁₀ and PM_{2.5} concentrations.

The size distribution of the PM in any given region can be characterized by a particle size distribution (PSD), which may describe the distribution of particle mass, volume, or number of specifically sized particles contained in the aerosol. Ambient aerosols are often characterized by PSDs with one or more modes. Each mode can be characterized by a lognormal distribution described by a mass median diameter (MMD) and geometric standard deviation (GSD) (Hinds, 1999). The MMD describes the particle diameter at which half the total mass of the aerosol lies on either side of. The GSD is related to the ratio between the MMD and the particle diameters at where either 15.9% or 84.1% of the mass is less than (equation 50).

$$\text{GSD} = \frac{d_{84.1}}{\text{MMD}} = \frac{\text{MMD}}{d_{15.9}} = \sqrt{\frac{d_{84.1}}{d_{15.9}}} \quad (50)$$

where:

$d_{84.1}$ = the particle diameter at 84.1% of the total mass; and

$d_{15.9}$ = the particle diameter at 15.9% of the total mass.

The Code of Federal Regulations (CFR) Title 40, Part 53 (1987a) states that any inlet that is to be used in monitoring networks for PM₁₀ NAAQS compliance must be designated as either a FRM or FEM sampler inlet. Inlets are classified as FRM inlets if they meet the requirements of 40 CFR Part 53. Subpart D of 40 CFR Part 53 (hereafter “Subpart D”) states that FRM PM₁₀ inlets are designed to perform with a cutpoint (d₅₀) of 10±0.5 micrometers (μm). The d₅₀ of a sampler is the particle size at which 50% of the particles of that size penetrate the inlet to the filter and the remaining 50% are removed from the sampled air upstream of the filter. Candidate inlets must also pass a series of rigorous tests to achieve FRM designation. Subpart D outlines the procedures and

requirements for testing candidate PM10 inlets with mono-dispersed liquid and solid particles in the controlled confines of a wind tunnel. Per Subpart D, the sampling effectiveness for ten specific particle sizes across three wind speeds is determined with a minimum of three replicates per particle diameter to establish repeatability (table 1).

Sampling effectiveness values for particles of various sizes are used to generate a performance curve for the sampler. This curve is considered the performance curve of the inlet and is often referred to as the Fractional Efficiency Curve (FEC). The FEC shown in figure 1 was constructed using the “ideal” sampler penetrations of specific particle sizes shown in Table D-3 (CFR, 1987b) of Subpart D.

Candidate inlets that do not meet the performance standards required by Subpart D cannot receive FRM designation or be deployed in monitoring networks to collect and report PM10 emissions.

Testing inlets per the requirements of Subpart D is both time consuming and costly. In order to determine the performance of a candidate inlet per Subpart D, one must have a wind tunnel with the ability to achieve both the wind speeds and cross sectional wind speed uniformity, a vibrating orifice aerosol generator to produce mono dispersed particles from solutions of varying concentrations of uranine (liquid particles) or ammonium fluorescein (solid particles), a microscope or aerosol particle sizer to measure the particle sizes and determine the concentration of particles that are or are not the correct size, a reliable flow system to consistently deliver the required flow rate to the candidate inlet, and a fluorometer with specific light wavelength filters to analyze the solutions containing captured particles.

In addition to the cost of equipment to conduct Subpart D analyses, a minimum of 96 tests must be conducted to complete the Subpart D testing. This number includes three tests at each particle size and wind speed combination to demonstrate the repeatability of the candidate inlet's performance. Additional tests may be needed due to issues with equipment. Test times will increase as the size of the particles being evaluated increases. This is due to a decreased number of particles penetrating the inlet's impactor and the need to overcome analysis equipment signal-to-noise concerns.

For inlets that do not pass Subpart D testing initially or to decrease the amount of time an inlet needs for Subpart D evaluation, it may be possible to use computational fluid dynamics (CFD) to estimate the results of Subpart D testing prior to physically conducting the tests with the inlet. Computational fluid dynamics is a robust tool that can be used to model the motion and deposition of particles under the influence of specific flow fields and conditions. Use of this tool could allow for quicker, more effective evaluation of FRM candidate inlets. Additionally, application of this tool during the design phase of candidate inlets would allow inlet development to focus on specific design considerations that could improve the performance of their inlet.

The objective of this research was to determine if computational fluid dynamics software could be used to return statistically similar performance results for an inlet as those produced through Subpart D testing. This study is a proof of concept demonstration that analyzed the various penetration efficiencies of particles sized as shown in table 1 through the impactor section of the SA246b FRM PM10 inlet (identified in figure 20).

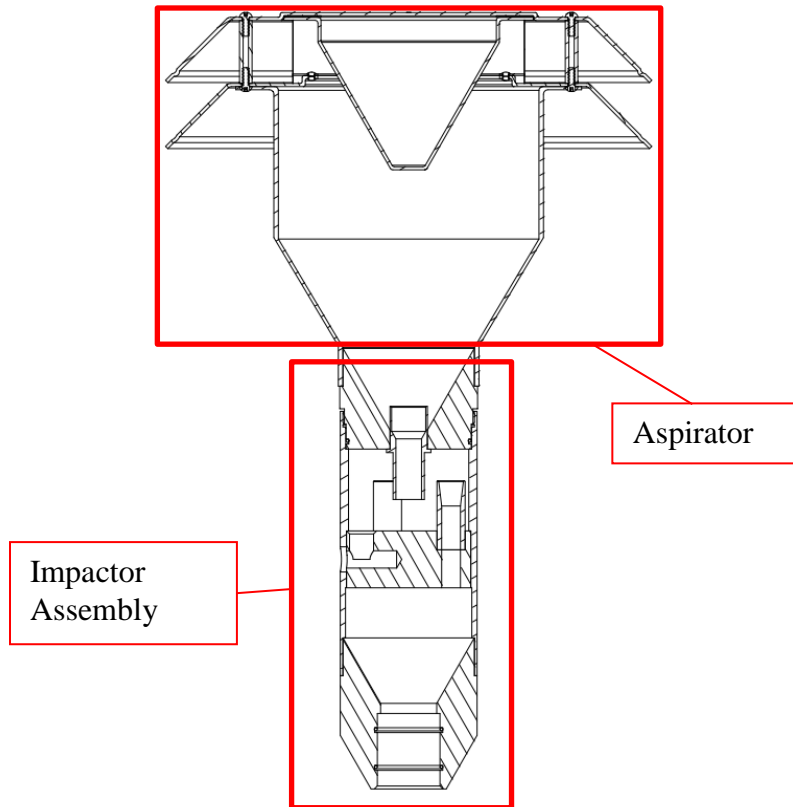


Figure 20. Hatched view of the SA246b FRM PM10 inlet by BGI Instruments.

Methodology

Determination of Inlet Performance Characteristics with a Subpart D Wind Tunnel

Subpart D wind tunnel testing of an FRM PM10 inlet, the SA246b, was previously been conducted and discussed as part of this thesis work in Chapter 2. The results of that study were used in this analysis of the CFD modeling of the SA246b impactor.

Calculation of SA246b Impactor Characteristics using CFD

Computational fluid dynamic is a numerical analysis to model fluid flow systems. Star CCM+ (STAR CCM+, V5.06.010, CD-adapco, Melville, NY) was the CFD program

that was used to model the motion and deposition of particles injected into the Lower Inlet Assembly, simply known as the impactor assembly for this study, of the SA246b shown in figure 21.

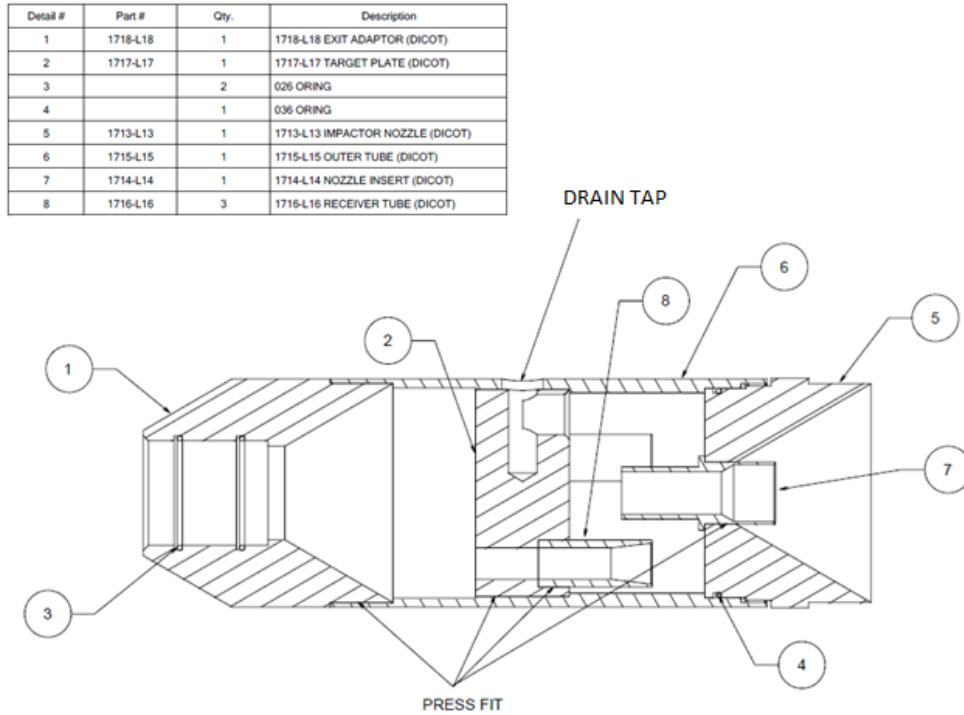


Figure 21. "Lower Inlet Assembly" of the SA246b inlet (BGI Instruments). No dimensions are included to prevent the divulging of proprietary information.

In order to perform a successful computational fluid dynamics simulation, several steps were involved. The initial step was the reproduction of the specified impactor nozzle in a 3D drawing program. SolidWorks (2009 SP2, Dassault Systèmes, Concord, MA) was used to draw and assemble the parts of the impactor assembly into a single piece based on manufacturing schematics of the SA246b inlet, provided by BGI Instruments. The

dimensions of the inlet provided by BGI Instruments are considered proprietary information and will not be presented here in full, but critical dimensions are: the smallest diameter of the nozzle insert was 0.013 meters (0.512 inches); the distance between the nozzle insert and the impaction plate surface was 0.015 meters (0.575 inches); and the receiver tube diameters were 0.01 meters (0.375 inches). The finished drawing was then exported as a specific file extension (a STL file) for later importation into Star CCM+.

After importing the SolidWorks drawings into Star CCM+ and confirming that drawn parts imported correctly, additional components were added to the assembly. Inlet and outlet derived parts (i.e. planes or shapes placed at the inlet and outlet of the impactor assembly that will be used in the CFD simulation to make calculations, measurements, or perform actions such as injecting particles into the system) were developed and added to the impactor assembly in order to insert the particles and determine the mass flux of particles leaving the inlet. The inlet derived part was a cylinder inserted at the top of the impactor assembly (where bubble 7 is physically located in figure 21) with a diameter to match that of the impactor nozzle (figure 21, balloon 5). This derived part was used to inject the particles into the impactor assembly. The outlet derived part was a cylinder inserted at the outlet of the of impactor assembly, where the O-rings marked with balloon 3 in figure 21 are located. The outlet derived part will be used to provide the 1 cubic meter per hour (16.67 liters per minute) of suction that the SA246b was designed to operate with and to measure the amount of particles, injected into the system by the inlet derived part, that penetrate the impactor. Particles that pass through the outlet derived part are particles that penetrate the impactor and would be collected on the filter for gravimetric analysis.

Prior to simulating flow fields or particle behavior in the impactor assembly, a mesh was generated. The meshing process produced a new part that was formed from the void space within the impactor assembly, referred to as a volume mesh. To generate the volume mesh, the assembly and added parts were selected and used to generate a new region with the “one boundary per part surface” and “one feature curve per part curve” options selected. Next, a new mesh was introduced into the continua. The meshing models used in this project were the surface remesher, the surface wrapper and the polyhedral mesher. After selecting the meshes, the reference values of the meshes were adjusted as follows:

- The base size was set equal to 0.013 m (the diameter of the nozzle insert),
- The surface curvature was set to 100,
- Surface growth rate was set to 1.2,
- Surface proximity was set to 5E-5,
- The relative minimum surface size was set to 2.5%, and
- The relative target size was set to 25%.

Using these settings, the surface mesh and volume mesh were generated. Figure 22 is a screenshot of the completed volume mesh.

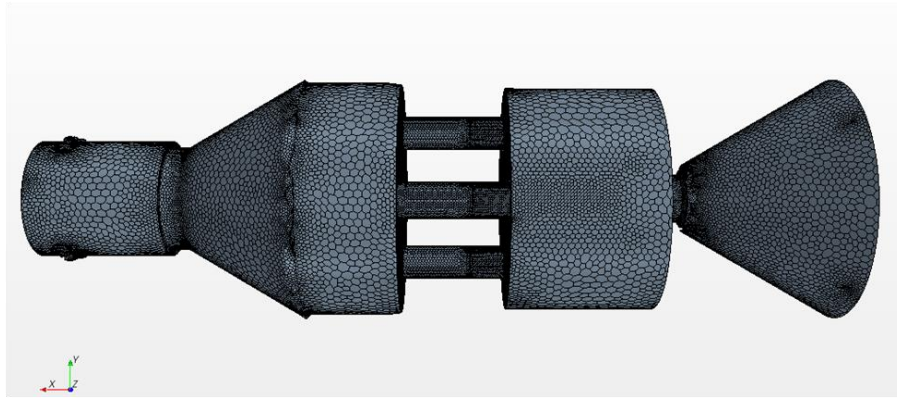


Figure 22. Volume mesh results.

Next, the flow field was generated. The simulated flow field was comprised of all the streamlines on which the particles may travel. To produce the flow field, several control models were chosen in Star CCM+: the generic flow model with air (as an ideal gas) as the working fluid, three-dimensional flow, two-layer all y^+ treatment, and the two-layer linear pressure strain models. Gravity was also considered to act in the x direction (as if the inlet were upright, as in normal operation) of the compass shown in figure 22.

Before determining which flow models to use in the simulation, a Reynolds number calculation was performed. This calculation determined which flow model was most appropriate. Reynolds number was calculated using equation 51.

$$Re = \frac{\rho V d}{\mu} \quad (51)$$

where:

ρ = the density of the working fluid (air) in the system (1.2 kg m^{-3} at 20°C and 760 mmHg),

V = the relative velocity of the working fluid (m s^{-1}),

d = the smaller diameter of the nozzle insert (1.3E-02 m), and

η = the viscosity of the working fluid (air) (1.86E-05 at 20°C and 760 mmHg).

For Reynolds Numbers less than 2,300, the flow is considered laminar. If the Reynolds' number is greater than 4,000, the flow is considered turbulent. The remaining Reynolds number values fall into the transitional region where the flow may be either laminar or turbulent. Based on the supplied flow rate to the inlet of 16.67 L min⁻¹ and the nozzle diameter of 1.3E-02 m, the velocity of the working fluid through the nozzle was determined to be 2.09 m s⁻¹. This air velocity resulted in a Reynolds number of 1759.65, or laminar flow through the nozzle.

Regardless of the Reynolds number determination, two sets of simulations were run on the impactor assembly using turbulent or laminar flow models, with the control models kept constant between the simulations. For the turbulent flow simulation, the Reynolds stress turbulence, steady flow, and turbulent flow models were added to the system. The turbulent flow simulation was conducted based on the conservative assumptions that a greater degree of mixing occurs in the impactor nozzle, and that the flow through the nozzle, impactor area, and the receiving tubes of the assembly actually experienced turbulent flow. In the laminar flow simulation, only the laminar flow model was used.

The control and flow models were used together to simulate the 16.67 L min⁻¹ of flow rate through the impactor assembly over 1000 iterations to produce flow and vector flow fields. a color graded flow field and vector field were generated. Two dimensional,

cut away views of the resulting internal laminar and turbulent flow fields are shown in figures 23a and 23b, respectively.

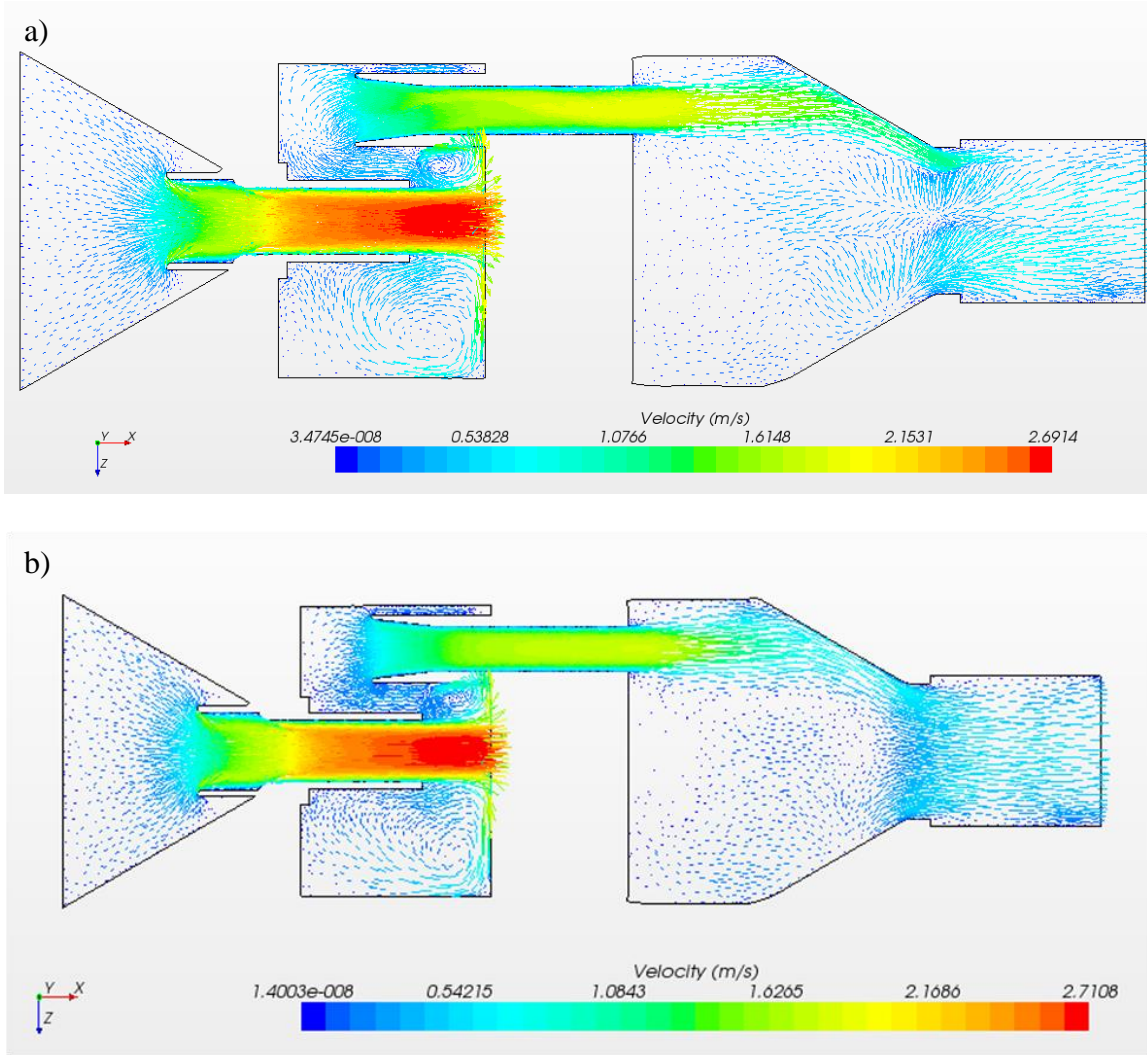


Figure 23. Resulting (a) laminar vector flow field simulation and (b) turbulent vector field simulation.

Following flow field simulation, particle tracking was setup and conducted using a Lagrangian Phase particle model that included drag force on liquid particles with a density of 937.7 kg m^{-3} in order to emulate the behavior of uranine-tagged, oleic acid

particles used in Subpart D wind tunnel evaluations. Particles were set to be removed from the system if they came into contact with a surface. An injector was then set up on the surface inlet derived part to inject particles into the impactor assembly. To ensure that enough particles were injected into the system, particles were injected at a mass rate of 1 kg s^{-1} . While this mass flow rate value was much higher than what would typically be seen during Subpart D testing, there was no buildup of particles that may cause the system to act differently over time. The outlet derived part was set up report the mass flux of particles across its service for use in determining the penetration of particles through the impactor assembly. Penetration was calculated using equation 52.

$$P = \frac{SA * MF_o}{\dot{m}_{in}} \quad (52)$$

where:

P = the fraction penetration efficiency,

SA = the surface area of the outlet derived part ($7.9E-4 \text{ m}^2$),

MF_o = the mas flux of particles exiting the impactor assembly ($\text{kg m}^{-2} \text{ s}^{-1}$), and

\dot{m}_{in} = the mass flow rate of particles injected into the assembly by the inlet derived part (1 kg s^{-1}).

CFD Model Evaluation

Once enough data was collected, the cutpoint and slope performance characteristics of the impactor assembly were determined. The cutpoint was the particle size at which fractional penetration was equal to 0.5. The performance slope of an inlet was defined using equation 53 from Hinds (1999).

$$\text{slope} = \frac{d_{84.1}}{d_{50}} = \frac{d_{50}}{d_{15.9}} = \sqrt{\frac{d_{84.1}}{d_{15.9}}} \quad (53)$$

where

$d_{84.1}$ = the particle size at which the sampler has a 84.1% collection efficiency, and

$d_{15.9}$ = the particle size at which the sampler has a 15.9% collection efficiency.

The particle diameter of $d_{15.9}$ was also equivalent to the diameter at which 84.1% of the mass of the aerosol penetrates the impactor. Interpolation was used to estimate the particle diameters that would match the 50%, 84.1%, and 15.9% collection efficiencies.

The lognormal distribution function was used to generate the fractional efficiency curve for the performance of the impactor assembly based on the performance characteristics calculated from the CFD modeled data. The equation 54 was used to predict the sampling efficiency of the impactor assembly for any given particle.

$$\eta_{p,ln} = 1 - \frac{1}{d_p * \ln(\text{slope}) * \sqrt{2\pi}} \exp \left[\frac{-(\ln(d_p) - \ln d_{50})^2}{2 * (\ln(\text{slope}))^2} \right] \quad (54)$$

where:

$\eta_{p,ln}$ = fractional sampling effectiveness for particle size d_p calculated with the lognormal function

d_p = particle size (μm),

Typically, the slope function yields the same value no matter which form was used, however, due to the interpolation of the d_{50} , $d_{84.1}$, and $d_{15.9}$, three different lognormal distribution slopes were produced. The slope value that produced the lowest sum of square errors between the CFD results and the lognormal distribution model was selected and used for further analysis. The sum of square errors was calculated using equation 55.

$$\left(\sum (E_i - \eta_{ex,i})^2\right) = \text{minimum} \quad (55)$$

where:

E_i = CFD sampling effectiveness for particle size i , and

$\eta_{ex,i}$ = lognormal model sampling effectiveness for particle size i .

CFD Model Comparison

After obtaining the CFD lognormal performance curve for the impactor assembly, the model was compared to the ideal performance values of an FRM PM10 inlet and the results of the Subpart D wind tunnel testing conducted at 8 km h⁻¹ from Chapter 2 using the two-tailed paired t-test for two different particle size ranges:

1. particles with diameters between one and 50 micrometers; and,
2. particles with diameters between $d_{84.1}$ and $d_{15.9}$

The first comparison evaluated how well the two models agreed across a large range of particle sizes. The second comparison was used to determine how well the two models agreed around the cutpoint and performance slope of their curves.

After determining if the models were statistically similar, the CFD model was evaluated using the same evaluation process outlined in Subpart D. In this analysis, the sampling effectiveness curve produced from the CFD was multiplied with the corresponding interval mass concentrations provided by the EPA in Table D-3 of Subpart D to obtain the expected mass concentration. The expected mass concentrations were then summed across all the sizes to determine the expected sampler mass concentration,

$C_{sam(exp)}$ ($\mu\text{g m}^{-3}$). This value was then compared to the “ideal” expected mass concentration ($C_{ideal(exp)}$) for PM10 inlets (equation 56):

$$\Delta C = \frac{C_{sam(exp)} - C_{ideal(exp)}}{C_{ideal(exp)}} * 100\% \quad (56)$$

According to table D-1 of Subpart D, the expected and “ideal” mass concentrations, ΔC , must be within ten percent of each other.

Results and Discussion

The particle penetration of the impactor assembly results are summarized in the table 14 below.

Table 13. CFD simulation sampling effectiveness results.

d_p (μm)	Turbulent			Laminar		
	Mass Flux ($\text{kg m}^{-2} \text{s}^{-1}$)	Outlet Flux (kg s^{-1})	Sampling Eff.	Mass Flux ($\text{kg m}^{-2} \text{s}^{-1}$)	Outlet Flux (kg s^{-1})	Sampling Eff.
1	1221.23	0.97	0.97	1169.70	0.93	0.93
2	1223.64	0.97	0.97	1171.42	0.93	0.93
3	1218.77	0.96	0.96	1184.71	0.94	0.94
4	1221.78	0.97	0.97	1179.28	0.93	0.93
5	1223.25	0.97	0.97	1185.63	0.94	0.94
6	1218.83	0.96	0.96	1170.28	0.93	0.93
7	1210.87	0.96	0.96	1151.85	0.91	0.91
8	1191.35	0.94	0.94	1110.89	0.88	0.88
9	1169.52	0.93	0.93	1144.08	0.91	0.91
10	1158.36	0.92	0.92	1075.37	0.85	0.85
11	1107.42	0.88	0.88	1070.23	0.85	0.85
12	1121.64	0.89	0.89	1027.86	0.81	0.81
13	1110.95	0.88	0.88	988.50	0.78	0.78
14	1046.82	0.83	0.83	837.44	0.66	0.66
14.5	N/A	N/A	N/A	754.24	0.60	0.60
14.75	N/A	N/A	N/A	645.16	0.51	0.51
14.755	N/A	N/A	N/A	644.14	0.51	0.51
14.8	N/A	N/A	N/A	627.37	0.50	0.50
15	881.33	0.70	0.70	518.54	0.41	0.41
15.5	711.59	0.56	0.56	N/A	N/A	N/A
15.75	644.96	0.51	0.51	N/A	N/A	N/A
15.755	635.36	0.50	0.50	N/A	N/A	N/A
15.8	613.98	0.49	0.49	N/A	N/A	N/A
16	524.34	0.42	0.42	140.55	0.11	0.11
17	120.71	0.10	0.10	11.70	9.26E-03	9.26E-03
18	8.40	6.65E-03	6.65E-03	0.00	0	0
19	3.35	2.65E-03	2.65E-03	2.02	1.6E-03	1.6E-03
20	0.00	0.00	0.00	0.00	0.00	0.00
21	0.00	0.00	0.00	0.00	0.00	0.00

Interpolation of the data in table 14 was used to determine the values of d_{50} , $d_{84.1}$, and $d_{15.9}$. The resulting cutpoints and slopes are shown in table 15.

Table 14. Interpolation results of critical diameters.

Flow Model	Cutpoint (μm)	Slope Calculation		
		d84.1/d50	d50/d15.9	√(d84.1/d15.9)
Laminar	14.79	1.07	1.32	1.19
Turbulent	15.76	1.07	1.15	1.11

Based on the results of table 15, the laminar flow model produced a cutpoint closer to what is required by Subpart D than the turbulent flow model. These results coupled with the Reynolds number yielding a determination that the flow through the nozzle was laminar, resulted in including only the laminar flow data in the remaining analysis.

Using the laminar simulation results from table 15, the lognormal distribution curves were fit to the data. The resulting curves are shown in figure 24.

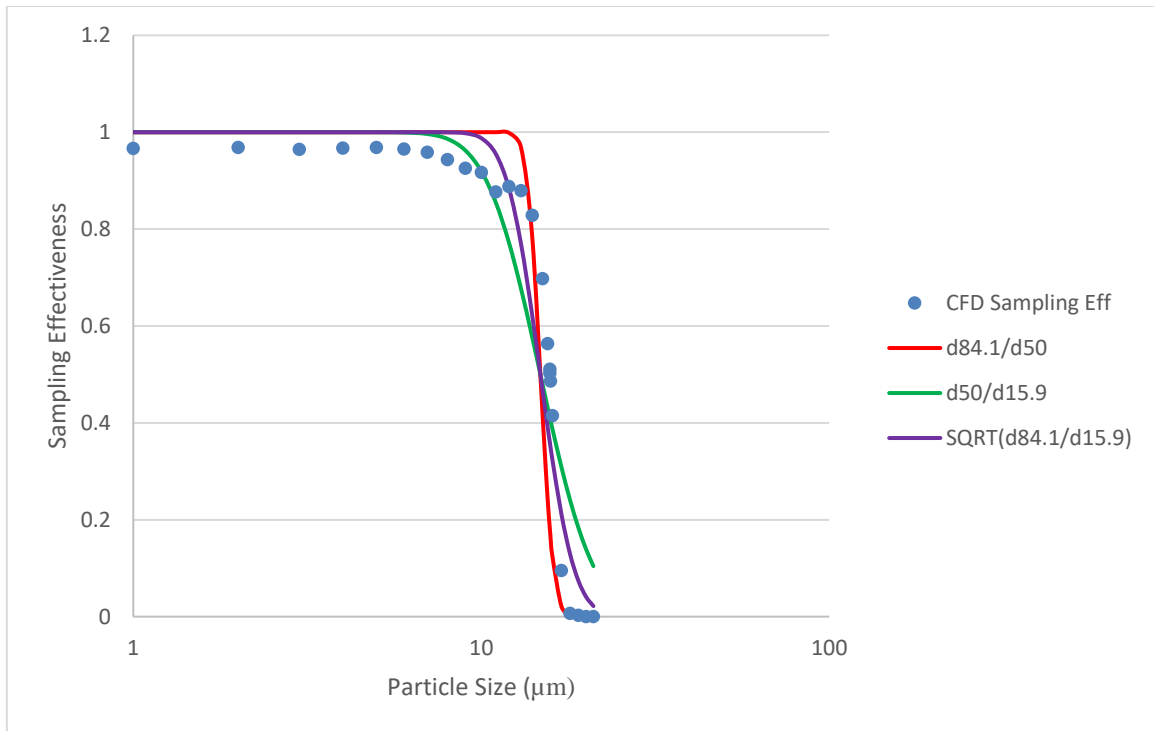


Figure 24. Laminar CFD lognormal curve fitting of modeling results with all three slope calculations.

The sum of squared errors for all three forms of the slope calculations for the laminar flow data is shown in table 16.

Table 15. Sum of Square error results between simulation and lognormal model.

Flow Model	Sum of Square Error (CFD v Lognormal)		
	d84.1/d50	d50/d15.9	$\sqrt{(d84.1/d15.9)}$
Laminar	0.64	0.38	0.27

The form of the slope function that produced the lowest sum of square error when comparing the lognormal curve fit to the simulation data was the third form of the function, where the performance slope was equivalent to the square root of $d_{84.1}$ divided by $d_{15.9}$, or

approximately 1.19. This slope was used in the remainder of the evaluation. The final form of the lognormal curve for the CFD analysis of the impactor assembly was described by a cutpoint of 14.79 μm and a slope of 1.19. An ANOVA analysis between the CFD simulation results and the lognormal curve fit revealed there was no statistical difference between the two data sets at a 95% confidence level (p-value of 0.6).

The laminar lognormal model and data set were graphed alongside the ideal FRM inlet sampling effectiveness curve and the Subpart D wind tunnel testing results in figure 25. Plotting the CFD performance curve with the Subpart D ideal and the SA246b performance curves from Chapter 2 expresses the difference in cutpoints between the CFD analysis and was previous evaluated.

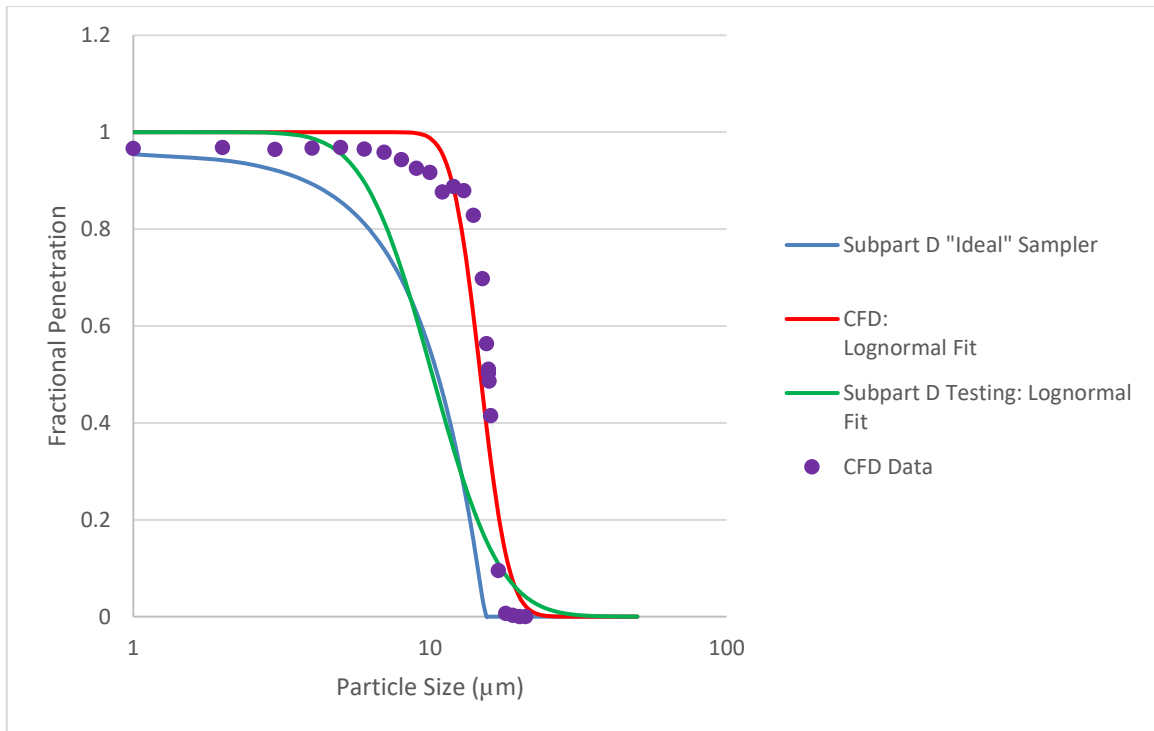


Figure 25. Graphical comparison of CFD results, the ideal sampling effectiveness for FRM PM10 inlets, and the Subpart D wind tunnel testing results.

According to the first paired t-test between the models across the full range of particle sizes, the models are statistically different (p-value of 0.0002) at a 95% confidence level. Further, the second analysis around the cutpoint of the two models also asserts that the two models are statistically different (p-value of 4.8E-5) at a confidence level of 95%. The paired t-test results demonstrate that CFD modeled curve was not equivalent to the performance curve developed for the SA246b in Chapter 2.

The CFD model was then used in the expected mass concentration analysis described by Subpart D. Table D-3 was adapted from Subpart D and completed as shown in table 17.

Table 16. Expected mass concentration for PM10 samplers (40 CFR Part 53 Subpart D - Table D-3).

d_p (μm)	CFD Lognormal Model			Ideal Sampler		
	Sampling Eff.	Interval Mass Concn. ($\mu\text{g m}^{-3}$)	Expected Mass Concn. ($\mu\text{g m}^{-3}$)	Sampling Eff.	Interval Mass Concn. ($\mu\text{g m}^{-3}$)	Expected Mass Concn. ($\mu\text{g m}^{-3}$)
<1.0	1.000	62.813	62.813	1.000	62.813	62.813
1.5	1.000	9.554	9.554	0.949	9.554	9.067
2.0	1.000	2.164	2.164	0.942	2.164	2.038
2.5	1.000	1.785	1.785	0.933	1.785	1.665
3.0	1.000	2.084	2.084	0.922	2.084	1.921
3.5	1.000	2.618	2.618	0.909	2.618	2.380
4.0	1.000	3.211	3.211	0.893	3.211	2.867
4.5	1.000	3.784	3.784	0.876	3.784	3.315
5.0	1.000	4.300	4.300	0.857	4.300	3.685
5.5	1.000	4.742	4.742	0.835	4.742	3.960
6.0	1.000	5.105	5.105	0.812	5.105	4.145
6.5	1.000	5.389	5.389	0.786	5.389	4.236
7.0	1.000	5.601	5.601	0.759	5.601	4.251
7.5	1.000	5.746	5.746	0.729	5.746	4.189
8.0	1.000	5.834	5.833	0.697	5.834	4.066
8.5	0.999	5.871	5.867	0.664	5.871	3.898
9.0	0.998	5.864	5.851	0.628	5.864	3.683
9.5	0.995	5.822	5.790	0.590	5.822	3.435
10.0	0.988	5.750	5.680	0.551	5.750	3.168
10.5	0.976	5.653	5.515	0.509	5.653	2.877
11.0	0.956	8.257	7.891	0.465	8.257	3.840
12.0	0.885	10.521	9.315	0.371	10.521	3.903
13.0	0.771	9.902	7.633	0.269	9.902	2.664
14.0	0.624	9.250	5.770	0.159	9.250	1.471
15.0	0.467	8.593	4.017	0.041	8.593	0.352
16.0	0.325	7.948	2.586	0.000	7.948	0.000
17.0	0.211	7.329	1.549	0.000	7.329	0.000
18.0	0.129	9.904	1.279	0.000	9.904	0.000
20.0	0.041	11.366	0.469	0.000	11.366	0.000
22.0	0.011	9.540	0.106	0.000	9.540	0.000
24.0	0.003	7.997	0.021	0.000	7.997	0.000
26.0	0.001	6.704	0.004	0.000	6.704	0.000
28.0	0.000	5.627	0.001	0.000	5.627	0.000
30.0	0.000	7.785	0.000	0.000	7.785	0.000
35.0	0.000	7.800	0.000	0.000	7.800	0.000
40.0	0.000	5.192	0.000	0.000	5.192	0.000
45.0	0.000	4.959	0.000	0.000	4.959	0.000
		C_{CFD} =	194.07		C_{ideal} =	143.889

The ΔC was determined to be 34.88% for the CFD lognormal model comparison. The calculated percent difference between the “ideal” and CFD model concentrations was not within the 10% requirement of Subpart D.

As demonstrated with figure 25, the statistical comparison, and the mass concentration analysis, the CFD results do not match the “ideal” sampler performance requirements of Subpart D or the empirically derived performance curve of the SA246b. It was hypothesized that the main reason behind this discrepancy was most likely due to the fact that only the lower section of the inlet was represented with the CFD simulation and not the complete assembly of the SA246b. Based on the work done by Nene (2006), the inlets of ambient samplers have performance characteristics due to the aspiration of the inlet itself, therefore, the FRM PM10 inlet performance of 10 ± 0.5 micrometers and a slope of approximately 1.5 must be achieved through a combination of the inlet aspirator and the impactor.

Conclusion and Future Work

In order to determine if the CFD simulation of a candidate inlet sampling effectiveness was an accurate method for measuring the inlet’s performance, CFD simulation was conducted on an inlet that had already achieved FRM designation. The impactor assembly of the FRM PM10 inlet, the SA246b manufactured by BGI Instruments, was recreated in SolidWorks, imported into Star CCM+, and challenged with an array of particle sizes using turbulent and laminar flow models. The laminar flow results were selected as the appropriate data to proceed with analyses. The resulting

sampling effectiveness values for the laminar were converted to a lognormal model that was not statistically different from the raw data. The CFD lognormal model was found to be statistically different from the “ideal” sampler effectiveness curve defined by Subpart D. The results of this study have shown that CFD simulation of the impactor assembly of the SA246b alone did not accurately estimate sampler performance. However, there are several additional items that can improve the results of the CFD simulation in future work.

The main goal of future work should be to conduct the simulation of the SA246b’s performance using both the aspirator and the impactor assembly. This would include importing the entire inlet into the CFD program and adding a derived part around the inlet to act as a wind tunnel. This would allow one to simulate the wind tunnel testing of Subpart D and the impact of aspiration on the sampling effectiveness results as compared to the results from the simulation of the impactor assembly alone. Figure 26 consists of screenshots of flow field generation from preliminary work on simulating performance of the complete SA246b assembly in Star CCM+.

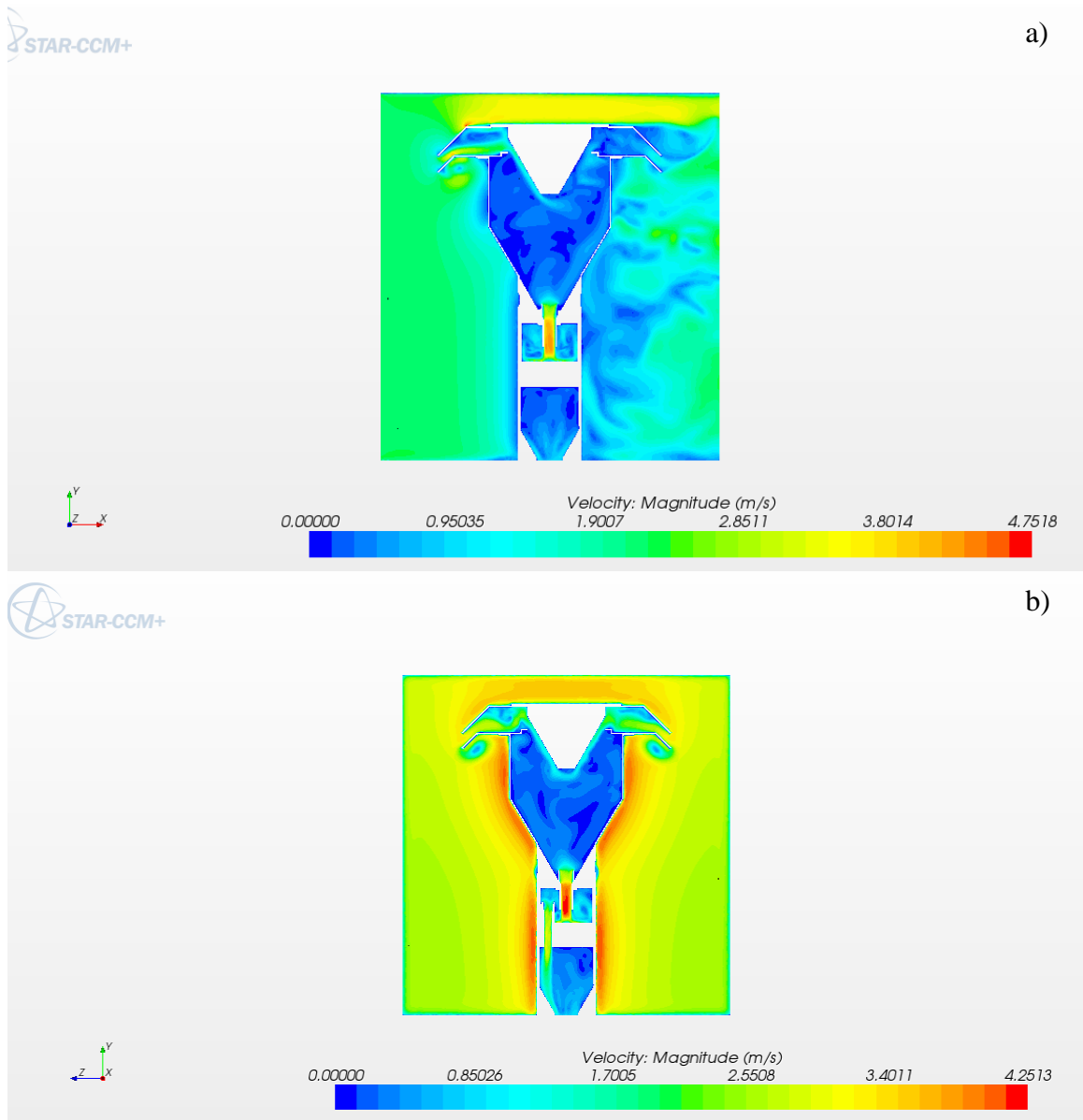


Figure 26. Preliminary flow field work for the SA246b taken from the (a) z-direction and (b) x-direction.

The next item that can improve future work is the optimization of the various model parameters. By increasing the density of polygons that are created through the meshing process, finer model estimates can be obtained. Additionally, the injector mass

flow rate of particles can be reduced from 1 kg s^{-1} to much more appropriate mass flow rates in order to ensure that this value is not adversely affecting the simulation results. The adjustment of these values will increase processing time and require additional computing power.

By incorporating these two concerns, a CFD simulation may produce a sampling performance curve that is statistically comparable to the “ideal” penetration curve of Subpart D and could be used to accurately predict sampler effectiveness.

REFERENCES

- AP-42: Compilation of Air Emission Factors. (1995). Fugitive Dust Sources. Retrieved from <http://www.epa.gov/ttnchie1/ap42/ch13/final/c13s02.pdf>
- Berglund, R. N., and Liu, B. Y. H. (1973). Generation of monodisperse aerosol standards. *Environmental Science and Technology*, 7(2), 147-153.
- BGI Instruments. (1997). Inlet assembly engineering drawings. Provided by BGI Instruments.
- Buser, M. D, Parnell Jr., C. B., Shaw, B. W., and Lacey, R. E. (2007). Particulate matter sampler errors due to the interaction of particle size and sampler characteristics: Ambient PM10 samplers. *Transactions of the ASABE*, 50(1), 229-240.
- Buser, M. D., Wanjura, J. D., Whitelock, D. P., Capareda, S. C., Shaw, B. W., and Lacey, R. E. (2008). Estimating FRM PM10 sampler performance characteristics using particle size analysis and collocated TSP and PM10 samplers: cotton gins. *ASABE*, 512(2), 695-702.
- Clean Air Act. (2004). The clean air act, 42 USC §7401. Retrieved from <http://www.epw.senate.gov/envlaws/cleanair.pdf>
- Code of Federal Regulations (1987a). Title 40 Part 53 Subpart A - Definitions.
- Code of Federal Regulations (1987b). Title 40 Part 53 Subpart D - Procedures for Testing Performance Characteristics of Methods for PM10.
- Cooper, C. D., and Alley, F.C. (2002). *Air Pollution Control*. 3rd ed. Long Grove, IL: Waveland Press, Inc.
- Faulkner, W. B., Shaw, B. W., Lacey, and R. E. (2007). Coarse fraction aerosol particles: Theoretical analysis of rural versus urban environments. *ASABE*, 23(2), 239-244
- Faulkner, W. B., and Haglund, J. S. (2012). Flattening coefficient for oleic acid droplets on treated glass slides. *Aerosol Science and Technology*, 46(7), 828-832
- EPA. (2006). Particulate matter (PM) standards – Table of historical PM NAAQS. Retrieved from https://www3.epa.gov/ttn/naaqs/standards/pm/s_pm_history.html
- EPA. (2011). Particulate matter (PM) basics. Retrieved from <https://www.epa.gov/pm-pollution/particulate-matter-pm-basics#PM>

- Haglund, J. S., Chandra, S., and McFarland, A. R. (2002). Evaluation of a high-volume aerosol concentrator. *Aerosol Science and Technology*, 36:690–696.
- Hinds, W. C. (1999). *Aerosol Technology*. 2nd ed. New York, NY. Wiley-Interscience.
- Kim, T. K., Seshadri, S., Kihm, K. D., Phares, D. J., and McIntyre, P. M. (2004). Visualization of defect particle transmission to the major flow of a slit virtual impactor. *Aerosol Science and Technology*, 38,870-880.
- McFarland, A. R and Ortiz, C. A. (1982). A 10 μm cut point ambient aerosol sampling inlet. *Atmos. Environ.* 16: 2959-2965.
- McFarland, A.R., and Ortiz, C.A. (1984). Characterization of Sierra-Andersen PM-10 inlet model 246B. Air Quality Laboratory Report, Texas A&M University, College Station, TX, 4716/02/02/84/ARM.
- Nene, R. R. (2006). Design of bio aerosol sampling inlets. MS thesis. College Station, Texas. Texas A&M University, Department of Mechanic Engineering.
- Tolocka, M. P., Peters, T. M., Vanderpool, R. W., Chen, F., and Wiener, R. W. (2001). On the modification of the low flow-rate PM10 dichotomous sampler inlet. *Aerosol Science and Technology*, 34: 407-415.
- TSI, Inc. (2009). Model 3450 vibrating aerosol generator operation and service manual. Rev. M. Shoreview, MN.
- Vanderpool, R. W. (2016). PM sampling: Collaborative study between Texas A&M and USEPA. Agricultural Air Quality Task Force Meeting. Sacramento, CA.
- VanOsdell, D. W., and Chen, F. L. (1990). Wind tunnel test report no. 28: Test of the Sierra Andersen 246B dichotomous sampler inlet. United States Environmental Protection Agency. U.S. Government Printing Office, Washington, D.C.
- Wang L., Parnell Jr., C. B., Shaw, B. W., Lacey, R. E., Buser, M. D., Goodrich, L. B., and Capareda, S. C. (2005). Correcting PM10 over-sampling problems for agricultural particulate matter emissions: Preliminary study. *Transactions of the ASABE*, 48(2), 749-755.
- Wanjura, J. D., Parnell Jr., C. B., Shaw, B. W., and Lacey, R. E. (2005). Design and evaluation of a low-volume total suspended particulate sampler. *Transactions of the ASAE*, 48(4), 1547-1552.

APPENDIX A

OPERATION OF THE SCOATES HALL 2X2 WIND TUNNEL

Scope: Outlines the start-up, testing parameters used, operation and shutdown of the 2x2 wind tunnel.

Purpose: To ensure the quality and repeatability of aerosol sampler evaluation tests in accordance with the Code of Federal Regulations, Title 40, Part 53, Subpart D.

PROCEDURE

1.1 General

The following procedures outline the appropriate way to effectively and accurately collect data for the characterization of Federal Reference Method candidate inlet according to Subpart D. This document will frequently reference other, separate procedures that must be used in tandem with this document.

1.2 Wind Tunnel Start Up

1. Turn on the wind tunnel, compressed air, PQ200, aerosol particle sizer (APS), frequency generator and HPLC pump.
 - a. Ensure that all equipment is plugged into it's appropriate power source.
 - b. To turn the wind tunnel on, flip the switch on safety box on the central column in the room to "ON," set the motor controller to the appropriate frequency using the up and down keys and pressing the "FWD" key on the motor controller. The frequency settings for desired wind speeds are shown in table A-1. Note that to achieve 24 km h⁻¹, the 4" squeezing panels must be installed inside the wind tunnel.

Table A-1. Frequencies required to generate specified wind speeds.

Wind Speed (km h ⁻¹)	Controller Frequency (Hz)	
	w/o Panels	w/ Panels
2	9.00	N/A
8	29.00	22.30
24	N/A	60.00

- c. To turn on the compressed, air, proceed to the West side of the room and find the compressed air line running under the window that is closest to the wind tunnel. Turn the valve counterclockwise until it is parallel with the air hose.
 - d. The switch to turn on the APS is located on the back of the device next to the power plug.
 - e. Press the red button on the front of the frequency generator to turn it on.
2. Turn on the HI-Q by flipping the switch on the front of the device to “ON.” Let the HI-Q warm up until it displays the main menu. Press the [1] key and then the [] key to display the flow rate in standard liters per minute.
3. Turn on the isokinetic pump by pressing the switch on the surge protector the pump is plugged into. Turn the isokinetic pump off prior to jet formation (Step 10).
4. Ensure that the HPLC pump input line is attached to the amber glass jar labeled “ETHANOL,” the drain valve switch on the VOAG is set to “OPEN” and the 500 mL glass beaker under the drain is empty. If the beaker is not empty, dispose of the contents by pouring them into the carboy located in the lab near the fluorometer.
5. Set the HPLC pump to a flow rate of 0.225 mL/min using the up and down arrow buttons. Press the “Prime” button on the HPLC pump and allow the pump to prime for 5 minutes. Stop the HPLC pump after 5 minutes by pressing the “Run/Stop” button.
6. Unscrew the “ETHANOL” jar from the HPLC pump inlet line cap by twisting the jar and not the cap to avoid tangling the lines. Transfer the cap to the selected particle solution and the screw the jar into the lid.
7. Once the cap is secured onto the test solution, prime the test solution for 5 minutes. Proceed to steps 8 through 10 while priming occurs.
8. Set the frequency generator parameters as follows:
 - a. Ensure that the BNC cable is connected to the “Output” port on the front of the frequency generator.
 - b. Rotate the frequency selector knob carefully until the desired frequency is displayed.
9. Fill out the System Data Wind Tunnel Log Sheet. If they need to be printed, the log sheets can be found on the research drive under Parnell on Research>Raleigh>Wind Tunnel>ScoatesTunnelLogSheets.xls. When printing, go to the print options and print the entire work book to obtain all 3 work sheets.
 - a. Fill the “System Data” form out as shown below (figure A-1). Include any additional information such as satellites appearing in APS samples, changes in frequency, etc. in the “Notes” section.

System Data

	Start-Up	Shut-Down
Date	3/19/2012	
Time	0930	1315
VOAG		
	Solution ID	10 um 1/12/2012
	Freq (khz)	56.7
	Press (psi)	Tank: 10 VOAG: 19
	O. Plate Size (um)	20
Tunnel Speed (km/hr)	8	
Barometric Pressure (mm HG)	756	
Temperature (C)	22.5	
Relative Humidity (%)		
APS file name: test_3_19_2012.A21		

Test Data

Test ID	1 - iso	2 - inlet	3 - iso	4 - inlet	5 - iso	6 - inlet
APS Sample #	3	4	6	8	9	10/11
Duration	30 min	1 hr				
Time Start						
Time Stop						

Notes:

Figure A-1. Example of the “System Data” form.

10. Using the recorded room temperature and pressure, calculate the flow set point for the isokinetic pump. To determine the set point, use equation 1 where Q_s is the flow rate set point in standard liters per minute, P_b is the barometric presume in millimeters of Mercury, and T is the room temperature in Kelvin.

$$Q_s = \frac{44.1375 * P_b}{T} \quad \text{Eq. 1}$$

11. Once the HPLC pump has primed for 5 minutes, disengage the prime function and ensure the pump is now operating at 0.225 mL/min.

**** The system is now ready for particle generation. See Appendix B, “Particle Generation,” for details. After successfully generating a particle stream, proceed with Section 1.3.

1.3 Wind Tunnel Operation/Testing

1. Inlets being tested in the wind tunnel are not collocated with reference samplers (isokinetic nozzles) so testing must be alternated between inlets and reference samplers for penetration calculations.
2. A minimum of 3 inlet tests are required per particle size per wind speed. There must be at least 1 reference sampler test per inlet test for comparison.
3. Any test conducted must be a minimum of 30 minutes in duration.
4. An APS sample must be taken before and after each test is started. The APS sample taken after one test counts as the APS sample prior to the subsequent test.

1.4 Taking an Isokinetic Sample

1. Number large filter and nozzle wash jars. Weigh and record the weight of the nozzle wash jars.
2. Take the appropriate sized isokinetic nozzle loaded with a filter and install the assembly in the wind tunnel.

Table A-2. Isokinetic Nozzle Sizes

Wind Speed (km/hr)	Isokinetic Nozzle Inlet Diameter (in)
2	2.6
8	1.3
24	0.75

- a. Open the access panel to the testing section of the wind tunnel.
- b. Place the support stand in the wind tunnel.
- c. Place the isokinetic inlet assembly inside the wind tunnel with the nozzle opening pointed at the wind tunnel entrance.
- d. Slip the open end of the 90-degree stainless steel fitting onto the upright stainless steel tube located inside the wind tunnel.
- e. Push the nylon ferrule and compression fitting up the tube and tighten the fitting onto the open threads of the 90-degree fitting.
- f. Move the stand located inside the wind tunnel under the isokinetic assembly to support the nozzle and prevent the assembly from being cantilevered on the vertical rod.
- g. Ensure that nozzle assembly is pointed directly at the wind tunnel intake (the direction particles will be coming from).

2. Close the access panel on the side of the wind tunnel.
3. Ensure the particle generation system is operating properly (see Particle Generation Appendix E) and that generated particles are being directed into the wind tunnel.
4. Start the isokinetic pump and the timer at the same time.
5. Once the desired testing time has been reached, stop the isokinetic pump. Record the testing duration.
6. Remove the panel from the side of the wind tunnel.
7. While wearing gloves, unscrew the isokinetic inlet assembly at the base and remove the entire assembly from the wind tunnel.
8. Unscrew the knurled sleeve of the isokinetic nozzle and set it to the side. Remove one glove.
9. Using the gloved hand, remove the isokinetic nozzle. Turn the nozzle upside down (smaller opening pointed down) over a nozzle wash jar. With the ungloved hand, use the isopropanol squirt bottle to apply the alcohol all around the inside of the nozzle. Additionally, spray the alcohol on the outside of the nozzle no more than an inch up the nozzle from the opening pointed down. Ensure all applied liquid is collected in the plastic jar. Because particles collected on the inlet are technically collected, this allows these particles to be considered as part of the analysis.
10. Weigh and record the weight and number of the jar used.
11. Screw a lid on to the nozzle wash jar.
12. Wipe nozzle inlet edge with a kim wipe to remove any hard residue and set aside to dry.
13. Extract the 90-mm filter from the inlet assembly using the ungloved hand and tweezers. Ensure that the tweezers DO NOT contact any of the sampling surface area as to prevent contamination. Place the filter in the larger filter jar.
14. Set assembly aside and remove/dispose of gloves.
15. Weigh the large filter jar with the filter in it. Record the weight and the number.
16. Add the isopropyl solution to the large filter draw. Add enough solution in order to fully submerge the filter.
17. Weigh the large filter jar with the filter and solution. Record the weight.
18. Screw a lid on to the large filter jar.
19. Let jars soak overnight before conducting the fluorometric analysis (see Appendix D).

1.5 Taking a SA246b Inlet Sample

1. Number filter jars.
2. Inspect the SA246b inlet for defects, obstructions, or other anomalies.
3. Open the access panel to the testing section of the wind tunnel.

4. Ensure the isokinetic nozzle support stand is not in the wind tunnel.
5. Place the SA246b inlet in the wind tunnel. The inlet should be placed in the large hole in the center of the test section.
6. Using fresh gloves and tweezers, place a 47-mm filter in the filter cartridge base (the side with the machined slits). Place the filter cartridge upper (the piece with the o-ring) onto the assembly and press the pieces together to ensure the assembly secures the filter properly.
7. Place the loaded filter cartridge in the filter holder and latch the holder closed. The filter cartridge should be placed in the filter holder such that the cartridge base is in immediate contact with the holder base. When the holder is closed, you should be able to look down the open end (the end opposite the hose connection) and have an unobstructed view of the filter.
8. Ensure that the hose from the PQ200 is securely screwed into the base of the filter holder.
9. Holding the SA246b inside the wind tunnel with one hand, use the other to insert the open end of the of the filter hold into the base of the SA246b inlet that should be visible on the underside (outside) of the wind tunnel testing section.
10. Remove gloves and secure the test section access panel.
11. Ensure the particle generation system is still producing particles and the particles are being directed into the wind tunnel.
12. Enter the appropriate options on the PQ200. Start the PQ200 and the timer at the same time. You may also use the programed time function on the PQ200.
13. Once the desired testing time has been reached, stop the PQ200. If using the internal timer on the PQ200, wait until the PQ200 is no longer drawing air through the sampling system. Record the testing duration.
14. Remove the filter folder from the SA246b by pulling the holder straight down.
15. While wearing gloves, open the filter holder and using one hand (Hand A), remove the filter cartridge from the holder. Set aside. Place the holder to the side.
16. If possible, remove the cartridge upper with Hand A. If unable to remove the upper piece by hand, using Hand B, insert a flat head screwdriver into the groove on the edge and twist slowly.
17. Once the upper piece is removed, set it aside. Pick up the filter cartridge base and turn it over so that that the filter falls out of the base and into one of the numbered filter jars.
18. Weigh the filter jar with the filter in it. Record the weight and the number.
19. Add the isopropyl solution to the filter draw. Add enough solution in order to fully submerge the filter.
20. Weigh the filter jar with the filter and solution. Record the weight.

21. Screw a lid on to the filter jar.
22. Let jars soak overnight before conducting the fluorometric analysis (see Appendix D).
23. Remove the SA246b from the wind tunnel by open the testing section access panel and, while wearing gloves, remove the inlet from the testing section. Place the inlet in its designated resting place.

1.6 Taking a LVTSP Sample

1. Number filter jars.
2. Open the testing section access panel and set aside.
3. Using fresh gloves and tweezers, place a 47-mm filter in the filter cartridge base (the side with the machined slits). Place the filter cartridge upper (the piece with the o-ring) onto the assembly and press the pieces together to ensure the assembly secures the filter properly. Set to the side.
4. While wearing gloves, inspect the round-top, LVTSP inlet for damage, blockages, or other anomalies. If you pick up or touch the inlet during inspection, only use one hand; that hand will be denoted as Hand A.
5. Using Hand A, place the LVTSP inlet in the PVC pipe used to hold and elevate the inlet. Undo the latch of the inlet and open the inlet.
6. Using Hand B, place the loaded filter cartridge in the open LVTSP inlet. Close and latch the inlet closed with Hand A
7. Remove the LVTSP inlet from the PVC pipe with Hand A and set aside.
8. Using Hand A, place the PVC pipe in the center of the testing section in the holder for the SA246b.
9. With Hand B, feed the air line from the PQ200 up through the sampler access port at the bottom of the testing section and through the PVC pipe.
10. With Hand A, pick up the LVTSP inlet and with Hand B screw the air hose from the PQ200 into the bottom of the LVTSP inlet.
11. With Hand A, place the LVTSP inlet back into the PVC pipe being careful to feed the excess air hose back down through the pipe.
12. Remove gloves and secure the test section access panel.
13. Ensure the particle generation system is still producing particles and the particles are being directed into the wind tunnel.
14. Enter the appropriate options on the PQ200. Start the PQ200 and the timer at the same time. You may also use the programed time function on the PQ200.
15. Once the desired testing time has been reached, stop the PQ200. If using the internal timer on the PQ200, wait until the PQ200 is no longer drawing air through the sampling system. Record the testing duration.
16. Open the access panel to the testing section of the wind tunnel.

17. Wearing new gloves, reach into the wind tunnel with Hand A and pull the LVTSP inlet up out of the PVC holder and then out of the wind tunnel through the access port.
18. Unscrew the air hose from bottom of the LVTSP inlet with Hand B and let it drop back through the PVC holder and out of the wind tunnel. Set the LVTSP inlet to the side.
19. Remove the PVC pipe with Hand A and set it on the nearby table.
20. Holding the LVTSP inlet with one hand, unlatch and open the inlet. Ensure the open LVTSP is stable and then change gloves to a new set. Dispose of the old ones.
21. If possible, remove the cartridge upper with Hand A. If unable to remove the upper piece by hand, using Hand B, insert a flat head screwdriver into the groove on the edge and twist slowly.
22. Once the upper piece is removed, set it aside. Pick up the filter cartridge base and turn it over so that that the filter falls out of the base and into one of the numbered filter jars.
23. Weigh the filter jar with the filter in it. Record the weight and the number.
24. Add the isopropyl solution to the filter draw. Add enough solution in order to fully submerge the filter.
25. Weigh the filter jar with the filter and solution. Record the weight.
26. Screw a lid on to the filter jar.
27. Let jars soak overnight before conducting the fluorometric analysis (see Appendix D).

1.7 Wind Tunnel Shutdown

1. Shutdown procedures can be started once the final test for the testing period is completed.
2. After stopping the final test, take an APS sample. While the APS sample is running, remove the sampler from the wind tunnel and jar the filter appropriately.
3. After completion of the APS sample, make sure a 250-mL beaker no more than half full is under the drain spout on the VOAG and flip the toggle switch on the VOAG labeled "DRAIN" to the "OPEN" position. Fluid will drain out.
4. Press "Run/Stop" button on the HPLC pump to stop the pump. The green light next to RUN will turn off.
5. Unscrew the amber jar containing solution used in testing from the HPLC inlet line cap. Cap solution jar.
6. Open the "Rinse Solution" ethanol jar and dip the stone filter on the end of the HPLC inlet line into the rinse solution several times.

7. Leave the HPLC pump inlet line in the rinse solution and press “Prime” on the HPLC pump. Prime for 30 seconds to a minute. Stop the pump and carefully lift the stone filter from the solution for inspection. If the HPLC pump inlet line just after the cap is not clear or the stone filter is not white after inspection, prime for another 30 seconds. Repeat as needed.
8. Remove the lid from the amber jar labeled “ETHANOL.” Insert the HPLC pump inlet line into the ethanol jar, making sure the stone filter is fully submerged, and screw the jar into the cap. Cap the rinse solution jar.
9. With the inlet line in the ethanol, press the “Prime” button on the HPLC pump and flush the system for 5 minutes. Proceed with steps 10 - 14 while flushing.
10. While system is flushing, carefully lower the cross bar holding the charge neutralizer onto the VOAG head low enough to remove the charge neutralizer. Remove the charge neutralizer and set aside, upright.
11. Cover the hole of the dispersion cap with a finger until the cap comes free from the VOAG head. Set aside.
12. Press “STOP” on the variable speed motor controller to turn off the wind tunnel fan.
13. Rotate the red switch on the air clockwise until it stops to stop the flow of compressed air.
14. Turn off the APS. Ensure the microscope light is turned off.
15. After the system has flushed for 5 minutes, press the “Run/Stop” button on the HPLC pump until the green light next to “RUN” turns off. Flip the switch below the front display to turn the pump off.
16. Carefully unscrew the piezo-electric crystal from the VOAG head. Using the isopropyl squirt bottle, spray the outer and inner surfaces of the crystal and wipe dry with Kim-wipes. Set aside to dry.

APPENDIX B

PARTICLE GENERATION

Scope: Outlines the start-up, testing parameters used, operation and shutdown of the 2x2 wind tunnel.

Purpose: To ensure the quality and repeatability of aerosol sampler evaluation tests in accordance with the Code of Federal Regulations, Title 40, Part 53, Subpart D.

PROCEDURE

1.1 General

The following procedures describe the procedures and techniques used to produce and evaluate a persistent, quality stream of particles. The steps involved with particle generation fall between Wind Tunnel Start-Up/Set-Up and Sample Collection. At this point, the particle generation system has been primed with the test solution but no particles have been generated.

Ideally, these steps will only need to be done once per experiment, however, the VOAG can be a temperamental machine and regeneration of particles may be required.

1.2 Jet Formation

1. After priming the test solution for 5 minutes, flip the drain valve switch on the VOAG to "CLOSED." If solution is still draining, flip the switch from "OPEN" to "CLOSED" until solution stops draining.
2. Test solution is pumped up through the piezoelectric crystal cap screwed onto the liquid base chamber and then down to the drain. Once the drain is closed, pressure in the VOAG head increases until the fluid is forced up through the orifice plate set in the piezoelectric crystal cap. This causes the particle "jet."
3. As the system pressures up, liquid will begin to pool on the surface of the piezoelectric crystal cap. Use a Kim wipe to remove this material so that it doesn't obstruct the jet.

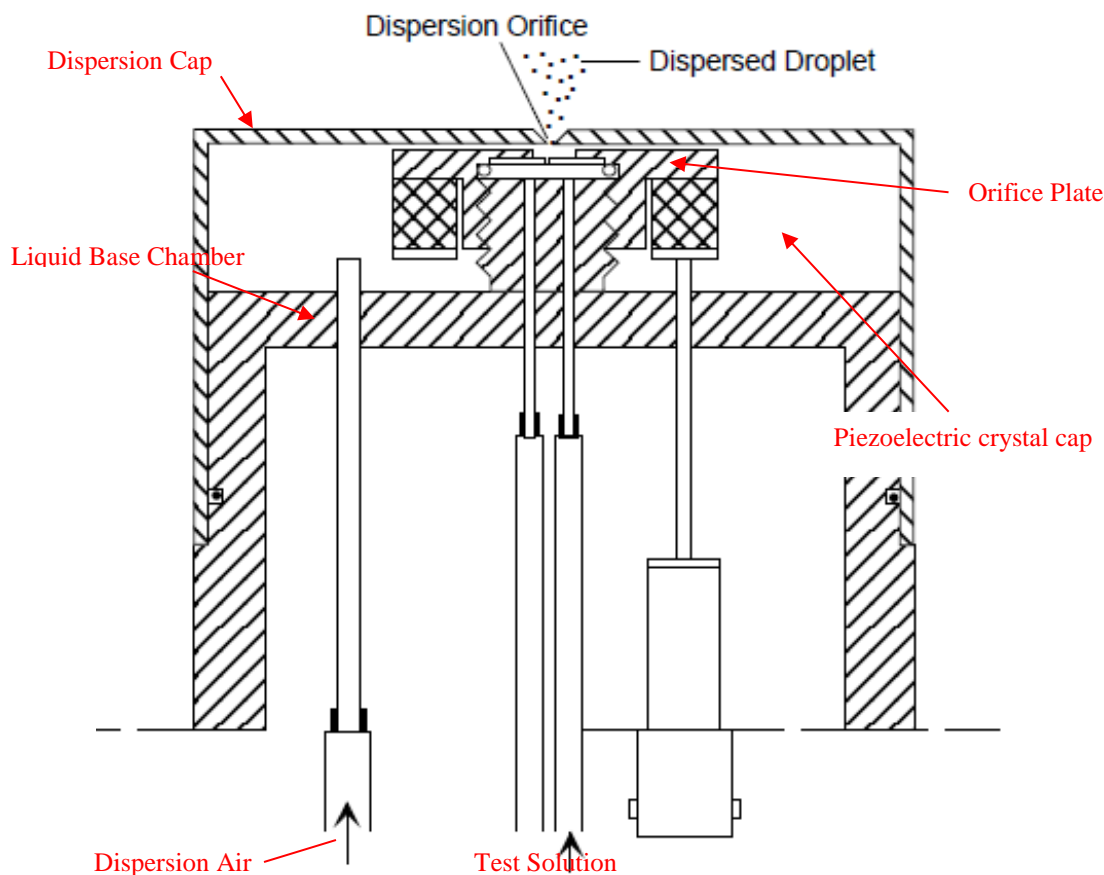


Figure B-1. Hatched image of the VOAG head (TSI, 2009)

4. The pressure required to produce the jet will cause enough back pressure in the test solution line to cause a pressure fault in the HPLC pump. Press “Run/Stop” on the HPLC pump to remove the fault. Wait for the pressure gauge on the VOAG to fall between 20 and 30 psi and then press the “Run/Stop” button to begin pumping the test solution at 0.225 mL/min. If running smaller particles, use the flow rate shown in table B-1. Ensure the frequency generator is on and set the initial supplied frequency to the values shown in table B-1 on the frequency generator.

Table B-1. Initial frequency generator and liquid feed pump rate settings.

	3 μm and Smaller Solutions	5 – 25 μm Solutions
Generator Frequency (Hz)	150,000	56,500
Liquid Feed Rate (mL/min)	0.093	0.225

5. Wait for the pressure gauge on the VOAG to stabilize and ensure the jet is a single, vertical stream. The next step is to evaluate that the jet consists of monodispersed particles.

1.3 Jet Evaluation

1. Connect the deflection nozzle to the dispersion air tube on top of the liquid base chamber.

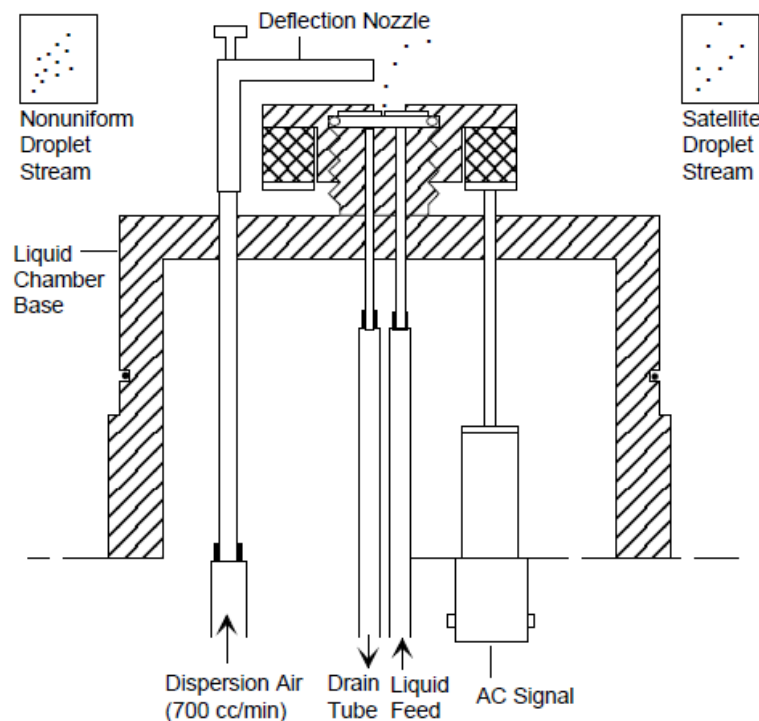


Figure B-2. Use of the deflection nozzle to deflect the jet (TSI, XXXX).

2. While adjusting the amount of dispersion air applied, deflect the particle jet using the dispersion nozzle by placing the nozzle up near the jet. You will also move the nozzle up and down the jet to ensure that it deflects consistently as the particles become more disperse.

3. A monodisperse particle will deflect as a straight line. If two distinct lines are observed during deflection, satellite particles are present, meaning that polydisperse particles (particles of distinctly different sizes) are being formed.
4. To correct the polydisperse particle issue, begin to adjust the frequency supplied to VOAG while continuing the deflection evaluation. If a potential frequency is found, allow the jet to settle for approximately 1 minute and then reevaluate the stream with the deflection nozzle.
5. Once a frequency has been selected, turn down the dispersion air, place the dispersion cap on the liquid chamber base, line up the thumbscrew indents with the thumb screws on the base, and push the cap down. Screw the thumb screws in to secure the dispersion cap.
6. Adjust the dispersion air knob by rotating it clockwise or counterclockwise until the ball in the flow meter stays at approximately 15 cc/min*100.
7. Place the acrylic drying column over the dispersion cap, dropping it gently into place. Insert the K85 charge neutralizer into the top of the drying column. Make sure to push the charge neutralizer in all the way that it seals around the O-ring properly.
8. Point the outlet of the charge neutralizer towards the inlet of the wind tunnel.
9. Connect the APS to the charge neutralizer via the plastic tube, and collect an APS sample. Ensure that the APS readout shows a single peak (1 local maximum) on the particle count graph. If multiple peaks are shown, the particle jet will need to be re-evaluated. Repeat the previous steps as necessary until you achieve a single peak you have a monodispersed particle. Record APS output by saving the file.
10. Ensure you remove the tube from the APS and the charge neutralizer and set it aside before proceeding.

1.4 Particle Impaction

1. After recording an APS measurement, impact particles on a coated slide.
2. Place a coated slide in the PVC slide impactor. The coated side of the slide should face the gray impactor nozzle of the impactor. Place the cap on the impactor to ensure the slide is secured.
3. Attach the hose from the small blue pump to the connection on the end of the impactor.
4. Turn the pump on and place the impactor inlet on the side of the PVC impactor in front of the outlet of the charge neutralizer. The amount of time the impactor

should be held there varies. The smaller the particle, the longer the wait time. 25 micrometer particles should only take a second. The 3 micrometer particles may take up to 10 seconds or more.

5. Remove the impactor from in front of the charge neutralizer and turn off the blue pump.
6. Disconnect the hose from the pump and remove the cap from the impactor cap.
7. Remove the slide and place it impacted/coated side up on the microscope. Ensure impacted particles are circular and well-spaced as shown below.

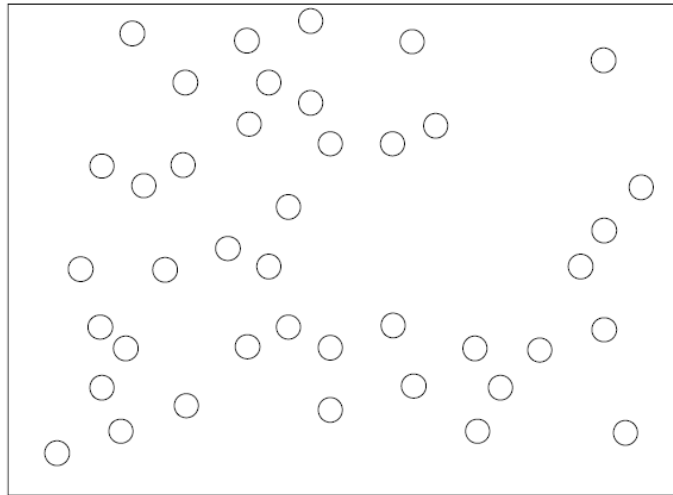


Figure B-3. Example of particles impacted on a coated slide as seen through the microscope (TSI, XXXX).

8. Using the particle sizing worksheet measure at least 10 particles using the slider. To measure a particle, move the line slider to the left edge of the particle and record the number on the knob of the line slider. Move the line slider to the right edge of the particle and record that number. If you rotate the number past 100, remember to account for that by adding 100 to the reading for each time you rotate past 100. The difference between the left and right numbers is the number of ticks wide the particle is. Approximately 42 ticks = 10 micrometers.
9. Complete the particle diameter measure for all particles. Calculate the average particle diameter and record the value. If the particle diameter is as desired, proceed with collecting samples. If the need be repeat the previous jet evaluation and APS steps until you achieve the desired particle sizes.

APPENDIX C

OPERATION OF THE QUANTECH DIGITAL FILTER FLUOROMETER

Scope: Outlines instrument setup, sample preparation, and instrument operation for Quantech Digital Filter Fluorometer.

Purpose: To ensure quality assured and controlled analysis of the fluorescein content of filters used for aerosol sampler evaluation.

PROCEDURE

1.1 General

The Quantech Fluorometer directs light in the wavelength range of 340-750 nm through a narrow band pass filter to determine the absorption of light by fluorescein in a liquid sample. The photomultiplier tube (PMT) measures the fraction of light that penetrates through a liquid sample in a test tube. Narrow band pass filters and sharp-cut filters reduce light attenuation of the PMT at certain wavelengths to reduce measurement noise. The primary excitation filter for fluorescein is NB490 and the secondary emission filter is SC515. The filters are manufactured by Quantech. The numbers are found on the top of the filters.

1.2 Fluorometer Setup

1. Install the NB490 (primary) and SC515 (secondary) filters by opening the top door on the fluorometer.
2. When viewing the chamber from the top, the primary excitation filter (NB490) should be placed in the slot at the top position and the secondary emission filter (SC515) should be placed at the left position (figure C-1).

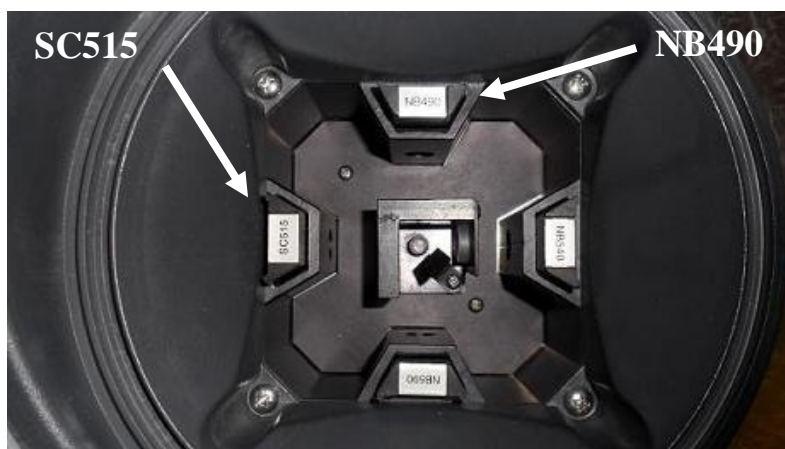


Figure C-1. Overhead view of fluorometer chamber.

1.3 Sample Preparation

1. Background Information for analysis of samples from the Subpart D Wind Tunnel
 - a. Five samples are collected for each test run in the wind tunnel, including:
 - i. Inlet filter
 - ii. Front isokinetic nozzle filter
 - iii. Back isokinetic nozzle filter
 - iv. Front isokinetic nozzle wash
 - v. Back isokinetic nozzle wash
 - b. The filters are removed from the wind tunnel after each test and are placed in 250mL Nalgene jars. Five mL of 50% water, 50% isopropanol solution are added to each jar immediately after the filter is placed into the jar. One drop of 1M sodium hydroxide is added to each jar directly after the filter is placed into the jar. The jars must sit for a minimum of four hours before the solutions are analyzed with the fluorometer to allow the fluorescein on the filters to dissolve into the alcohol solution.
 - c. One drop of 1M sodium hydroxide is added to the jars with wash solution (i.e. those without filters) immediately before they are analyzed.
 - d. After each test, the front and back isokinetic nozzles are washed with 50% water, 50% isopropanol solution. The wash is collected into a 250 mL Nalgene jar.
 - e. Each jar is labeled to indicate the test number and what type of sample is in the jar.

- i. Jars with an inlet filter are labeled with an “I”
 - ii. Jars with a front isokinetic nozzle filter are labeled with an “F”
 - iii. Jars with a back isokinetic nozzle filter are labeled with a “B”
 - iv. Jars with wash liquid from a front isokinetic nozzle are labeled with an “FW”
 - v. Jars with wash liquid from a back isokinetic nozzle are labeled with a “BW”
2. Place a 12 x 75mm test tube into the test tube rack for each jar. There should be 5 test tubes for each test. The empty sample test tubes for each test should be placed in the same row. The inlet sample (I) test tube should be placed in the first column, the front isokinetic nozzle sample (F) test tube should be placed in the second column, the back isokinetic nozzle sample (B) test tube should be placed in the third column, the front isokinetic nozzle wash sample (FW) test tube should be placed in the fourth column, and the back isokinetic nozzle wash (BW) sample test tube should be placed in the fifth column (figure C-2).

1I	1F	1B	1FW	1BW
2I	2F	2B	2FW	2BW
3I	3F	3B	3FW	3BW
4I	4F	4B	4FW	4BW
5I	5F	5B	5FW	5BW

Figure C-2. Overhead schematic of test tube rack.

3. Take the cap off of a jar. If the sample does not have a filter in it, put one drop of 1M sodium hydroxide into the jar and swirl the jar. If the sample has a filter in it, do not add anything.
4. Use a 1mL pipette to put ~2mL of liquid from a jar into the corresponding test tube. The exact volume is not important, but the level of the liquid needs to be higher than the light shining through the aperture in the chamber. The distance from the bottom of the test tube to the liquid surface should be ~1 cm.
5. Prepare a blank sample. Put ~2mL of 50% water and 50% isopropanol solution into a test tube. Place the blank sample into the test tube rack.

1.4 Running Samples with the Fluorometer

1. Turn on the fluorometer with the switch on the back located near the power cord.
2. Allow the fluorometer to warm up for 30 minutes.
3. Analyze a calibration standard.
 - a. The initial screen will read “Main Menu.” Press the right arrow button once and the screen will read “Advanced Functions.” Press the “Enter” button.
 - b. Press the left arrow button twice. The screen will read “Manually Set Gains and PMT Voltages.” Press the “Enter” button.
 - c. The first screen will read “Turn off Auto-Gain? No” Press the “Up Arrow” button.
 - d. The screen will read “Turn off Auto-Gain? Yes.” Press the “Enter” button.
 - e. The screen will read “Set Gain, 1.” Press the up and down arrow buttons to change the gain setting to “1”.
 - f. Press the left arrow button once and the screen will read “Set PMT Voltage, High.” Use the up and down arrow buttons to change the voltage setting to “Medium High.” Press the “Enter” button.
 - g. The screen will read “Main Menu.” Press the “Enter” button.
 - h. The screen will read “Choose Method.” Use the left and right arrow buttons until the screen reads “Raw Fluorescence.” Press the “Enter” button.
 - i. The screen will read “Enter Concentration 0000.000 <FIU>.” Press the “Enter” button.
 - j. The screen will read “Insert Known Sample.” Place a sample from one of the isokinetic nozzles into the fluorometer. A sample with one of the highest concentrations of fluorescein should be used because the fluorometer uses this reading to set the range of the voltage and gain. Therefore, if one of the tests were run for longer than the average test time, use either the front or back isokinetic nozzle sample from that test. If all the tests were of approximately the same duration, it does not matter which isokinetic nozzle sample is used. Place the sample into the chamber and press the “Enter” button. The fluorometer uses this reading to scale the PMT voltage and gain settings.
 - k. The screen will read “Insert Blank Sample? No.” Take the sample out of the chamber and press the “Enter” button. The sample that was taken out of the chamber should be replaced into the test tube rack. It will need to be analyzed

with the rest of the samples. The screen will read “Insert Unknown Sample.” The fluorometer is now ready to read all of the samples.

4. Order of Sample Analysis

- a. Before analyzing a test sample, the blank sample should be analyzed by following steps 5a through 5e.
- b. Once the blank sample is analyzed, the samples from the first test should be analyzed. The samples for the inlet, front isokinetic nozzle, back isokinetic nozzle, front isokinetic nozzle wash, and back isokinetic nozzle wash should be analyzed by repeating steps 5a through 5e. If the reading from one of the isokinetic nozzles is >3000 , the voltage setting should be changed to medium low.
 - i. Press the main menu button and repeat steps 3a through 4b.
 - ii. When it says to change the voltage setting to “Medium High” in step 3f, change the voltage setting to “Medium Low.”
- c. The blank sample should be analyzed after all five samples have been analyzed for each test.
- d. After every sample has been analyzed, steps 4a through 4c should be repeated once. There should be two fluorometer values for each test tube.

5. Analyzing Samples

- a. Open the chamber door on the top of the fluorometer (figure C-3).



Figure C-3. Fluorometer with chamber door open.

- b. Place a test tube into the chamber.
- c. Close the chamber door.
- d. Read the screen to the left of the chamber door on the top of the fluorometer. Record the reading on the data sheet in the space that corresponds to the sample. The fluorometer gives readings in Fluorescent Intensity Units (FIUs). An FIU is the uncalibrated output of the electrical conditioning circuit

that processes the raw signal from the photomultiplier tube. FIU is directly proportional to the concentration of the fluorescent tracer material.

- e. Open the chamber door, take the test tube out of the test tube holder, and place it back in the test tube rack.

1.5 Disposing of Samples

1. Pour the remaining liquid from Nalgene jars into the waste disposal carboy* beneath counter. Put the jars in the “Used Jar Rack” to be washed.
2. Put used filters from the Nalgene jars into the trash.
3. Pour the remaining liquid from the test tubes into the waste disposal carboy beneath counter.
4. Put used test tubes into the “Glass Waste” box.

* When the waste disposal carboy is full, contact the “TAMU Environmental Health and Safety Department” at (979) 845-2132 and they will pick up the carboy, dispose of the contents and return the carboy to the lab.

1.6 Washing Nalgene Jars and Lids

1. Over the sink, fill a used jar with tap water.
2. Pour the water from the first jar into another used jar. Continue pouring the water between the two jars four times.
3. Repeat steps 1 and 2 until all the jars are clean.
4. Place the cleaned jars into the “Clean Jar Rack.”
5. Over the sink, spray the underside of a used lid with tap water. Repeat for all of the used lids.
6. Place the cleaned lids into the “Clean Lid Rack.”

APPENDIX D

GLASS SLIDE COATING PROCEDURE

Scope: Outlines the procedure to be used when coating of glass slides for use in measuring aerosols generated by the VOAG during aerosol sampler test evaluations.

Purpose: To ensure the quality and repeatability of aerosol sampler evaluation tests in accordance with the Code of Federal Regulations, Title 40, Part 53, Subpart D.

PROCEDURE

1.1 General

The following procedures outline the appropriate way to correctly prepare glass slides for the effective impaction of both liquid and solid particles generated by the VOAG for subsequent sizing with the microscope.

1.2 Cleaning/Prep

1. Put on a pair of gloves.
2. Take the desired number of slides to be coated by slide treat procedure from the box and place them on a clean, flat surface or propped up against the slide holder. The number of slides to be coated for the impaction of liquid particles must be an even number as these slides are coated in pairs.
3. Pickup a slide and, using the isopropyl spray bottle, squirt a relatively small amount of isopropyl on both sides of the glass slide. Use a Kimwipe to rub both sides of the glass slides. Inspect both sides of the slide to make sure no smudges or lint residue is visibly present. Set aside to dry.

1.3 Coating Slides for Liquid Particles

1. Open the bottle of NyeBar Solution, Type Q, by unwrapping the tape seal around the cap. Place the cap and tape aside. A solution of NyeBar other than Q may be used but it must be noted according to Step 1.3.9.
2. Take two slides to be coated with NyeBar for liquid particle impaction and determine which side is the “frosted” side. At one end of each slide, there is an opaque, textured section that is known as “frosting.” The NyeBar coating **MUST ALWAYS** be on the frosted side of the slide.

3. Once it has been determined which sides of the two slides are frosted, take the pipette, dip it into and draw up some of the NyeBar from the bottle. Take one of the two slides, holding it by the frosting, and place between 6-8 drops of NyeBar onto the frosted side of the slide in a line from the unfrosted edge of the slide toward the frosting.
4. Take the second slide and, holding it by the frosting, place it on top of the slide with the NyeBar solution frosted side down. Apply light pressure.
5. Slowly pull the two slides apart, horizontally and longitudinally, so as to coat the the surface of each slide with NyeBar. This step is to be done quickly after placing the two slides together as the NyeBar dries quickly and can cause the slides to stick to one another.
6. Visually inspect the coated slides after pulling them apart. The NyeBar will produce an oleophobic coating on the frosted side of each slide that has a “rainbow-like” sheen when held at the correct angle to a light source. The coating must extend from the unfrosted edge of the slide to at least three quarters of the slide towards the frosting and the full width of the slide.
7. If both slides do not meet the criteria of Step 1.3.6, the slides can be cleaned according to step 3 and the NyeBar coating reapplied. Be sure there is no “rainbow-like” sheen prior to re-application. If only one slide of the pair do not meet the requirements of Step 1.2.6, it can be cleaned as previously stated and the coating replied using a different paired slide.
8. Slides that meet the coating requirements of Step 1.3.6 may be place in the top row of the slide box. Slides placed in the box should be placed with the frosted/coated side facing to the right, the frost edge pointing the opposite direction of the slide box lid and towards the second row, and in the second slide holder to the left of slides currently in the box (if the box is such that the lid is away from the user).
9. If a slide is coated with a NyeBar solution other than Type Q, the coating should be noted in any testing documentation as well as on the slide itself by writing the letter of the solution on the frosting of the slide coated with the solution. Different solutions have different flattening factors.

1.4 Coating Slides for Solid Particles

1. Open the tube of Dow Corning High-Vacuum silicon grease by unscrewing the cap. Set the cap aside.
2. Take a single slide and determine which face of the slide is “frosted.” This is the side of the lside that the grease will be applied to.

3. Apply an amount of grease, equivalent to the diameter of a dime and the thickness of a quarter, to the frosted side of the slide.
4. Using your finger, spread the grease across the entire un-frosted surface of the slide.
5. Take a Kim-wipe, fold it in half and place the slide between within the fold. Applying pressure to the Kim-wipe with one hand, pull the slide through the Kim-wipe, by holding onto the frosted section of the slide. Repeat until it feels like the slide no longer resists being pulled through the Kim-wipe.
6. Inspect the grease coated slide. The slide should have dramatically increased opacity on the coated surface. The grease coating should be unbroken across the entire non-frosted surface of the slide.
7. If a slide does not meet the criteria of Step 1.4.6, steps 3 through 6 may be repeated with a reduced amount of grease.
8. Slides that meet the coating requirements of Step 1.4.6 may be place in the bottom row of the slide box. Slides placed in the box should be placed with the frosted/coated side facing to the right, the frost edge pointing the opposite direction of the slide box lid and towards the side of the slide box, and in the second slide holder to the left of slides currently in the box (if the box is such that the lid is away from the user).

1.5 Clean Up

1. Recap the NyeBar solution by screwing the cap back onto the bottle and reapplying the sealant tape to the cap to cover the gap between the cap and threads.
2. Ensure that the silicon grease cap is screwed down onto the grease tube.
3. Return both containers to their appropriate drawer.
4. Any slides that broke, fractured, cracked or are otherwise unusable need to be disposed of with the sharps/glass disposal box found under the analysis counter.
5. Close and latch the slide box.

APPENDIX E

PARTICLE SOLUTION CONSTRUCTION

Scope: Describes the procedure to be used when mixing solutions for the generation of specific sized particles.

Purpose: To ensure the quality and repeatability of aerosol particle solutions for use in sampler evaluation tests under the guidelines of the Code of Federal Regulations, Title 40, Part 53, Subpart D.

PROCEDURE

1.1 General

The following procedures describe the appropriate way to correctly prepare both uranine and fluorescein based solutions to be used in conjunction with a vibrating orifice aerosol generator (VOAG) for the generation of liquid and solid particles of desired particle diameter.

1.2 Cleaning/Prep

1. ALWAYS wear a pair of powder-free latex gloves.
2. Ensure that the ethanol squirt bottle is full by pouring ethanol from the 4 L bottle into the squirt bottle. If there is not enough bulk ethanol in the 4 L bottle, additional ethanol can be obtained by acquiring a PO for the BSBE stockroom and taking the jug to the Biological Sciences Building East (BSBE), Room to purchase a refill of the 4 L container.
3. Fill the DI water squirt bottle from the DI Water storage carboy. If the DI water carboy is low, additional carboy can be obtained from Dr. Carmen Gomez's lab in Scoates Hall, Room 219.
4. When using any equipment or materials in any lab, observe all warnings and safety precautions required for the facility. Clean and return all borrowed equipment/materials in a timely manner and in working condition.

1.3 Mixing a Solution for Liquid Particle Generation

1. Open the file "Oleic Acid Solution Master" in the address R:\Raleigh\Wind Tunnel\ScoT Data\Solution Construction\Oleic Acid. Press the "Enable" button in the orange security warning bar at the top of the spreadsheet and immediately use the "Save As" command and save the in the "Oleic Acid" folder with the master file as "[Particle Size] um Solution Prep [date of solution construction],"

replacing the [brackets] with the desired generated particle size of the solution and the date on which the solution is being prepared in the month-day-year format, respectively.

2. On the “Oleic Acid – Desired” tab, fill the cells highlighted yellow with the appropriate information according to table E-1. The “Desired Aerodynamic Diameter D_{pa}” is the desired particle size of the solution (the same particle size as listed in the file name).

Table E-1. Spreadsheet parameters used to obtain appropriate masses of oleic acid and uranine for solution preparation.

	3 um and Smaller Solutions	5 – 25 um Solutions
Generator Frequency (Hz)	150,000	56,500
Liquid Feed Rate (mL/min)	0.093	0.225
Desired Uranine/Oleic Acid Ratio (g/mL)	0.100	0.100
Container Volume (mL)	1,000	1,000

3. Record the mass of oleic acid and uranine required for the solution. These cells are highlighted green.
4. Place a 250 mL beaker in the 0.0001 resolution scale on the desk next to the wind tunnel. Shut the glass doors and allow the scale to equalize. Once the mass reading stops changing, tare the scale.
5. Remove the jar of uranine from the solutions cabinet located next to the flammables cabinet and place it on the desk.
6. Open the jar of uranine and using the spoon labeled uranine, carefully and slowly add small amounts of powdered uranine to the beaker on the scale. When approaching the mass required for the solution, close the glass doors of the scale after adding additional uranine in order to allow the mass reading to stabilize.
7. Repeat step 1.3.6 until the desired mass of uranine ± 0.0001 g has been added to the beaker. Record the mass of uranine actually in the beaker.
8. After the desired mass of uranine has been weighed out, remove the beaker from the scale and add between 10 – 20 mL of DI water to the beaker by sight, using the DI water squirt bottle. **DO NOT** squirt the water directly onto the mound of uranine in the beaker. Spray the interior sides of the beaker with the water while slowly rotating the beaker. Lightly swirl the solution to try and wet most of the uranine.

9. After adding the DI water, add between 150 – 200 mL of ethanol to the beaker using the ethanol squirt bottle in the same manner as the DI water squirt bottle. Lightly swirl the solution after adding the ethanol to try and break up all the uranine.
10. Take the beaker containing the uranine solution and place it in the ultrasonic bath. The water level in the ultrasonic bath should be just slightly below the solution level in the beaker. Place a Kim-wipe over the top of the beaker and sonicate the solution for 30 minutes.
11. While the uranine solution is sonicating, get a new pair of gloves, take a volumetric flask (make sure it is not labeled for use with ammonium hydroxide) and place it in the .001g resolution scale located in the filter analysis station. Ensure that the mass reading on the scale plus the desired mass of oleic acid will not exceed that maximum mass reading of the scale. If it does exceed the limits of the scale, use the secondary scale (.01 g resolution) located on the counter under the solutions cabinet. Tare the scale.
12. Retrieve the oleic acid from the solutions cabinet and pour a volume of oleic acid to use with a cap into a clean, filter analysis cup. Return the oleic acid bottle to the cabinet. There may already be a cup of oleic acid ready for use. If so, use it.
13. Add the oleic acid carefully and slowly to the volumetric flask using a 1 or 3 mL disposable pipette. When adding the oleic acid with the pipette, make sure to insert the end of the pipette inside the flask to prevent any oleic acid from getting on the outside of the flask. It is acceptable if some oleic acid ends up on the inside surface of the volumetric flask neck, but avoid this if possible.
14. Add oleic acid until the desired mass has been reached. Record the actual mass of the oleic acid added to the flask. It is very difficult to get exactly the required mass of oleic acid due to a certain amount of mass being associated with individual drops/ It's better to be slightly over the required mass than slightly under.
15. Using the ethanol squirt bottle, add approximately 20 mL of ethanol by spraying the interior surfaces of the flask to recover any oleic acid that may have stuck to the surfaces of the flask neck.
16. Place the funnel in the top of the flask and add approximately 150 mL of ethanol from the 4 L ethanol bottle.
17. Remove the funnel and set aside to dry. Insert the flask stopper and move the flask into the ultrasonic bath. Sonicate the solution for at least 10 minutes or for the time remaining in step 1.3.10, whichever is longer.

18. After the 30 minute sonication period has ended, check the uranine solution. If large chunks of uranine have not dissolved, swirl the solution and replace the solution in the ultrasonic bath covered by the Kim-wipe; add ethanol if needed. Sonicate for 10 minutes. Repeat this step as needed.
19. Remove the volumetric flask from the bath and dry it off. Place the flask on some paper towels. Remove the stopper and insert the funnel. Remove the uranine solution from the bath and dry it off. Carefully pour the uranine solution into the funnel.
20. Use an ethanol squirt bottle to spray the entire inside surfaces of the uranine beaker to recover any additional solution. Also spray any of the outside beaker edges to recover any other solution. Set the beaker aside. Use the ethanol squirt bottle to clean the funnel of any more uranine solution into the flask.
21. Fill the flask with ethanol from the 4 L bottle using the funnel to within 1 inch of the 1000 mL line on the flask. Replace the stopper in the flask and return the flask to the ultrasonic bath. Sonicate for 30 minutes to an hour.
22. Fill the flask to the 1000 mL line using the ethanol squirt bottle. Sonicate again for 10 minutes. If the flask gets filled over the line, estimate the volume of overage and record the total volume of solution in the flask.
23. In the solution workbook, switch to “Oleic Acid – Actual” tab and enter the masses of uranine and oleic acid used and the total volume of the solution into the appropriate sections of the spreadsheet. Ensure that the resulting particle size (green highlighted cell) is within the range of the desired particle size ± 0.5 microns. If the resulting solution particle size is outside these bounds, dispose of it using the carboy located in the filter analysis station. Save the file.
24. If the prepared solution meets the requirements in step 1.3.24, fill an empty 1000 mL amber glass jar with the completed solution. Screw the glass jar cap onto the jar and set aside.
25. Use the labeler to label the jar as “[Particle size] um Uranine Solution [Solution preparation date],” replacing the [brackets] with the target particle size of the solution and the date of solution prep date using the month/day/year format, respectively.
26. Place the completed solution in the solutions cabinet in consecutive order according to particle size and any solution already present for that particle size.

1.4 Mixing a Solution for Solid Particle Generation

1. Open the file “Ammonium Hydroxide Solution Master” in the address R:\Raleigh\Wind Tunnel\ScoT Data\Solution Construction\Ammonium. Press

the “Enable” button in the orange security warning bar at the top of the spreadsheet and immediately use the “Save As” command and save the in the “Ammonium” folder with the master file as “[Particle Size] um Solution Prep [date of solution construction],” replacing the [brackets] with the desired generated particle size of the solution and the date on which the solution is being prepared in the month-day-year format, respectively.

2. On the “Ammonium Flourescein – Desired” tab, fill in the “Desired Aerodynamic Diameter, Dpa” cell (highlighted yellow) with the desired particle size of the solution. Use the parameters listed in table E-1 under the “5 – 25 um Solutions” heading for the remaining highlighted cells.
3. Record the required volume of ammonium hydroxide and mass of fluorescein required for the solution preparation.

****WARNING**** *Ammonium hydroxide* is a very hazardous chemical. **NEVER** open the ammonium hydroxide bottle outside of the fume hood. **ALWAYS** wear gloves when handling the NH₄OH bottle or materials inserted inside the bottle and **DO NOT** let it get on your skin. Refer to the bottle for procedures if the solution does come into contact with skin. When mixing chemicals into the volumetric flask, do so in a well-ventilated area or near an open window, **DO NOT** leave the stopper out for too long and **DO NOT** stand directly over the opening or inhale deeply. Respirator masks are helpful and are available on the counter next to the sink. These same rules apply for the carboy containing waste ammonium hydroxide.

4. Request the use of a fume either in the Food Lab (Scoates Hall, Room 318) or Dr. Gomez’s lab (Scoates Hall, Room 219). Collect the volumetric flask labeled for use with ammonium hydroxide, a volumetric flask stopper, the pipette hand pump, and a 0.01 increment disposable pipette. Add approximately 100 mL of DI water to the flask from the DI water storage carboy and take the gathered materials to the fume hood. Retrieve the ammonium hydroxide from the storage cabinet (next to the solutions cabinet) and take the bottle to the fume hood. Place the bottle in the hood.
5. Prior to opening the NH₄OH bottle, turn the fume hood ON. Assemble the disposable pipette and hand pipette pump such that the disposable pipette is parallel and connected to the “S” valve. To operate the hand pump, release the air out of the pump by squeezing the air chamber and holding the “A” valve open. Insert the disposable pipette into the ammonium hydroxide, and slightly squeeze the “S” valve to obtain solution in the pipette. Insert the pipette into the volumetric flask to discard the ammonium hydroxide. Do this by squeezing the “E” valve. Repeat this procedure as necessary until the final volume of required ammonium hydroxide is obtained. To operate the hand pump.

6. Insert the pipette into the bottle of ammonium hydroxide and draw out the solution. Slowly transfer the pipette to the volumetric flask and dispense the solution.
7. Repeat step 1.4.6 until the desired volume of ammonium hydroxide has been added to the flask. Place the stopper in the flask and recap the 4 L bottle. Rinse or dispose of the pipette as needed. Let the equipment sit in the fume hood for several minutes to draw off any excess NH_4OH fumes.
8. Take the volumetric flask and place it in the ultrasonic bath. The water level in the bath should be at or just above the liquid level in the flask. Sonicate for 10 minutes. Retrieve all the materials from the fume hood and return them to their appropriate locations in the lab.
9. Place a 250 mL beaker in the .0001g resolution scale on the desk next to the wind tunnel. Shut the glass doors and allow the scale to equalize. Once the mass reading stops changing, tare the scale.
10. Remove the jar of fluorescein from the solutions cabinet located next to the flammables cabinet and place it on the desk.
11. Open the jar of fluorescein and using the spoon labeled fluorescein, carefully and slowly add small amounts of powdered fluorescein to the beaker on the scale. When approaching the mass required for the solution, close the glass doors of the scale after adding additional fluorescein in order to allow the mass reading to stabilize.
12. Repeat step 1.3.6 until the desired mass of fluorescein ± 0.0001 g has been added to the beaker. Record the mass of fluorescein actually in the beaker. Change gloves.
13. Once the sonication time from step 1.4.8 has elapsed, remove the flask from the bath and dry with paper towels. Set the flask in a well-ventilated or near an open window. Put on a respirator mask if available.
14. Take the beaker of fluorescein, the squirt bottle of DI water, and the funnel to the flask. Remove the stopper of the flask and place the funnel in the opening. Carefully tilt the fluorescein beaker in order to slowly pour the fluorescein into the funnel. Use the DI water to affect the fluorescein along as need but DO NOT squirt the fluorescein powder directly with the water. Ensure that all of the fluorescein makes it into the funnel and down into the flask. Use the squirt bottle to recover any fluorescein from the surfaces or edges of the beaker, the funnel and the inside surfaces of the flask neck. Place the stopper in the flask and set the funnel aside to dry.

15. Add DI water directly to the beaker either with the squirt bottle or from the carboy to the 1000 mL line on the volumetric flask.
16. Sonicate the mixture for 30 minutes. Make sure the stopper is firmly in place.
17. In the solution workbook, switch to “Ammonium Hydroxide – Actual” tab and enter the mass of fluorescein and volumes of the ammonium hydroxide used and total solution into the appropriate sections of the spreadsheet. Ensure that the resulting particle size (green highlighted cell) is within the range of the desired particle size ± 0.5 microns. If the resulting solution particle size is outside these bounds, dispose of it using the carboy located in the filter analysis station. Save the file.
18. After 30 minutes the solution should be fully mixed and dissolved. Remove the flask from the bath and dry. If the flask is warm to the touch, set aside to cool.
19. If the prepared solution meets the requirements in step 1.4.17, fill an empty 1000 mL amber glass jar with the completed solution. Screw the glass jar cap onto the jar and set aside.
20. Use the labeler to label the jar as “[Particle size] um Fluorescein Solution [Solution preparation date],” replacing the [brackets] with the target particle size of the solution and the date of solution prep date using the month/day/year format, respectively.
21. Place the completed solution in the solutions cabinet in consecutive order according to particle size and any solution already present for that particle size.

1.5 Clean Up

1. Clean up any spills using the manufacture provided techniques if available.
2. Clean all containers, tools, and other equipment using the lab sink. Place items in the appropriate drying racks or locations.
3. Wipe down surfaces using kim-wipes and ethanol.
4. Allow all used equipment to properly dry before next use.